A Geotechnical Study of the Eastern Flanks of the Rockall Trough

By

Eoin Wyse, B.Sc.

Thesis submitted in fulfilment of the requirements for the Degree of Master of Engineering Science to the Department of Civil Engineering, University College Dublin

Head of Department

Prof. Eugene O'Brien

Supervisor

Dr. Mike Long

University College Dublin, April 2004

Table of Contents

Chapter 1: Abstract

This project presents the results of a geotechnical analysis of the cores and tries to quantify some of the near surface lithologies in various slope settings along the Eastern Rockall Trough. Tests were carried out in order to classify the various materials. The classification tests carried out included moisture contents, specific gravities, plasticity indices and grain size analyses. One of the grain size analyses was also used to compare the traditional sieving and hydrometer methods and laser sizing methods. Some oedometer tests and shearbox tests were also carried out. Basic sets of lithologies were proposed and these were integrated with the classification data presented in this report and previous work. These lithologies were Carbonate-Rich Sandy Silts, Sandy Silts, Silts and Foraminiferal Sandy Silts. While some basic trends could be observed, since the samples were from a limited depth and over a relatively large geographical area, these trends may not have been accurate. Therefore to try and minimise this factor samples were grouped not only geographically but also according to the various lithologies, which were proposed. The oedometer tests were carried out to attempt to describe the stress history of the samples. This gave results implying that the material tested was overconsolidated, suggesting that the sample was buried under a greater depth of sediment at some stage in it's history. Shearbox tests were performed in order to determine the peak effective stress parameters of the sample and also look at the variation in the strength of the sample with regards to changing density and normal stress. These showed that the material has low strength at low effective stresses and implies that surface slides are more likely to occur than more catastrophic deep slides.

Chapter 2: Acknowledgements

I would like to thank Dr. Mike Long for his patience and help in this project. I'd also like to thank George Cosgrove and the other users of the Soils lab for their help and advice. A big thank you goes to the other post-graduate students, Lorraine, Caroline, Amir, Liang and especially Farzin Hosseini and Muhammad Ekhlasur Rahman. Thanks also have to go to the Rockall Studies Group and The Irish American partnership and Enterprise Ireland for their sponsorship. Of course, the biggest thank you has to go to my parents for their unfailing faith in me. Thanks also have to go to Lena Øvrebø (for help with the figures and digital photos), Dr. Peter Haughton, and Prof. Pat Shannon in the Geology Department, UCD.

This publication uses data and survey results acquired during a project undertaken on behalf of the Rockall Studies Group (RSG) of the Irish Petroleum Infrastructure Programme Group 2. The RSG comprises: Agip (UK) Ltd, Anadarko Ireland Company, ARCO Ireland Offshore Inc, BG Exploration & Production Ltd, BP Exploration Operating Company Ltd, British-Borneo International Ltd, Elf Petroleum Ireland BV, Enterprise Energy Ireland Ltd, Mobil Oil North Sea Ltd, Murphy Ireland Offshore Ltd, Phillips Petroleum Exploration Ireland, Saga Petroleum Ireland Ltd, Shell EP Ireland B.V., Statoil Exploration (Ireland) Ltd, Total Oil Marine plc, Union Texas Petroleum Ltd and the Petroleum Affairs Division of the Department of the Marine and Natural Resources.

Chapter 3: Introduction

With the discovery of various fossil fuel resources off the west coast of Ireland, i.e. the Corrib Gas Field, a large amount of research is now taking place with regards to possible petroleum production infrastructure in the Rockall Trough. This varies greatly covering many different disciplines and looking at many features of the Rockall area, with many of these projects being sponsored by the Petroleum Infrastructure Programme (PIP) and the Petroleum Affairs Division (PAD) of the Department of the Marine and Natural Resources. These projects range from studies of local wildlife, detailed surveys of the coldwater carbonate mounds in the area, to sedimentological analyses of the near bottom sediments. This project concerns an examination of the geotechnical characteristics of these sediments.

In 1998, a suite of 45 gravity cores was obtained from the slopes of the Rockall Trough. These cores were to be investigated both geologically and geotechnically and formed the basis of three Rockall Studies Group (RSG) projects, project 98/20 (Regional Geotechnical Characterisation of Near-Surface Sediments, Preliminary Geotechnical Assessment; UCD, JBA and TCD), project 99/1 (Sedimentological analysis of gravity cores from the Rockall Trough, Øvrebø, PhD study in progress) and 00/17, (this project) respectively. Project 99/1 looked at these cores in order to achieve a better understanding of factors influencing slope stability and the importance of bottom current processes on the flanks of the Rockall Trough. Project 00/17, the geotechnical analysis, was carried out in close conjunction with project 99/1.

Project 00/17 (the present project) involved an examination of these cores with a view to fulfilling some of the following objectives:

- To establish a relationship between the depositional and topographical environment and the basic properties of the materials.
- To try and explain the stress history of the material
- To look at the liquefaction potential and relationship between density or porosity and shear strength with regards to slope stability.

Initially, a literature review was carried out in order to address the basic theory of offshore slope stability. The results from a number of similar studies were examined. Particular attention was paid to projects that integrated both geological and geotechnical approaches to studying areas such as the fjords of Norway, the Mississippi Fan and the Ormen Lange Slide.

The next chapter involved presenting the different areas examined and describing their geographical location and a brief description of the lithologies found. Also included are seismic profiles of some of the areas (from Shannon and Praeg, 2001).

Sampling methodology and the testing methods for the classification tests are presented in the next chapter. These tests included moisture contents, specific gravities, grain size analyses and plasticity indices. The results of these tests are presented in the next section site by site and also by lithology, in order to limit the geographical influence on the results.

Another set of tests was also carried out to ascertain the stress history of some of the materials. This involved an oedometer test, the results of which can be used to determine whether a sample has been previously consolidated at some stage in its history.

Other tests included a shearbox test. This was used to calculate the strength of the sample. Both these tests are dealt with in their own sections.

Further chapters include stress history, discussions and conclusions. The stress history chapter deals with the results of a number of oedometer tests, which were used to try and determine the preconsolidation values for a number of samples. Two methods were utilised to obtain these preconsolidation figures, which are presented in this chapter.

Discussions and conclusions are presented in the relevant chapters and present respectively, options for further research and possible sources of errors present in this thesis, and also an overview of the findings presented in this thesis.

Chapter 4. Previous Research

Slope instability is a well-covered topic for onshore or near shore sites. However, in offshore settings, there is not as much data available. This literature survey examines some of the major papers published about the topic, which are relevant to this thesis. The papers examined fell into two main groups. The first group was papers dealing with the basic theory of offshore slope instability. These could again be split into three subheadings, dealing with (a) the potential of liquefaction in the sediments, (b) the various classes of failures and (c) the prerequisites for failures and the triggers of failures. A number of papers were examined which dealt with very similar studies to this project, in the sense that these papers described integrated studies looking at geological and geotechnical properties of offshore sites. These were studies, which took place in both the North Sea and in the Gulf of Mexico, together with a paper dealing with a general approach to carrying out these studies. Finally a paper was included which looked at the differences between laser grain sizing and the more traditional sieving and sedimentation method of determining grain sizes.

4.1: Theory of offshore slope stability

One of the centres for offshore slope stability studies is the Norwegian Geotechnical institute (NGI). Much of the early work in this field was done here. The work of their Director, L. Bjerrum, was especially important in helping our understanding of slopes. He looked initially at the shear strength parameters of the late glacial sensitive clays of Scandinavia (Bjerrum, 1961). However he also performed a similar examination of the fine sands and silts present in many of the fjords in western Norway, along with S. Kringstad and O. Kummeneje (1961). This work drew from the work of Terzaghi (1947),

which observed that slides of this type are characterized by a temporary liquefaction of large sand masses. Bjerrum (1971) went on to look at a number of flow slides, which occurred in fjords around central Norway including Trondheim Fjord (Figure 4.1). Since 1888, there had been two important slides in the Trondheim Harbour area. The largest and most important of these was the 1888 slide. This was observed to have begun out in the fjord and proceeded retrogressively towards the railway station. The part of the slide visible measured 170m in length. Eyewitness reports (Skaven-Haug, 1955) mention a 5 to 7m wave forming out in the fjord. This proceeded shorewards and when it receded, it took with it a 7m high jetty as well as the part of the railway tracks. Later investigations in the area in 1956/57 confirmed that the natural deposits of the area consisted of silty sands.

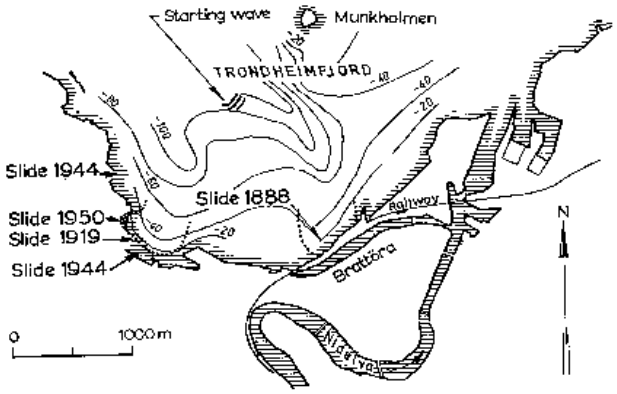

Figure 4.1: Trondheim harbour

Bjerrum (1961), demonstrated that the effective angle of internal friction, determined with drained tests in sensitive clays from the bottom of Trondheim Fjord, is in the order of 10^o. By using the expression below he proposes a theoretical relationship between ϕ' and S_u/p (the ratio between undrained shear strength and effective overburden pressure).

$$S_u/p = [(K+(1-K)A_f)\sin\phi']/[1+(2A-1)\sin\phi']$$

In order to use this equation we assume the cohesion term c'=0 in normally consolidated clay. We also need to introduce the initial stresses under which the clay was consolidated and the pore pressure parameter A. The value for A_f was measured in triaxial apparatus on a large number of samples of sensitive clays. K is the coefficient of earth pressure. If initial stresses are $\sigma I = p$ and $\sigma II = \sigma III = K_p$, with σI being the effective overburden pressure or normal stress and σII and σIII being the stresses acting on the soil perpendicular to σI, and the clay fails in compression we can use the above expression. Through use of the above expression he obtained similar values of S_u/p. He then went on to confirm this figure of 10^o in soils with a loose structure such as sands and silt with an *in situ* shearbox test. He proposed that the inflated effective ϕ' values between 25 and 32^o for quick clays and sands could be attributed to reconsolidation following sampling disturbance causing a change in the soil's properties.

Andresen and Bjerrum (1968) highlighted the possibility of liquefaction occurring at small strains in loose sands and silt. Terzaghi (1956) presented a more complete treatment of the various types of failures in submarine slopes. With materials of this type it helps to distinguish slope failures into two distinct types: Flow Slides and Liquefaction Slides. Flow slides develop retrogressively and generally start in the lower part of a slope as a result of a localised steepening due to erosion or due to the effect of seepage pressures during falling tides. The slide will continue until it reaches a layer of more dense sand deposits or where the loose sand disappears or is covered by layers of other types of soil or fill. Spontaneous Liquefaction type slides are where, due to an earthquake or some other source of vibration or shock, the loose sand undergoes liquefaction and this liquefaction in turn goes on to spread to neighbouring deposits of sand, which are prone

to liquefaction. These slides propagate in all directions, including upslope. They go on to describe how the “susceptibility of loose sand to liquefaction is the result of a small strain at failure, a low frictional resistance, a rapid rise in pore pressure during shearing and a rapid loss in strength after failure”. They also demonstrated that particle size and density are important factors. They propose a set of curves, which can be overlain onto a grain size distribution graph to bracket sediments, which are susceptible to liquefaction (Figure 4.2). These curves were taken from Langer (1958) and Watanabe (1965).

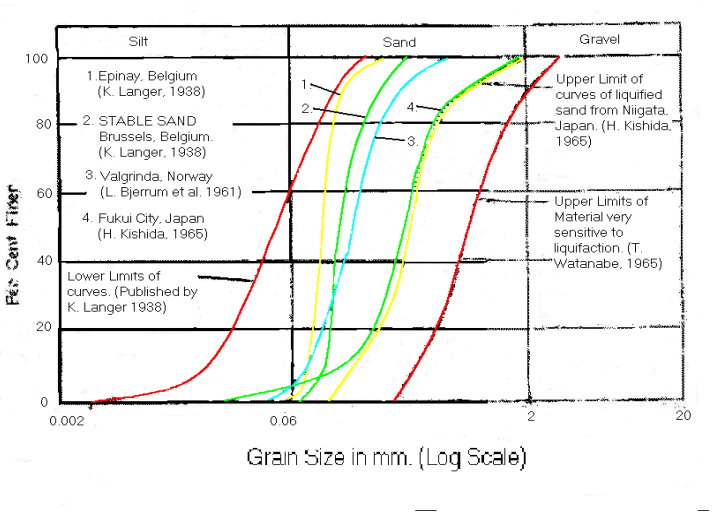

Figure 4.2: Grain size distribution curves for flow slide material and Valgrinda sand (Bjerrum, 1961; Langer, 1938; Watanaba, 1965; Kishida, 1965)

Edgers and Karlsrud (1985) used a theoretical viscous flow model to analyse submarine and subaerial quick clay slides for which velocity data was available. The scale of these slides varied greatly, from small coastal slides up to large slides with runout distances of up to 700km and flow velocities up to 25m/s. These models worked well with the observed data, indicating “soil flow may be an important factor in the runout of very large and rapidly moving submarine slides”. However, what these models

fail to address are the questions involved with the development of flow geometry and suggests examining existing submarine slide deposits more thoroughly.

Bjerrum (1971) dealt with six failures that occurred in Norway between 1930 and 1952. This paper lists the observations made during and after these slides and attempts to interpret them. He proposed a model explaining why these slides can reach such large dimensions. Bjerrum explains that due to the complete loss in strength, after a shear failure, “the slide assumes the nature of a viscous liquid”. This effectively complements Bjerrum’s previous paper describing liquefaction. As a result of the failure, the slide scar is left behind and this may undergo retrogressive propagation, due to the disappearing slide masses, leaving the scar unsupported. Another factor involved in the magnitude of these slides is that since these slides occur in fine sand and coarse silt, this material is very susceptible to erosion. In contrast to most onshore material, these sediments lack the vegetation, which helps to anchor the topsoil. This leads to the formation of channels and canyons, undermining any obstacles and leaving more slide scars and the opportunity for more retrogressive slides.

An example quoted by Locat (2001), which is that of the Grand Banks Slide of 1929 (Figure 4.3), is an interesting case. This covered a distance of over 1000km over twelve hours and also generating a tsunami. This was also a good example of how these marine movements are not composed of one type of failure. Here an earthquake triggered a submarine slide which then went on to generate a debris flow which then turned into a turbidity current and eventually caused a tsunami. Leroueil et al. (1996) used a number of stages to describe failures. The pre-failure stage, the failure stage and the post-failure stages are all represented in the above example. The fourth stage, which is not

represented, is the reactivation stage, which relates to further events on the failed mass or pre-existing failure planes. In stages 1 and 2 the differences between onshore and offshore failures are minimal, with soil or rock mechanics dictating the behaviour of the material.

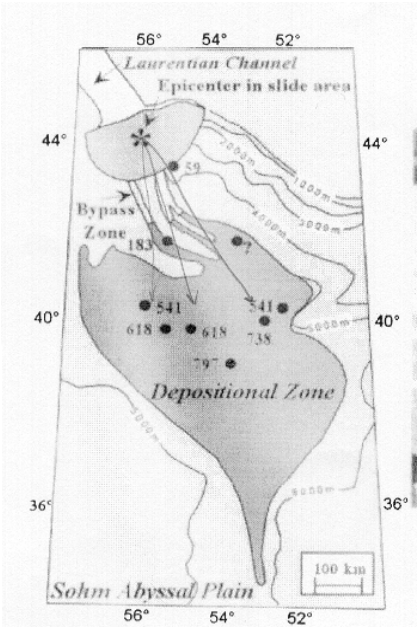

Figure 4.3: The Grand

Banks Slide, 1929 (Locat, 2001)

However, the third stage is substantially different with the behaviour of the failed body subscribing more to fluid mechanics principles. Locat (2001) mentions the use of sonar and swath mapping systems such as GLORIA and TOBI methods to be among the most useful tools in the analysis of geomorphological features on the sea floor. With both of these methods integrated with seismic surveys, an excellent picture of sea floor morphology can be obtained. Seismics especially prove invaluable in the analysis of shallow sediments (i.e. around the first 100m beneath seabed) and sonar itself can give an indication of even shallower material (up to 3m). Locat (2001) mentions the need for a

seismic system with a resolution of 10cm in the first 100m. However, all of these methods discussed so far are non-invasive, observational methods. When it comes to sampling these materials a whole set of problems are encountered that are not experienced in land-based operations. The majority of the scientific community uses 50-year-old coring technologies, and only box core type samples meet the quality requirements required by a standard study on land. Another of Locat's suggestions is to use the liquidity index of a sediment as a good parameter, which can help predict the undisturbed intact strength, or the rheological properties of clayey material involved in post failure stages of mass movement. The liquidity index (I_L) of a soil can be defined as:

$$I_L = (w_n - w_p)/(w_L - w_p),$$

where w_n is the natural water content, w_L and w_p are the liquid and plastic limits respectively. Coupling this alongside shear strength parameters of reconstituted sediments shows good agreement with measurements of the liquidity index. The remainder of this paper deals with the modelling of the post failure stages and risk and hazard assessment.

Nadim et al. (1997) examined the triggers for such slides particularly slides on relatively shallow slopes. They quoted figures for the inclination of such slopes of the order of 0.5^o up to $50\text{-}60^o$. They suggested that the critical angle depends "mainly on the properties of the sediment and the magnitude of the release factor". This paper summarized the three prerequisites for a slide to occur;

1) Topography favourable for slide activity.

2) Necessary amounts of sediments, which can be brought into a state of low shear strength.

3) Release mechanisms that temporarily reduce the stability of the sediments.

All three have to be present if a slide is to occur. Some of the most important release mechanisms are then construction activity, earthquakes, rapid sedimentation, blasting, sudden impact of soft sediments, erosion at critical sections due to currents and seepage of groundwater.

4.2: Previous Geological and Geotechnical Studies

Bryn et al (1998) attempts to lay down guidelines to slope stability investigations offshore. With little specific data previously recorded, the group started with a high resolution seismic survey and swath bathymetry data acquired in 1996/97 as part of the Seabed Project. The 'Seabed Project' was a joint project set up by 7 operators to assess the safety and feasibility of exploration activities and field developments around the Mid-Norwegian continental slope. Since earlier borings in this area were of a general nature with a focus on geological investigation, no in situ geotechnical tests were performed. This meant that any strength or deformation properties, which were determined, were not representative of undisturbed conditions. In the successive phases, four deep geotechnical borings were performed. These ranged from 106m to 310m in depth. Sediment sampling and cone penetration tests (CPTs) were performed at intervals. Vertical seismic profiling (VSP) and slimline logging were also carried out. Gravity cores were acquired mainly for site-specific investigations. The paper described some features present in the area such as slide scars and sediments (identified from both Towed Ocean Bottom Instrument, (a long range sidescan sonar combined with pinger (TOBI)) and ROV methods), diapirism (from high-resolution seismics) and BSRs (bottom simulating reflectors) (again from high-

resolution seismics). A diapir is an upward directed domelike intrusion of a lighter mass into a denser cover. In this case this could be sediment containing gas hydrates. BSRs represent possible gas hydrate bearing sediments where the BSR represents the base of the stable gas hydrates. Both of these last features can be potential triggers for the slides. In the example mentioned in this paper, the BSR is found at the same level as the shear surface for the slide but does not continue into the slide body. Along with BSRs, other features representing gas escape features are usually found, consisting of chimneys and vents, in the same sections. All of these features showed up on the northern flank of the Storegga Slide. One boring was planned to penetrate the BSR but no indications of gas hydrates or free gas were found and only a slight increase in gas in the pore water was documented below the BSR level. They then described some of the other major features around the slides, such as overconsolidated tills/debris flow deposits and seabed grooves.

The paper by Silva et al. (1999) deals with a project similar to this thesis and involved research in the Gulf of Mexico. That project was part of a longer five-year programme and the objective of was to investigate, understand and predict seabed processes on the continental slope in the northwest Gulf of Mexico, using an integrated geological and geotechnical approach. Water depths ranged from 800m to 2700m; with sediments (recovered by a large diameter gravity piston corer) mainly being laminated soft sediments. In situ shear strength and pore pressure measurements were taken. Further testing was carried out on board the research ship, generally within two days after retrieval of the samples. Tests included vane shear tests at selected intervals, density/water content sampling, triaxial consolidation and permeability testing. One of the main outcomes from this, however, is the usefulness of in situ testing such as vane

shear measurements and pore pressure measurements. Also to be noted is the fact that bulk density can be a very useful parameter in the study of marine sediments. It can be related to porosity and water content, and is also indicative of grain size and the degree of consolidation. For example, Silva et al. stated “Surficial sediment with bulk densities of 1.25to 1.45g/cm^3 are usually composed of clays. The addition of silt and sand raises the density as does the consolidation process” Therefore sediments with high bulk densities could contain sands and/or have undergone overconsolidation.

Silva et al, (2000) took four geotechnical stratigraphic units within part of the area of their 1999 paper and compared the plateau material with the low-lying basinal material. From these samples it was seen that the area suffered from slope failures in the past. Looking at the overconsolidation ratios from the basinal samples it was shown that possibly 8-12m of material was removed prior to the deposition of the current layer of overburden. It was concluded that the plateau regions were normally consolidated, with some underconsolidation observed. Samples underwent consolidation testing along with triaxial testing according to ASTM D 2435 and ASTM D 4767 respectively. In order to ascertain the quality of the samples gathered, large diameter gravity cores were taken at the sites where jumbo piston cores were taken. This was to make sure no core shortening or core-lengthening effects were present. As well as this, visual inspections were carried out on split cores and x-ray radiographs of the cores were also taken. This was to attempt to quantify the amount of sample disturbance, which was present. The paper then also compared and contrasted the stress history of the plateau sediments (which had a slope of approx. 1^o) to that of the basinal sediments (which had slope angles greater than 20^o).

Locat (2001) attempted to set down and describe the procedures, which could be useful in attempting to combine both a geological and geotechnical approach to offshore slope stability investigations as described in this section. He described the various triggers of offshore slope failures. Factors including plate tectonics and gas hydrate phase changes are mentioned, and landslide masses or scars evidenced the resulting instabilities. One of the main questions to be asked about these features is whether or not the processes involved with the previous failure are still at work. For example, the authors asked, if the initial trigger was an overloading of the slope due to increased deposition, is this increased rate of deposition still present? If this is the case, then it is a matter of time before the slope becomes overloaded again and another failure occurs. In this case the factor of safety (FOS) is considerably close to one. If on the other hand, sedimentation rate has reduced, the threat of further failure is reduced, as the slope, through failure, has reachieved an equilibrium state and so it's FOS is increased accordingly. Another difference to be accounted for between land and offshore slope failures is the fact that marine instabilities in general always contain more material than land-based instabilities. Not only this but also that they can cover a greater distance and area.

With the recent discovery of the Ormen Lange gas field in 1997, a large amount of study has taken place around the Storegga Slide area. This is described in T. Tjelta et al. (2002). The Ormen Lange gas field lies beneath the slide scar of the Storegga slide. The slide in question is found off the coast of Norway and involved 500m of sediment being removed approximately 8200 years ago. The study involved geological and geotechnical boreholes, or "geoborings", to several hundred meters below the seabed.

Water depths in the area range from 250m to 1630m. A high-resolution seismic survey of the area was also undertaken. The boreholes themselves targeted seismic units and horizons and a number of tests, both in situ and onshore were carried out. They also sampled regionally extensive strata in order to try and estimate the regional history along with the possibility of producing a model for estimating normalised in situ strength parameters for the area. Due to the presence of stones and boulders, various drill bits were used but this led to sample disturbance. In order to counteract this, all onshore testing was carried out on trimmed samples. The trimming was of the nature of only using $10cm^2$ out of a $40cm^2$ sample. One of the more innovative steps was to install piezometers on the seabed in order to continuously monitor in situ pore pressures. The two main methods for determining in situ pore pressures are by direct methods via piezometers or else via estimates prepared from a penetrometer dissipation test. The latter method is performed using CPT type equipment and is connected to the drilling equipment. Since the piezometers measure the pore pressure directly, it is a preferable and more reliable source of results. However, the dissipation test is relatively quicker, where the excess pore pressure observed during installation is observed to decrease towards a residual pressure level. However, a number of factors have to be taken into account in this case: The quality of the installation itself, the amount of time allowed (extent of dissipation permitted), and the amount of disturbance in the pore pressure field. In essence the problem may be that the residual pressure observed in the dissipation test may be a transitory state in a longer process around the borehole. From the piezometer data presented by Tjelta et al. (2002), it seems to suggest that a timescale of a number of days is required to reach stable pressures. While onshore it is possible to wait, in an

offshore setting it is more problematic due to the operational constraints of the vessel and the cost of the tests. This was done in order to prove one of the major assumptions with these studies, which is that the pore pressure is hydrostatic. However, because the Storegga Slide was initiated on a shallow slope and the last glaciation had a very high sedimentation rate, this had to be clarified. By using these “permanent” piezometers it was hoped to capture seasonal effects or long-term trends in pore pressure development. Since dissipation was slow in the area studied, piezometers were the most reliable source of pore pressure data. The assumption that pore pressures are hydrostatic is according to Tjelta et al. (2002) “a potentially erroneous and unconservative assumption”.

Further papers looked at during the course of this project include an important and informative paper “Comparison of Laser Grain Size Analysis with Pipette and Sieve Analysis: A Solution for the Underestimated Clay Fraction”, Konert et al (1997). Two almost identical samples were taken for grain size analysis, one of which was measured using laser sizing, while the other was measured using the sieve and hydrometer method. The disparity found could be explained by what was found in this paper with the laser-sized results coming out as slightly coarser than the sieving and sedimentation methods. This is due to the non-sphericity of clay particles.

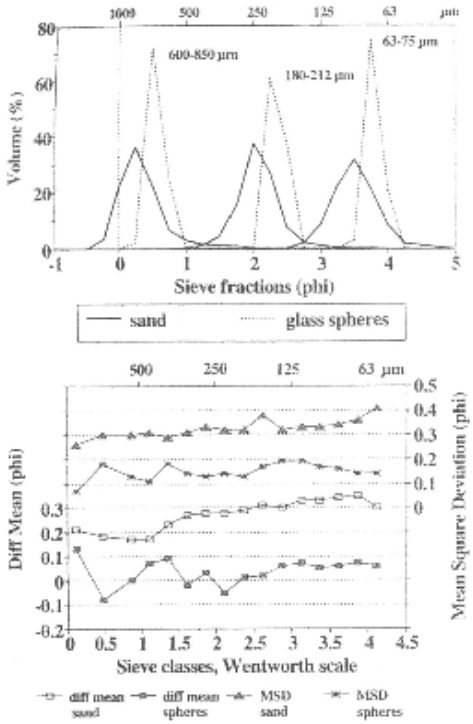

Fig 4.4 – Contrast between differences between spherical objects and sand grains. The top figure uses laser measurements, while the bottom uses traditional sieving methods and plots the deviation between both.

Chapter 5. Sites: Introduction

The main structural evolution of the Rockall Trough occurred due to continental rifting from the late Palaeozoic to early Cenozoic periods. Extensional activity along with some subsidence and inversion during the Mesozoic and Cenozoic periods led to extreme crustal thinning. Eventual continental break-up occurred between the Rockall Plateau and Greenland where seafloor spreading during Palaeogene times led to the formation of the Northeast Atlantic. The most recent period of tectonic activity here was the regional uplift of the British Isles and Scandinavia during the Neogene. After this period of uplift a period of subsidence outpacing sedimentation was observed (Shannon et al. 1994, 1999).

The post break-up period occurred during the early Neogene and at this time the North Atlantic area experienced deepwater circulation and drift sedimentation. Changing climate conditions and sea-level fluctuations influenced the onset of the late Palaeogene, early Neogene Antarctic Glaciation and also the late Neogene-Quaternary Arctic glaciation. In northwest Europe the first evidence of major cooling is seen at the base of the Pleistocene. Late Quaternary advances have been recorded as far westward as the Hebrides Shelf and the northeast Rockall Trough. The area referred to in this thesis could be therefore placed within the glaciated area covering the west of Ireland.

The samples used in this project (and 99/01) were obtained during a shallow drilling programme site survey from the 18th to 28th June 1998 onboard the RTS

Challenger. 45 cores were collected along with geophysical surveying. The samples taken were 87.5mm in diameter and were recovered with a 3m gravity core sampler. Sampling locations were recorded to DGPS (~~Digital~~ Differential Global Positioning System) accuracy. The cores were placed in a polycarbonate liner, which was cut to lengths not less than 0.75m and not more than 1m. If there was a discrepancy between the size of the sample and the length of the liner tube wax was placed to minimise sample disturbance as far as was practical. The sites which were chosen were areas targeted for deeper drilling, with some isolated cores acquired on seabed features identified on the basis of the sonar work (see Table 5.1).

Site	Block No.	Latitude	Longitude
1	83/24	52°14' N	15°16' W
1A	83/20	52°26' N	15°06' W
2	16/28	54°01' N	13°13' W
3	11/20	55°25' N	10°07' W
3A	11/20	55°25' N	10°02' W

Table 5.1: Site Terminology

The Rockall Trough is part of a chain of Palaeozoic-Cenozoic sedimentary basins extending from Norway to Ireland along the North Atlantic Seaboard, stretching from the Porcupine Abyssal Plain in the southwest to the Wyville-Thomson Ridge in the northeast. Depths range from 4500m in the southwest to 1250m in the northeast. The steepest slopes are found in the southeast with dips of up to 20°. The average slope is around 6°. This area is highly important to the exchange of water masses between the Nordic seas and the North Atlantic.

~~The main structural evolution of the Rockall Trough occurred due to continental rifting from the late Palaeozoic to early Cenozoic periods. Extensional activity along with~~

some subsidence and inversion during the Mesozoic and Cenozoic periods led to extreme crustal thinning. Eventual continental break-up occurred between the Rockall Plateau and Greenland where seafloor spreading during Palaeogene times led to the formation of the Northeast Atlantic. The most recent period of tectonic activity here was the regional uplift of the British Isles and Scandinavia during the Neogene. After this period of uplift a period of subsidence outpacing sedimentation was observed (Shannon et al. 1994, 1999).

The post break-up period occurred during the early Neogene and at this time the North Atlantic area experienced deepwater circulation and drift sedimentation. Changing climate conditions and sea-level fluctuations influenced the onset of the late Palaeogene, early Neogene Antarctic Glaciation and also the late Neogene-Quaternary Arctic glaciation. In northwest Europe the first evidence of major cooling is seen at the base of the Pleistocene. Late Quaternary advances have been recorded as far westward as the Hebrides Shelf and the northeast Rockall Trough. The area referred to in this thesis could be therefore placed within the glaciated area covering the west of Ireland.

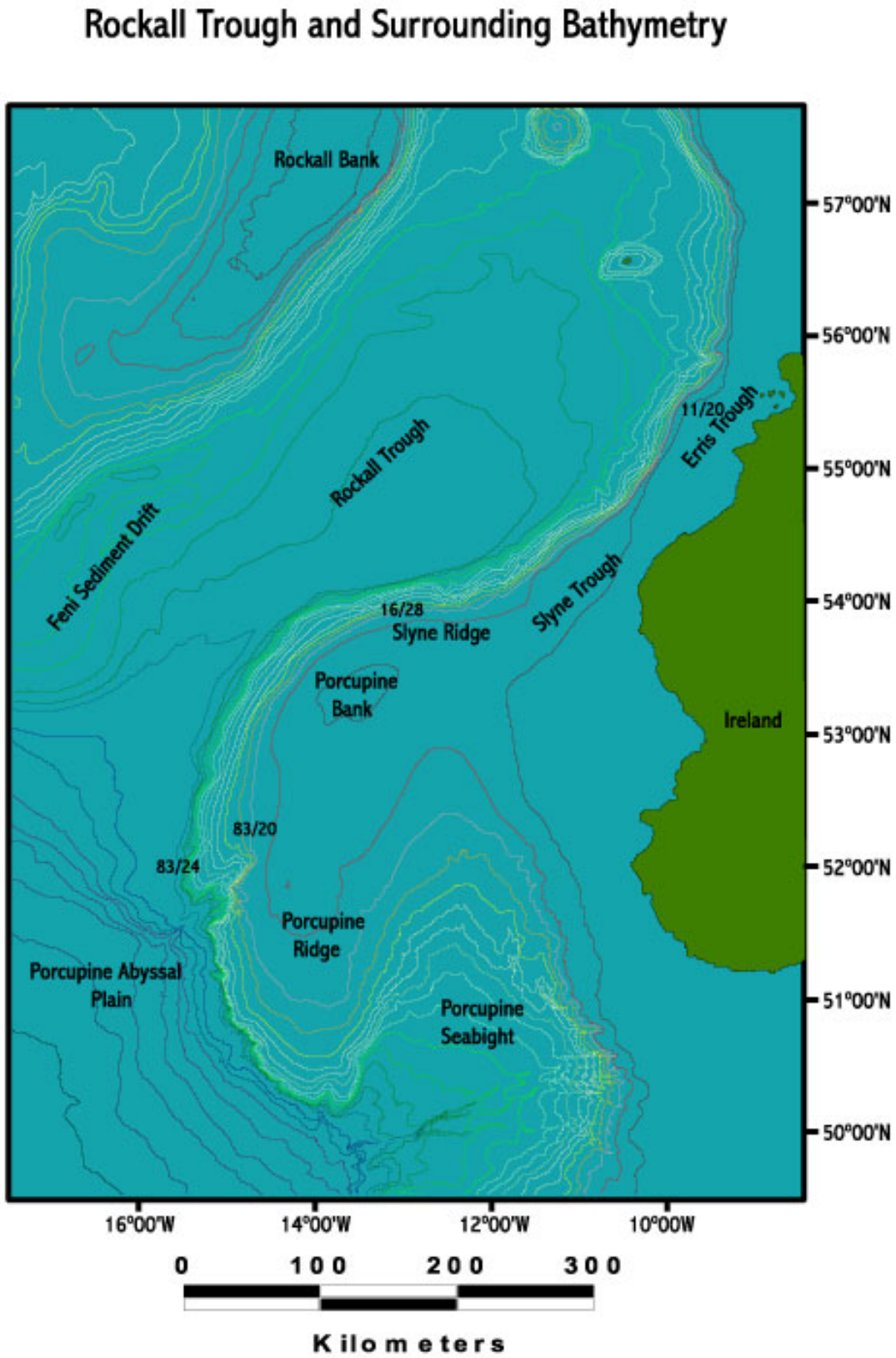

Figure 5.1 Bathymetric map of the Rockall Trough showing the location of the coring sites. The sites are labelled with the target names. Modified from Praeg and Shannon (2001).

5.1 Site 1($52^0$14'N, $15^0$16'W): Block 83/24

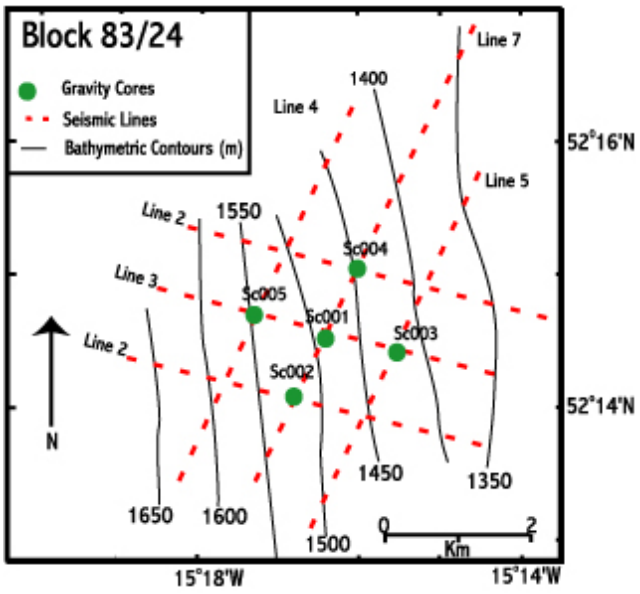

Figure 5.2: 83/24 map. Modified from Praeg and Shannon (2000), along with sample core (scale: 1m) from Site 1 (83/24-Sc001 Box 1).

This site is situated on the western side of a canyon complex, which itself lies on the western flank of the Porcupine Ridge (See Fig. 5.1/5.2). Samples were recovered from a maximum depth of 2.55m. These samples were taken from a layer of Plio-Pleistocene material, which is estimated to be approximately 10m thick from the seismic data illustrated in Figure 5.4. The lowest unit found consists of a brown sandy clay with some thick (~1cm) white bands present (See Figure 5.3). These were hypothesized to be possibly bioclastic (of biological origin, i.e. shell or fossil fragments) clays (L. Øvrebø, personal communication, 2001). Overlying this unit was found an upcoarsening sequence of clay, going into bioclastic sands. The rest of the area seems to be composed of these clayey bioclastic sands, with some bioturbation (disturbance by biological organisms). The changes observed in the sediments can be explained by changing climatic factors, such as deposition rates changing during glacial and periglacial periods. The material was probably deposited by fallout from melting icebergs. The slope around Site 1 was observed to be 3.5^{o}.

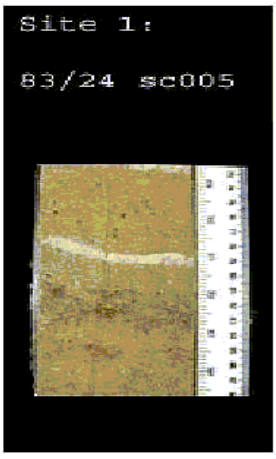

Figure 5.3: Possible Coccolith Clay band present in sample.

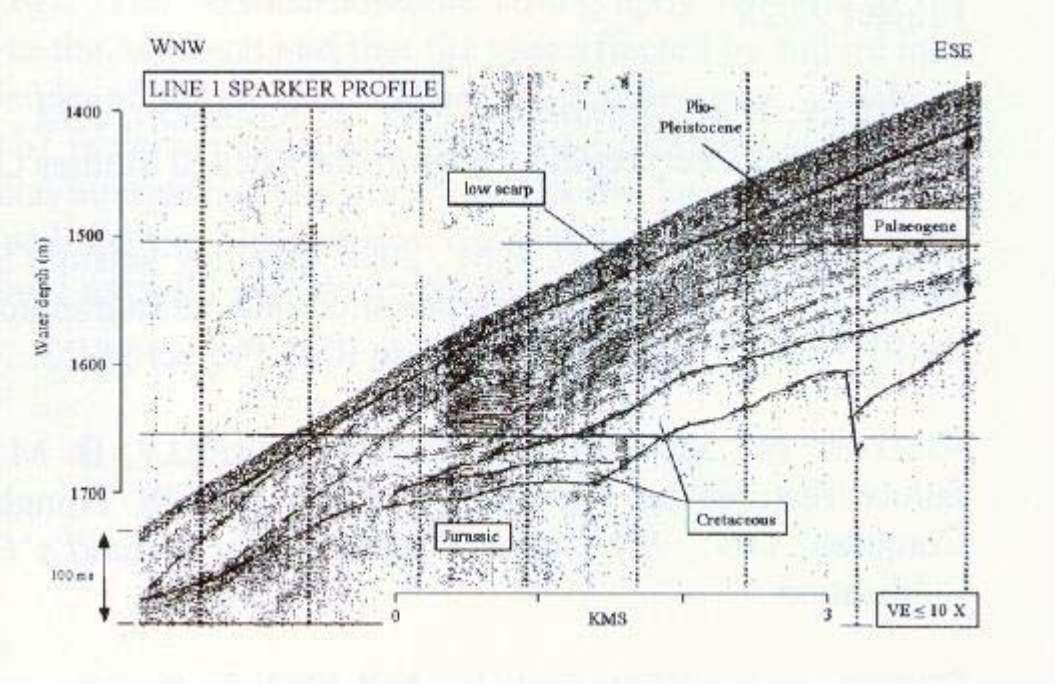

Figure 5.4: Sparker profile showing down slope thinning across a low scarp. Gravity core 83/24-Sc002 lies in the middle of this section. (Praeg and Shannon 2000.)

5.2 Site 1A ($52^0$26'N, $15^0$06'W): Block 83/20

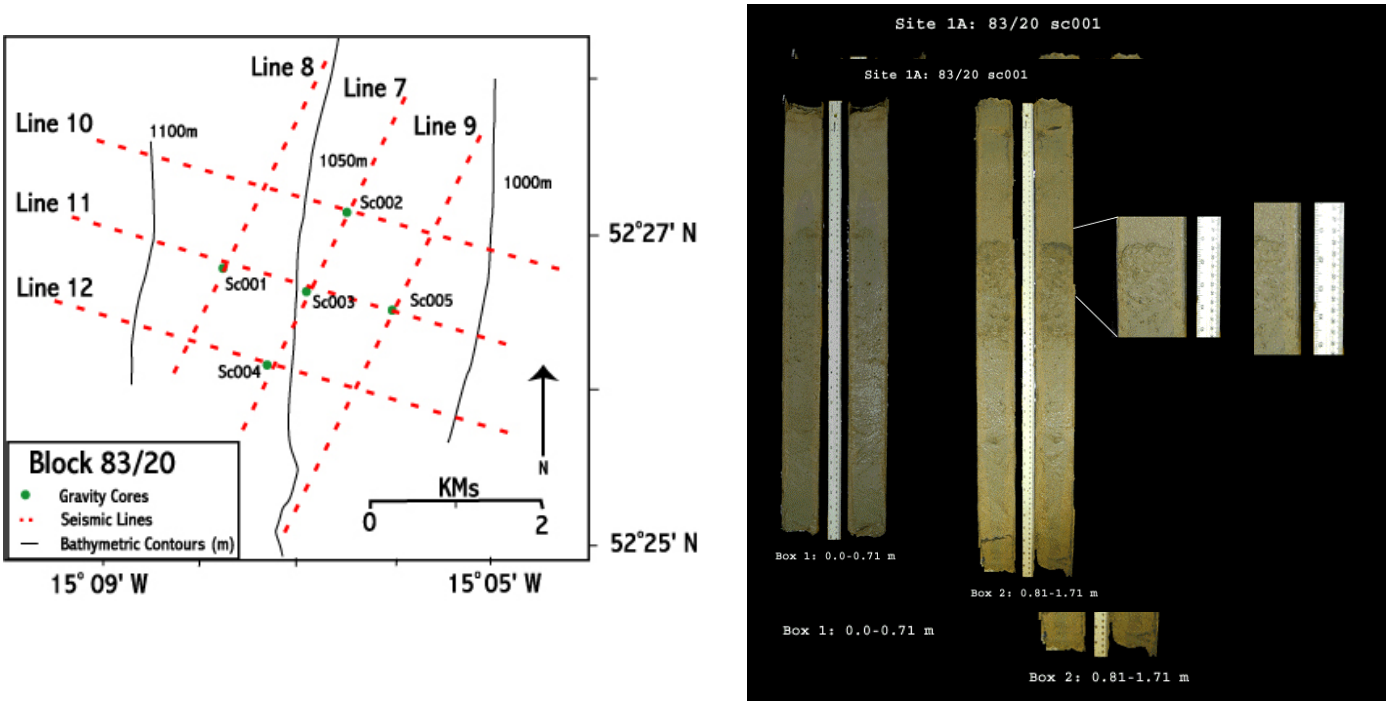

Figure 5.5: 83/20 map. Modified from Praeg and Shannon (2000), along with a sample core (scale 1m) from Site 1A (83/20-Sc001 Box1)

This site is situated upslope to the north-northeast of Site 1 (see Fig. 5.1/5.5). This area exhibits a negligible sea floor slope. Again the samples here were taken from the Plio-Pleistocene layer, which is thought to be approximately 10m thick in the area. It can be seen to be extensive across the area in the seismic profile of the area (See Fig. 5.6). The stratigraphy of this area is very similar to Site 1 with clayey bioclastic sand passing into sandy clay. Two upward fining sequences were observed, but it is uncertain if these represent mass flow events. Again it is interpreted that this succession represents changing deposition rates due to glaciation and the retreat of the glaciers. Another notable fact is that these cores, while very similar to Site 1, contain small spicules, rod shaped fragments of glass sponges, which are otherwise not recorded in Site 1.

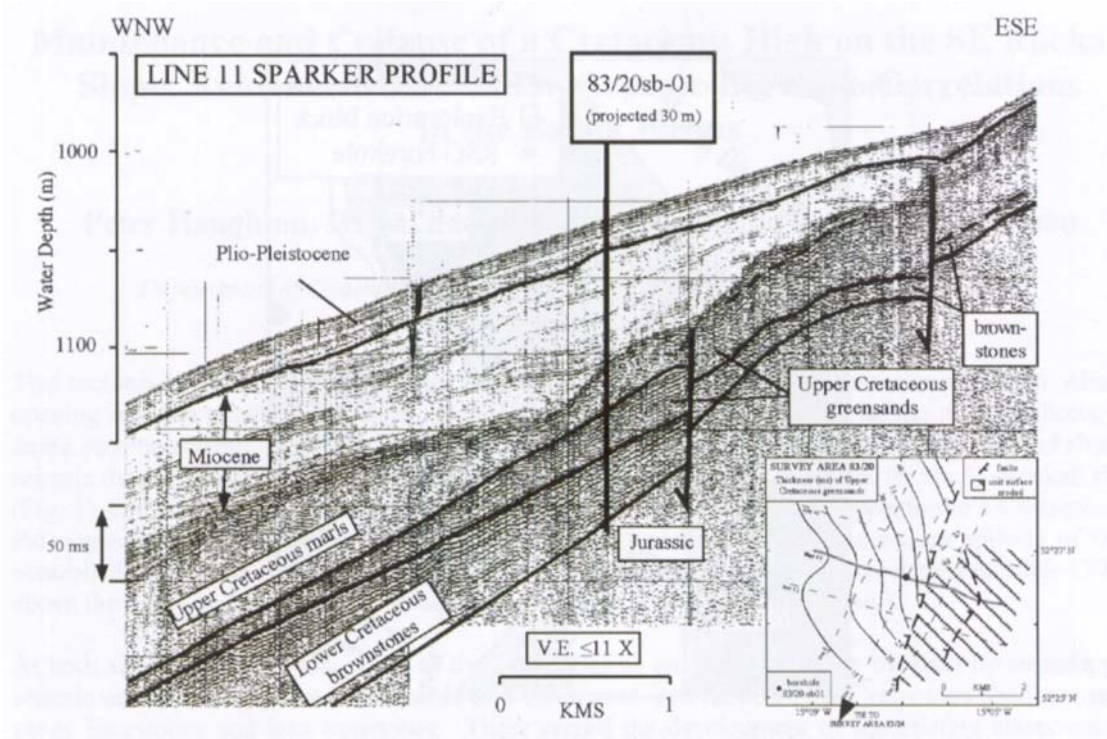

Figure 5.6: Sparker profile across the 83/20 survey area. Borehole 83/20-Sb02 corresponds to gravity core 83/20-Sc003. (Praeg and Shannon 2000.)

5.3 Site 2 ($54^0$01'N, $13^0$13'W): Block 16/28

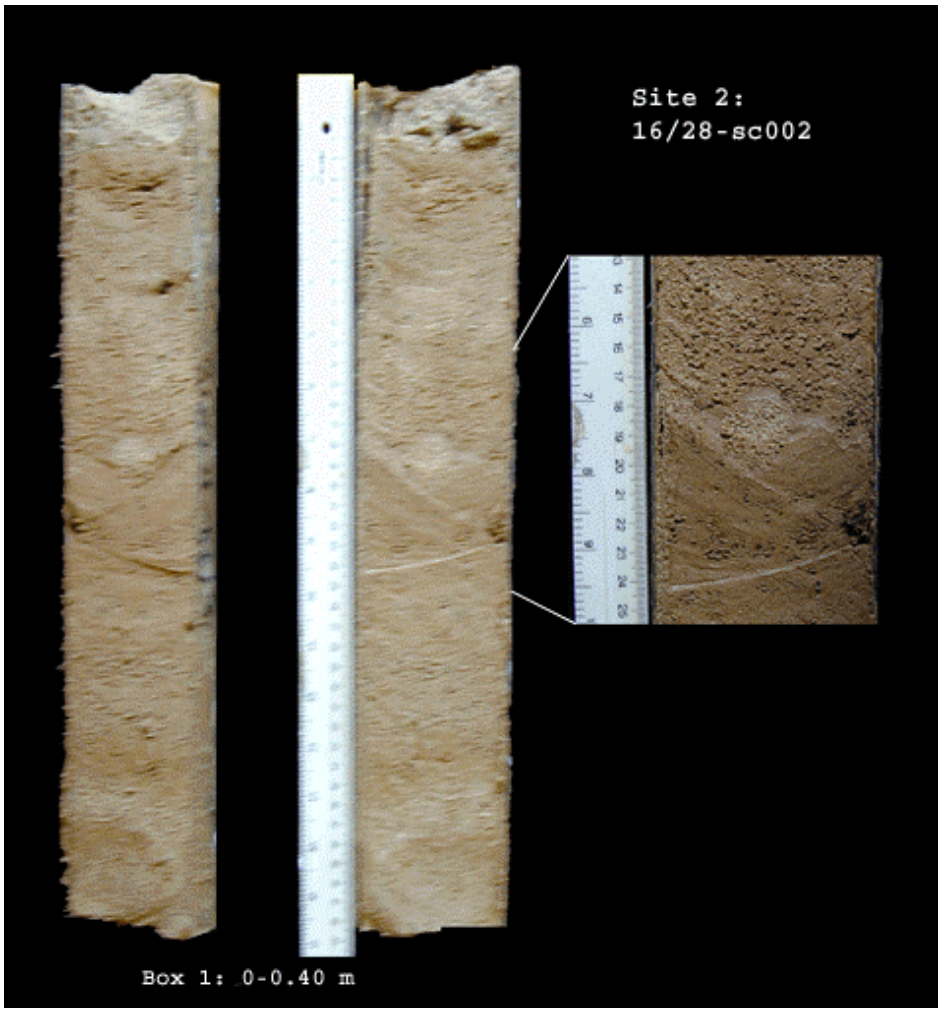

Figure 5.7: Sample Core from Site 2 (16/28-Sc002 Box 1)

Unfortunately this site had the least amount of cores available for sampling with only two cores, both under 2m, being recovered. The deepest sample recovered reached 1.3m. It was noted in the borehole logs that this was an area of hard sea floor and had undergone recent slumping. It was also noted to contain muddy sand, forams and rounded lithic fragments. The site is located Northward of Sites 1 and 1A, to the west of Slyne

Ridge (See Fig. 5.1). The cores themselves consist of brown coarse bioclastic sand, fining upwards. However, with only two cores and overall less than 3m of material, not much analysis could be carried out on this site.

5.4 Site 3 and Site 3A ($55^0$25'N, $10^0$07'W, and $55^0$25'N, $10^0$02'W)

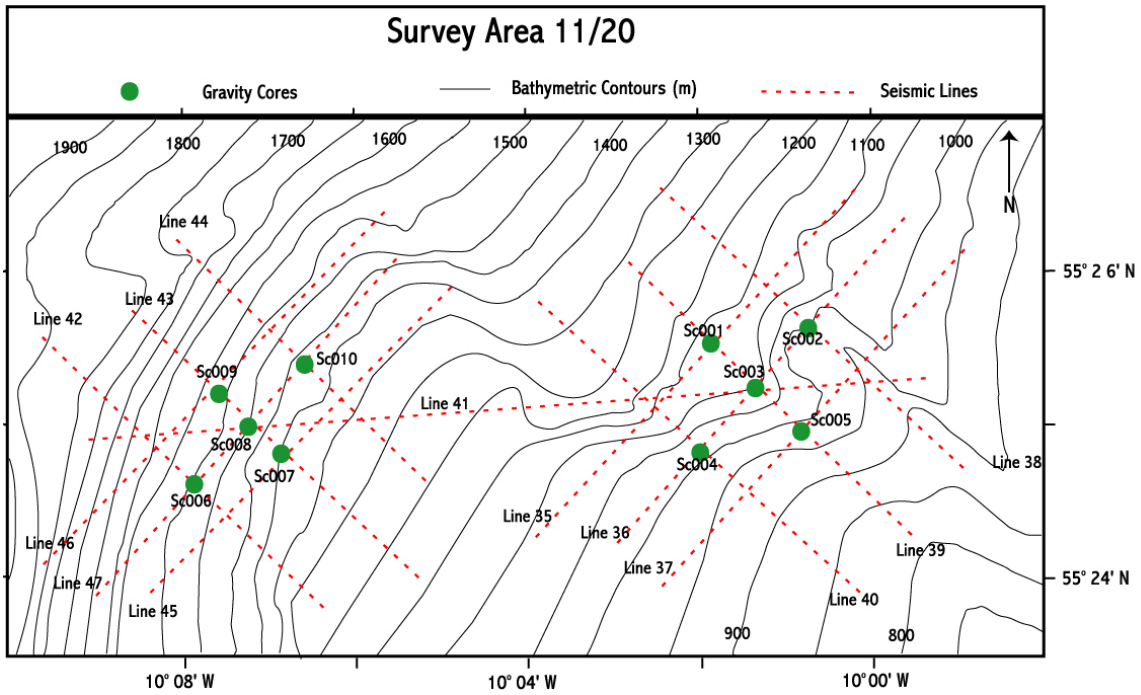

Figure 5.8: 11/20 map. Modified from Praeg and Shannon.

This site (Figure 5.8) provided the most cores and also potentially the simplest stratigraphy at shallow levels. Both sites were found near the Erris Trough. Shannon et al. (2001) used this to illustrate debris flows as observed by TOBI sidescan sonar imaging. Here the area was seen to exhibit some small canyon systems. These networks of canyon systems on the upper slope were seen to describe a cauliform or finger-like pattern. The incised canyons generally exhibited a v-shaped profile. From the TOBI images the aprons and fans resulting from these canyon systems are interpreted to be probable sandy to gravelly flows. However as seen below in the seismic section (Fig. 5.8) this area is possibly the most complex and disturbed site at depth. The material here is highly

disturbed and so it is difficult to determine the thickness of the upper layer of sediment. The cores are taken from slopes of 3.5^{o} at site 3A and 7.5-8^{o} at site 3. The deepest samples recovered from Site 3A were from 2.33m depth and the deepest samples recovered from Site 3 were from 2.42m. Both of these sites showed this simple shallow stratigraphy but as the seismic profile shows, this is not the case at deeper levels, with pockets of Palaeogene material found beneath the upper plio-pleistocene material found at the surface.

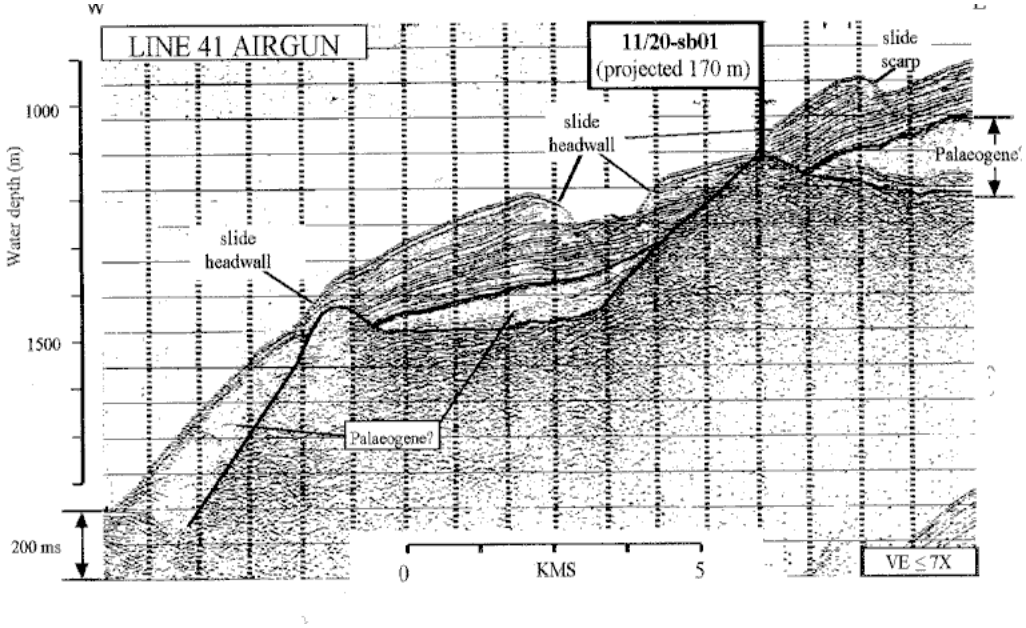

Figure 5.9: Airgun Seismic profile across the 11/20 survey area. Line 41 passes through both Site 3 and Site 3A. Praeg and Shannon 2000.

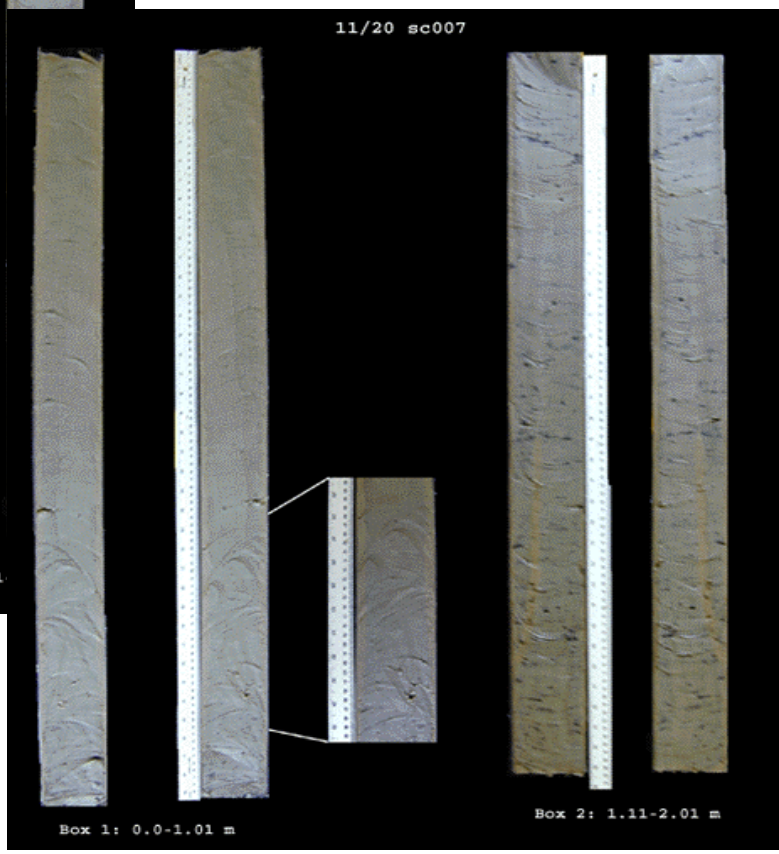

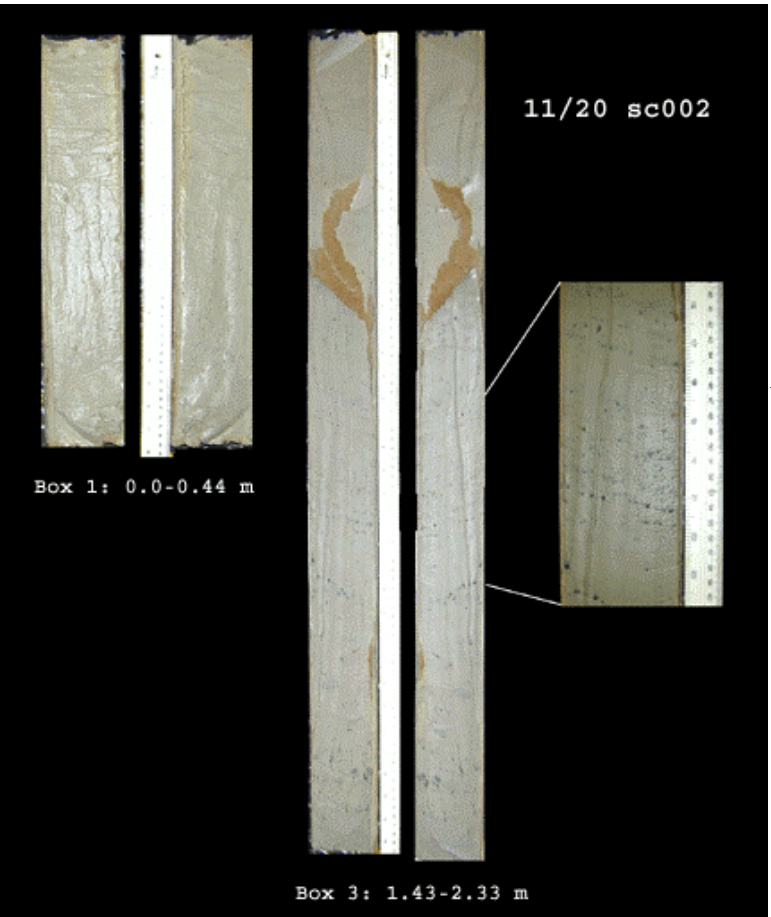

1/20-Sc007 Boxes 1 and 2) and 3A (11/20-

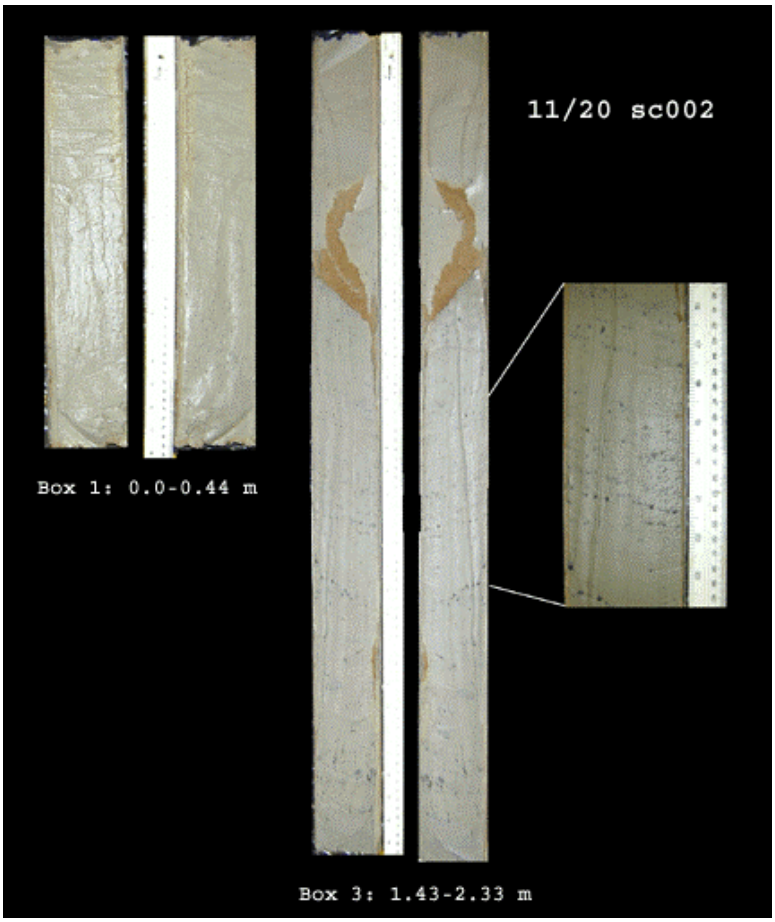

Chapter 6.

Methodology

Samples were selected from the newly opened cores and brought to Earlsfort Terrace for a series of tests to characterise the materials found and also to try and determine their stress history. This section explains how these samples were selected and also the basic characteristic tests performed on these samples.

6.1 Sampling

The samples tested in this thesis were obtained in 1998 using gravity coring techniques. The 45 cores were approximately 2-3m long and divided up into boxes varying in length from 20cm to 1m and had a diameter of 87.5mm. These cores were brought to the Geology Department in U.C.D. Belfield where two opposing longitudinal

grooves were cut with a mechanical saw to a depth of approximately 90% of the thickness of the Perspex casing. A blade was used to manually cut through the remaining Perspex casing along the groove. A guitar string was then drawn through the core dividing it into two halves. A digital camera was then used to take photographs of the split core immediately upon opening. One half of the core was used for sampling and the other half was preserved for reference and logging by Lena Øvrebø (PhD student in Geology). The half core kept for sampling was further divided longitudinally by using glass plates, with half the core reserved for geotechnical sampling and the other half being used for geological sampling. Samples were chosen so as to capture all the key lithologies in each core and spaced so as to avoid sampling over lithological boundaries.

6.2 Testing

A suite of classification tests was carried out on the samples. All tests were carried out according to the guidelines set out in BS1377 (parts 1 and 2).

Moisture contents look at the percentage of water present in a sample with relation to the dry weight of the sample. This is achieved by taking a sample (approx. 20g weight) of the material to be tested, drying it overnight in an oven, taking the weight of the dried sample and dividing the amount of water liberated by the dry weight of the material. Results are presented in the form of a percentage.

Specific gravities give an indication of the density of a sample. This involves determining the volume of a known amount of soil through the use of a small bottle

known as a pyknometer. The bottle is weighed when full of water, and then weighed again with a sample of dried soil and water, made up to the same volume as the bottle full of water. Sample sizes were on average around 10g. Care should be taken to ensure that there is no air trapped in the soil sample as this could lead to smaller values than the true specific gravity of the material. The majority of samples with values of less than 2.4 were observed to have sample sizes greater than 14g implying that trapped air could have been a factor in these lower values.

The plasticity index is the range of moisture contents, between which the material exhibits plastic behaviour. The test itself involves two tests; one to discover the liquid limit (the moisture content above which the material behaves like a liquid) and one to discover the plastic limit (the moisture content below which the material behaves like a brittle solid). The liquid limit is determined through the use of a falling cone penetrometer. The sample is prepared to a known moisture content and tested once. The penetration values should fall between 15 and 25mm. A number of tests are performed with moisture contents varied so as to give a spread of at least four results over the expected range. These are then graphed as penetration versus moisture content and the liquid limit is said to be the moisture content, which would give a penetration of 20mm. The plastic limit test is slightly more subjective as it involves rolling lengths of the sample into cylinders of approximately 1mm in diameter. This continues until the material cannot be rolled in this fashion and simply breaks up. This is known as the plastic limit. The plasticity Index is then determined by subtracting the plastic limit from the liquid limit.

Grain size analyses were carried out through a combined approach between sieve analyses and the hydrometer method. The sample is initially sieved through a set of sieves ranging from 2mm, down to 0.063mm. All material left which has passed through these sieves is then prepared for the hydrometer test. This determines the grain sizes present by looking at the sedimentation rate of the material in a 1000ml-measuring cylinder. By using a hydrometer and comparing the results between a control and the sample these sedimentation rates can be determined and grain sizes applied.

Chapter 7. Classification Tests Results

Samples were taken from Plio-Pleistocene material, which in general has an average thickness of approximately 10m (inferred from high-resolution seismic profiles of the areas (~~Ref~~Shannon and Praeg, 2000~~?~~)). This varies from site to site but from the high-resolution seismic profiles it can be assumed that the samples are all part of this layer. The results from the testing of these samples are presented here in a site-by-site format and later on the results from these samples shall be presented based on their lithologies. Also included here are the results of the previous investigation of some of these areas by JBA Ltd., UCD and TCD. These are referred to as “preliminary results”.

These results include moisture contents, specific gravities, plasticity indices and grain size analyses. All tests were performed according to the specifications outlined in BS1377 (Parts 1&2).

7.1 Site 1 (83/24)

In Site 1 (see Figure 5.2), where carbonate rich sandy silts, sandy silts, foraminiferal silt and another sandy silt unit were recorded, moisture contents range from 65% up to 73% with a basic trend of decreasing values with increasing depth, with the greatest variation of values found within the upper 1m (see Fig. 7.1). There is no obvious trend with regards to soil type apart from a general trend of decreasing values with depth. Moisture contents from the Preliminary Geotechnical Assessment carried out by UCD, TCD and JBA Ltd. (Project Number 98/20) have values ranging from 37% to 75%. The low value of 37% is an isolated, possibly erroneous, reading with the next sample being seen at approximately 55%.

Specific gravities show a trend where the values increase, corresponding to increasing depth. Values range from 2.25mg/m^3 up to 2.70 mg/m^3. This corresponds to values for a non-organic siliceous soil (2.65 mg/m^3), which agrees with geological results (Øvrebø, personal communication, 2001). The value of 2.25 mg/m^3 is an isolated point as can be seen from Fig. 7.1, with the rest of the samples giving readings between 2.43 mg/m^3 and 2.70 mg/m^3. This data point is also from a much shallower depth than the samples tested in the preliminary report. The readings from the preliminary study varied between 2.41 mg/m^3 and 2.60 mg/m^3.

Particle size data shows that the sample tested was a coarse SILT/fine SAND and the curve can be placed within the curves describing material susceptible to

liquefaction according to Andresen and Bjerrum (1968). The preliminary study described the material as a sandy CLAY or SILT. A comparison between using the hydrometer method for particle sizing as described in BS1377: 1990 and laser grain sizing was also carried out. This produced discrepancies, which could be attributed to the factors mentioned in section 4.5 (Konert and Van den Bergher (1997)). As can be seen in Fig. 7.1 there is a smoother, more gradual and coarser curve to be seen in the laser-sizing curve.

Plasticity indices also increase with depth. Results ranged from 28% up to 36%. Plastic limits varied from 23% to 46% with liquid limits reading from 52% to 74%. A good suite of results was found in borehole number 83/24-Sc002. The materials were plotted on a Plasticity Chart and were described as high plasticity materials. Project 98/20 gave two sets of results, one from a depth of 0.65m, the other from a depth of 1.4m. The plastic limit of the shallower sample was 27% and the liquid limit was 39%. The deeper sample was found to be non-plastic, with a liquid limit of 60%. The shallower sample plotted as intermediate plasticity silt on the Plasticity Chart. It should be noted here that the sandy silts group together on one side of the A-line in comparison to the carbonate rich sandy clays, which plot on the other side of the line. The shading in Fig. 6.1 is consistent throughout, i.e. yellow is Carbonate Rich Sandy Silt, green is Sandy Silt, blue is Foraminiferal Silt and red is another, lower Sandy Silt.

Table 7.1: Site 1 Results

** bsl. = Below Sea Level*

Core Number	Box No.	Core Length (m)	Depth bsl.* (m)	Sample No.	Depth (m)	Moisture Content (%)	Specific Gravity	Plasticity Index (%)
83/24-Sc001	1	0.0-0.65	1468	1	0.11-0.265m	71	-	LL, PL, PI
				2	0.38-0.5m	70	-	
	2	0.75-1.57			-	-	-	
83/24-Sc002	1	0.0-0.65	1503	1	0.14-0.22m	73	2.511	74, 46, 28
				2	0.27-0.37m	68	2.602	58, 27, 31
				3	0.475-0.585m	69	2.703	66, 30, 36
	2	0.65-1.55			-	-		
	3	1.65-2.55		4	1.91-1.96m	-		52, 23, 29
83/24-Sc003	1	0.0-0.96	1404	1	0.595-0.855m	69	2.432	
	2	1.06-1.96			-	-		
83/24-Sc004	1	0.0-0.39	1426		-	-		
	2	0.49-1.39			-	-		
83/24-Sc005	1	0.0-0.44	1527	4	0.145-0.165	73	2.254	
				5	0.33-0.41	70	2.554	
	2	0.44-1.34						
	3	1.44-2.34		1	1.57-1.79m	65	2.506	
				2	1.805-1.945m	73	2.506	
				3	2.11-2.22m	65	2.636	

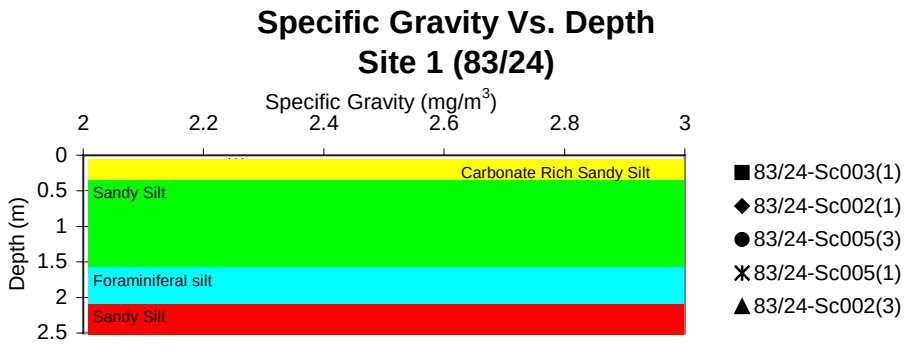

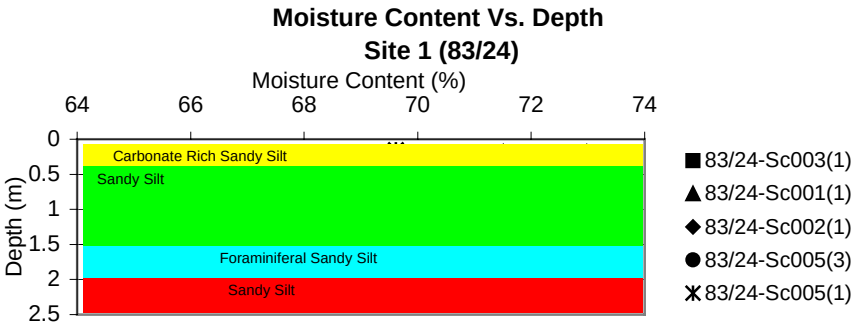

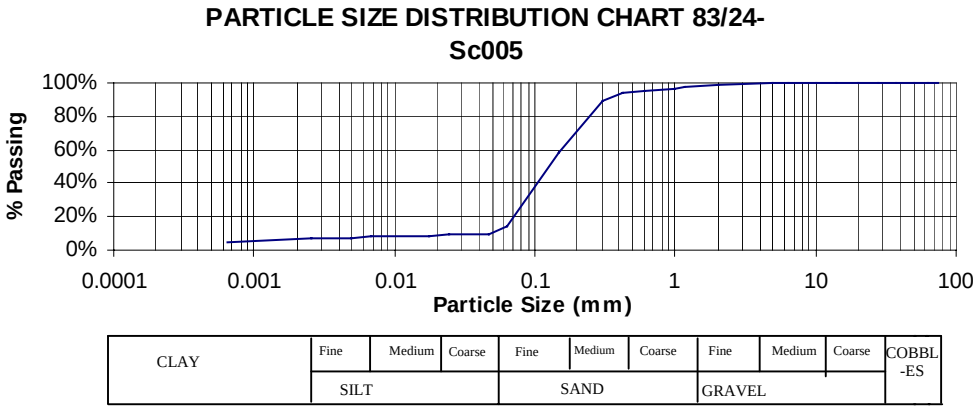

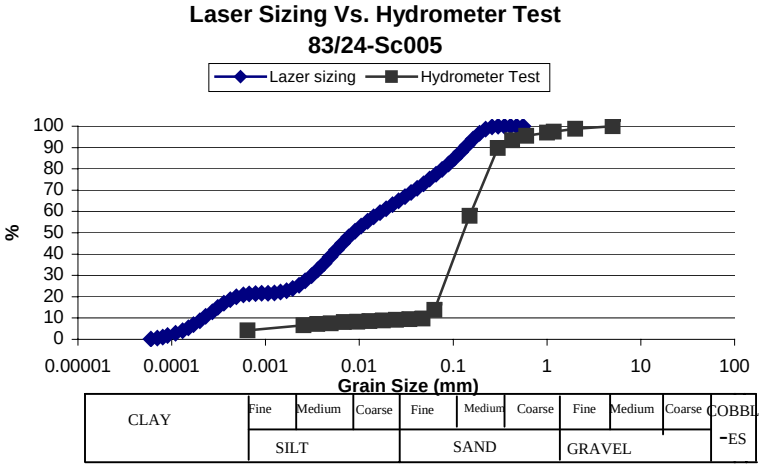

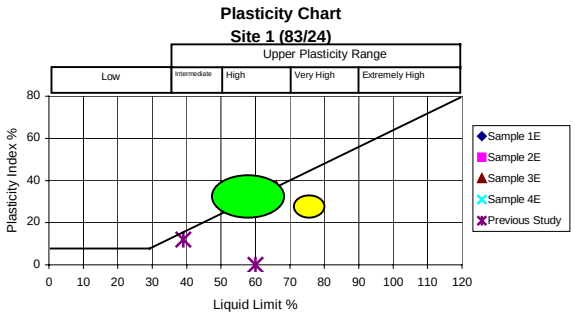

Figure 7.1: Site 1 Results

7.2 Site 1A (83/20)

In this area only 2 types of material were observed: A silt overlying a sandy silt. This area (see Figure 5.3) exhibited moisture contents that were generally much lower than those found in other areas. Values ranging from 21% up to 81% were observed (Figure 6.2 and Table 6.2) with no obvious trend with depth. The preliminary study noted that these samples exhibited high moisture contents, ranging from 51% to 61%. These cores could have undergone drying out and this would account for the lower values observed in this study. Values were seen to decline with depth as was expected. It should be noted, though, that the depths of these samples were not as large as those in the other sites, as they were confined to the upper 1.8m of sediment.

Specific gravities showed a different trend to the readings observed in Site 1 (83/24). Values were seen to decrease with depth in borehole 83/20-Sc001, with very little variation in borehole 83/20-Sc002. Values in this site ranged from 2.29 up to 2.71 (see Figure 6.2). No specific gravity data were obtained in the preliminary study.

Plasticity indices fell within the intermediate to high plasticity range with one sample proving to be non-plastic. Liquid limits were found to have values around 50% ranging from 46% to 52%. Plastic limits were between 23% and 28%. Plasticity indices were between 24% and 26%. These compare relatively well with the previously recorded values. With plastic limits of 23% to 30% and liquid limits from 44% to 74% these gave Plasticity indices of 21-45%. The results from this study plotted on the Plasticity Chart define the material in this area as intermediate to high plasticity clays (CI, CH). The preliminary study shows that the four samples tested in this area can be divided on the basis of their depth, with the upper samples (from 0.9m and 1.1m) giving values lying between 28% and 30% for their plastic limits and 72% and 74% for their liquid limits.

The results from 1.5m to 2.2m show lower values. Plastic limits varied from 23% to 25% with liquid limits also lower, giving 44% and 53%. Again the sandy silts plotted on the upper side of the A-line. Once again the colour of shading follows the pattern from the moisture contents and specific gravities.

Particle size distribution tests on one of the samples yielded a result that this could be classified as a coarse SILT, fine SAND. This again placed this material within the curves specified by Andresen and Van den Bergher (1968) (Section 4.5). This was classified as Silt according to the geological investigation.

Core No.	Box No.	Box Interval (m)	Depth bsl.* (m)	Depth (m)	Sample No.	Moisture Content (%)	Specific Gravity	Plasticity Index (%)
83/20-Sc001	1	0.0-0.71	1060	0.27-0.56	1	81.367	2.428	LL,PL,PI
	2	0.81-1.71		-		47.725	2.293	
83/20-Sc002	1	0.0-0.92	1025	0.48-0.64	1	31.162	2.706	52, 28, 24
	2	1.02-1.92		1.41-1.68	2	20.819	2.698	46, too sandy.
83/20-Sc003	1	0.0-0.40	1032	-		-	-	
	2	0.40-1.30		-		-	-	
	3	1.40-2.30		-		-	-	
83/20-Sc004	1	0.0-1.02	1043	-		-	-	
	2	1.12-2.02		1.305-1.57	1	39.086	-	49, 23, 26
83/20-Sc005	1	0.0-0.28	1007	-		-	-	
	2	0.28-1.06		0.83-1.11	1	32.304	-	
	3	1.16-2.06		-		-	-	

Table 7.2: Results for Site 1A

** bsl. = Below Sea Level*

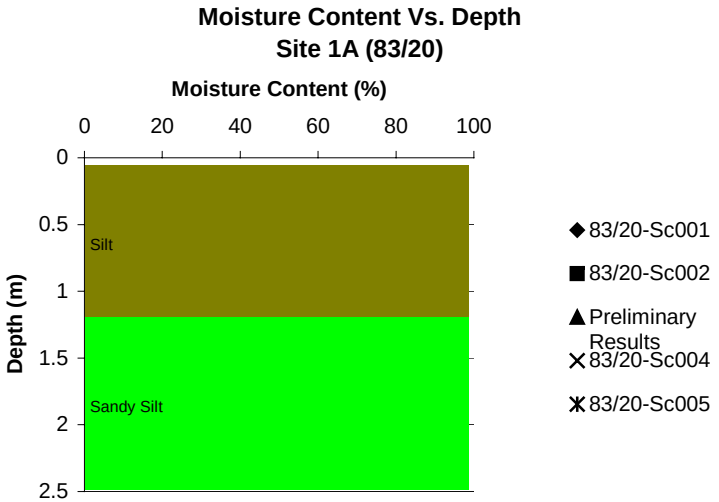

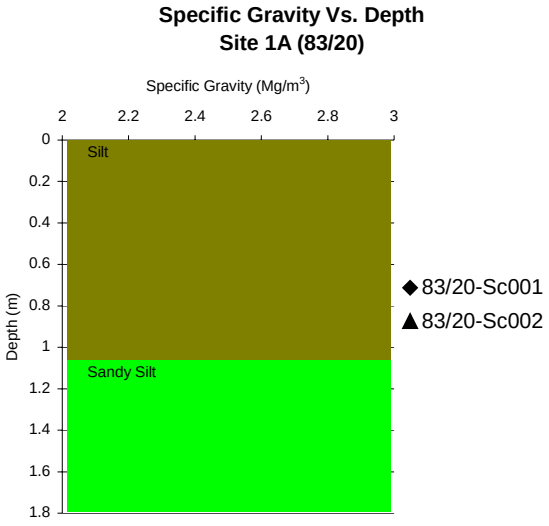

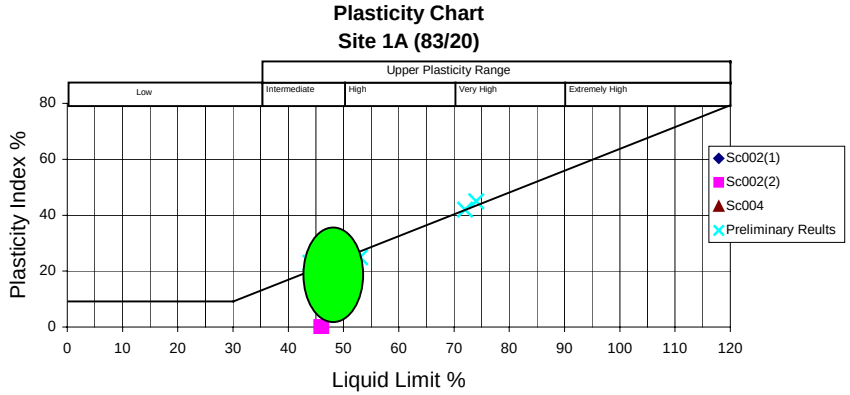

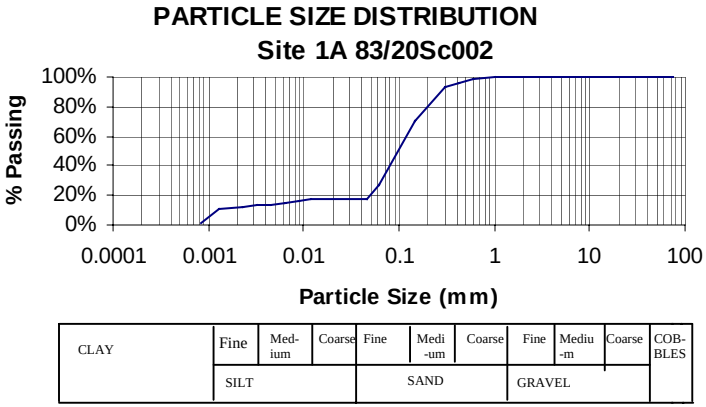

Figure 7.2: Results from Site 1A

7.3 Site 2 (16/28)

Due to the short length of these cores (both measure just over 1m), only a very limited programme of testing was carried out. Here foraminiferal sandy silt overlies sandy silt. Moisture contents here were observed to increase with depth going from 49% to 79% (see Figure 6.3). The preliminary study gave values of 51% to 66%.

Core Number	Box No.	Core Length (m)	Depth bsl.* (m)	Sample No.	Depth (m)	Moisture Content (%)
16/28-Sc001	1	0.0-0.57	1486			
	2	0.57-1.17		1	0.45-0.53m	78
				2	0.615-0.72m	79
16/28-Sc002	1	0.0-0.40	1465	1	0.055-0.18m	49
	2	0.40-1.30				

Table 7.3: Results for Site 2
** bsl. = Below Sea Level*

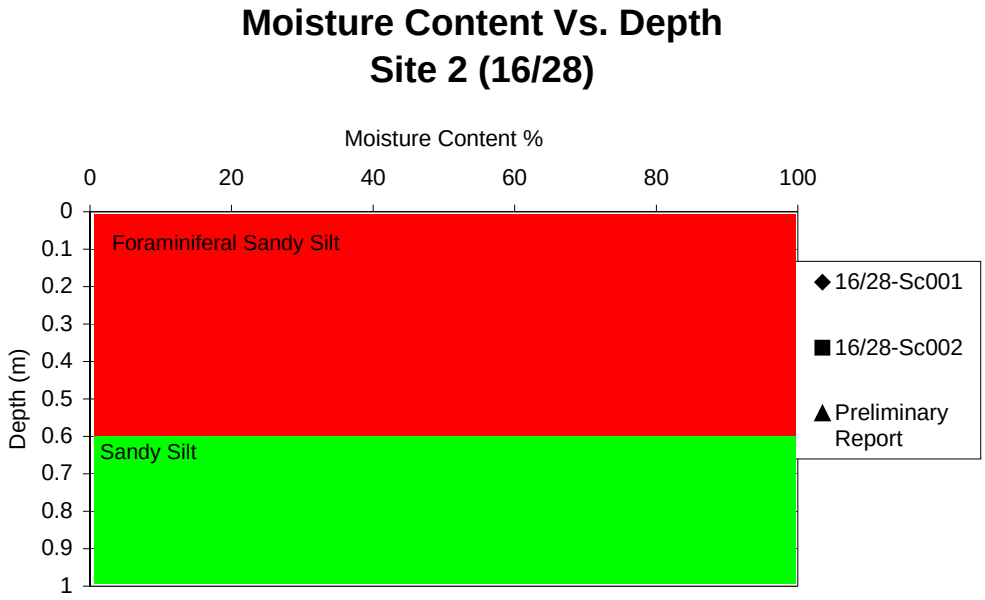

Figure 7.3: Moisture Contents for Site 2

7.4 Site 3 (11/20)

In this site foraminiferal silt overlying silts were recorded. In both this site and site 3A it was noted that a coarser material overlies the finer sediments in low standing areas or channels on the seabed. Given the nature of these sediments a possible deposition mechanism can be proposed. Since this material is quite fine grained it is possible that it could have been fallout from a melting glacier during the last ice age, with coarser material coming from the leading edge of the glacier as it retreated/melted, and therefore covering the preceding fine grained fallout. While the samples in the upper unit show little or no trends, a possible pattern of decreasing moisture content with increasing depth can be seen in the lower unit. Values between 50% and 39% were recorded (see Figure 6.4).

Core Number	Box No.	Core Length (m)	Depth bsl.* (m)	Sample No.	Depth (m)	Moisture Content (%)
11/20-Sc006	1	0.0-0.52	1496			
	2	0.52-1.42		1	0.58-0.865	50
				2	1.07-1.35	45
	3	1.52-2.42		3	1.99-2.23	39
11/20-Sc007	1	0.0-1.01	1365	1	0.39-0.59	
	2	1.11-2.01				
11/20-Sc008	1	0.0-0.41	1463	1	0.115-0.24	46
	2	0.41-1.31		2	0.865-1.135	45
	3	1.41-2.31				
11/20-Sc009	1	0.0-0.88	1522			
	2	0.98-1.98				
11/20-Sc010	1	0.0-0.31	1397			
	2	0.31-1.21				
	3	1.31-2.21		1	1.86-1.98	40
				2	1.62-1.72	39

Table 7.4: Site 3 Results

** bsl. = Below Sea Level*

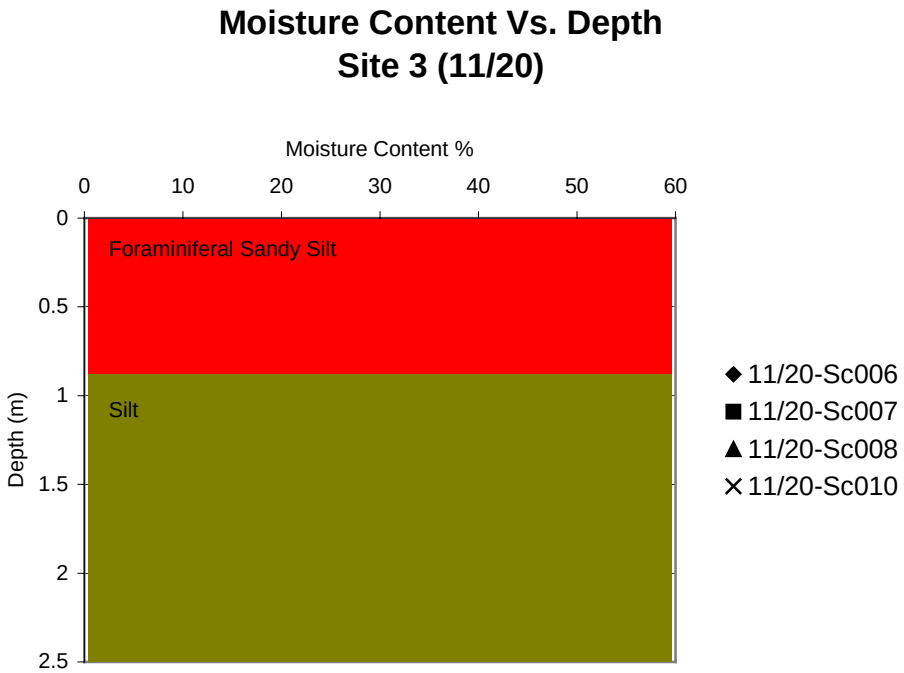

Figure 7.4: Site 3 Moisture contents

7.5 Site 3A (11/20)

This area was similar to site 3 in that foraminiferal sandy silts overlying silt were recorded. However, an overlap in depth was observed, with some of the samples with higher moisture contents and specific gravities proving to be silts, rather than foraminiferal sandy silts. No real trend can be observed in the upper unit but the lower unit exhibits a strong decreasing moisture content with increasing depth. Two of the samples tested in this area showed slight increases in their moisture contents with depth, with the rest showing a decrease with depth as seen in other areas. Another point of interest is that the two samples which showed increases with depth both had slightly higher values than the other samples, which were tested. This can be seen as one set can be observed straddling 50% and the other set lying between 60-70% (See Figure 6.5).

The specific gravities can be subdivided into 3 groups, each corresponding to a different borehole and each within it's own range with little overlap with the other samples. Sample 11/20-Sc002 has the greatest average value, between 2.75 and 2.77. Sample 11/20-Sc001 shows some overlap with Sc003 but mainly lies between 2.67 and 2.69. Sc003 is found between these two samples with values ranging from 2.71 to 2.73. Considering the fact that the second value in the Sc001 suite is so far outside of the expected range it could be possible that this ~~value could be incorrect, due to factors mentioned earlier.~~ material is very similar to, if not the same, as the material found at a similar depth in 11/20-Sc003.

Particle size distribution suggests that this is coarse Silt/fine Sand. This once again places it within the area described as potentially liquefiable in Andresen and Bjerrum (1968).

Core Number	Box No.	Core Length (m)	Depth bsl.* (m)	Sample No.	Depth (m)	Moisture Content (%)	Specific Gravity
11/20-Sc001	1	0.0-0.92	1144	1	0.07-0.565	43	2.67
				2	0.855-0.99	46	2.723
	2	1.02-1.92		3	1.61-1.715	36	2.689
11/20-Sc002	1	0.0-0.44	1007	1	0.0-0.185	66	2.754
				2	0.27-0.44	69	2.756
	2	0.44-1.33					
	3	1.43-2.33		3	1.77-2.18	62	2.77
11/20-Sc003	1	0.0-0.48	1110	1	0.105-0.205	49	2.711
				2	0.32-0.42	50	2.725
	2	0.58-1.47		3	0.73-1.315	53	2.727
11/20-Sc004	1	0.00-0.33	1025				
	2	0.33-1.13		1	0.38-0.84	42	
	3	1.23-2.12		2	1.595-1.83	38	
11/20-Sc005	1	0.0-1.0	991	1	0.47-0.77	39	
	2	1.10-1.99					

Table 7.5: Results For Site 3A
** bsl. = Below Sea Level*

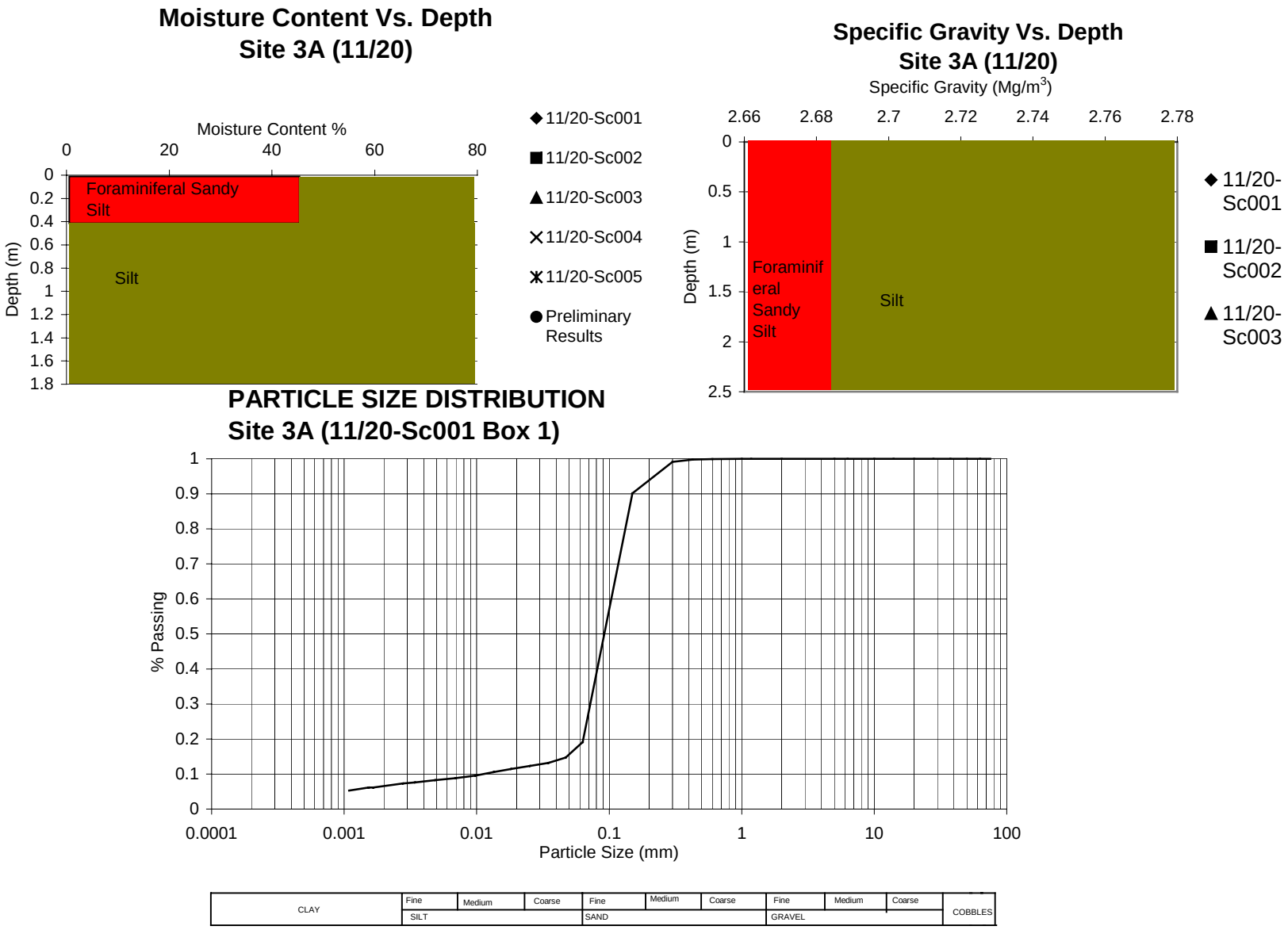

Figure 7.5: Results for Site 3A

7.6 Lithological Results

Using lithologies obtained from viewing the cores when opened, correlations were drawn between similar types of material. These are shown on the graphs of the various parameters such as the moisture contents, specific gravities and Plasticity Limits. In many cases, this entails a depth-based classification between carbonate rich sandy silts, sandy silts, foraminiferal sandy silts and silts. Trends are observed within some of these units and these are addressed here. This way of presenting the results was decided upon in the hope that it would help eliminate any geographical influence on the results. Some of these lithologies are found in boreholes, which are found some distance from each other.

7.6.1 Carbonate Rich Sandy Silts

The moisture contents for these materials show a general decrease with depth. However, these materials occur within a narrow range of just 8% (i.e. between 65% and 73%). The specific gravities of these materials are quite constant with depth giving values in or around 2.5mg/m^3. The Atterberg chart shows that these materials plot as very high plasticity silts.

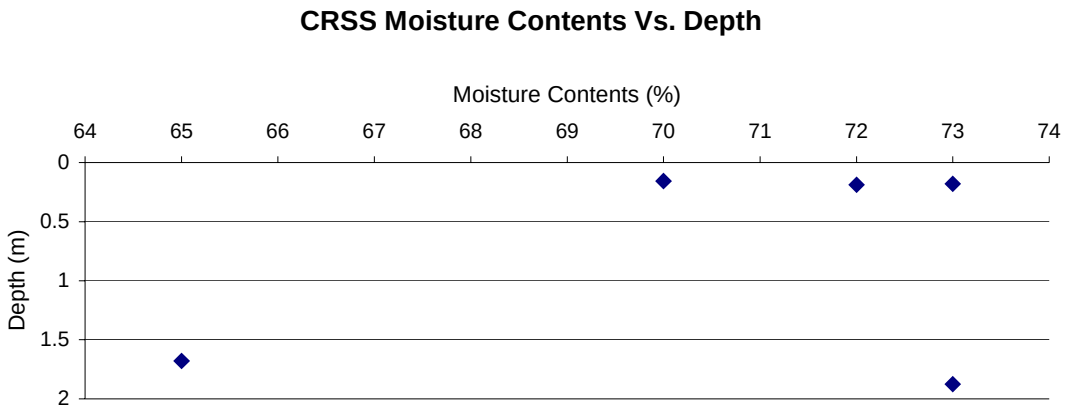

Figure 7.6: Moisture contents for Carbonate Rich Sandy Silts.

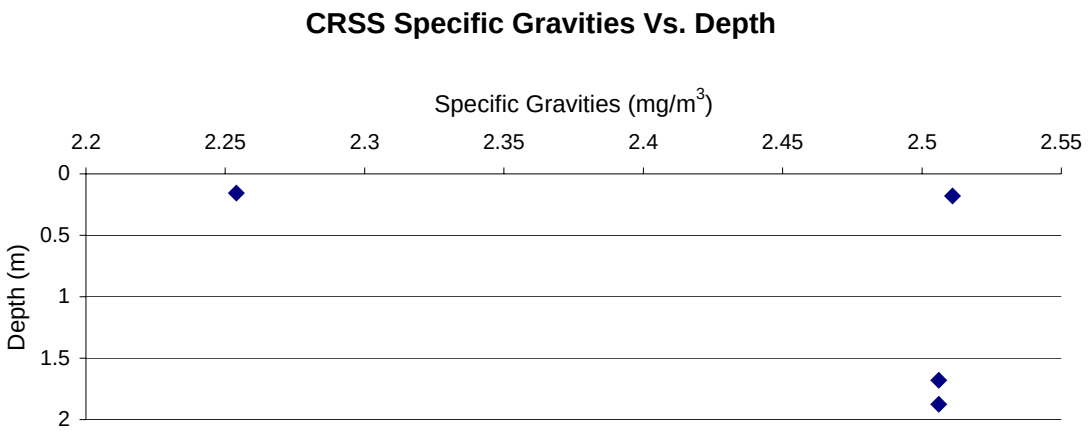

Figure 7.7: Specific Gravities for Carbonate Rich Sandy Silts.

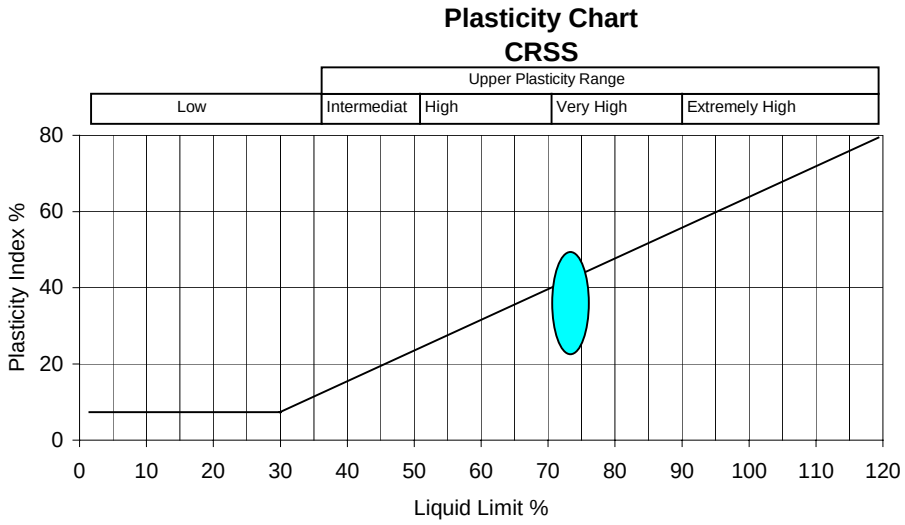

Figure 7.8: Atterberg Limit Tests for Carbonate Rich Sandy Silts.

7.6.2 Sandy Silts

In these samples~~'s~~, the ~~-~~moisture contents show ~~-~~a cluster of shallow samples at around 70%~~ are observed~~. Lower values are generally found at ~~larger~~ greater depths. The specific gravities for these samples are more widespread but showing a decrease with depth. Values range from 2.6mg/m^3 at shallow levels to 2.3mg/m^3 deeper down. This could possibly signify a fining ~~downwards~~ upwards unit representing a potential turbidity current or debris flow. Atterberg limit tests plot these samples as intermediate to high plasticity sandy silts with all of the samples either plotting on or near the Atterberg-line.

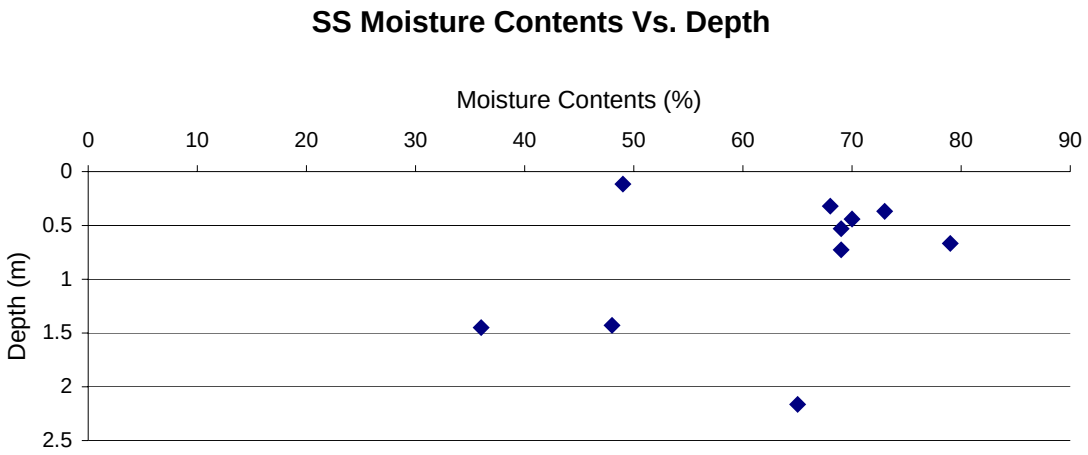

Figure 7.9: Moisture Contents for Sandy Silt.

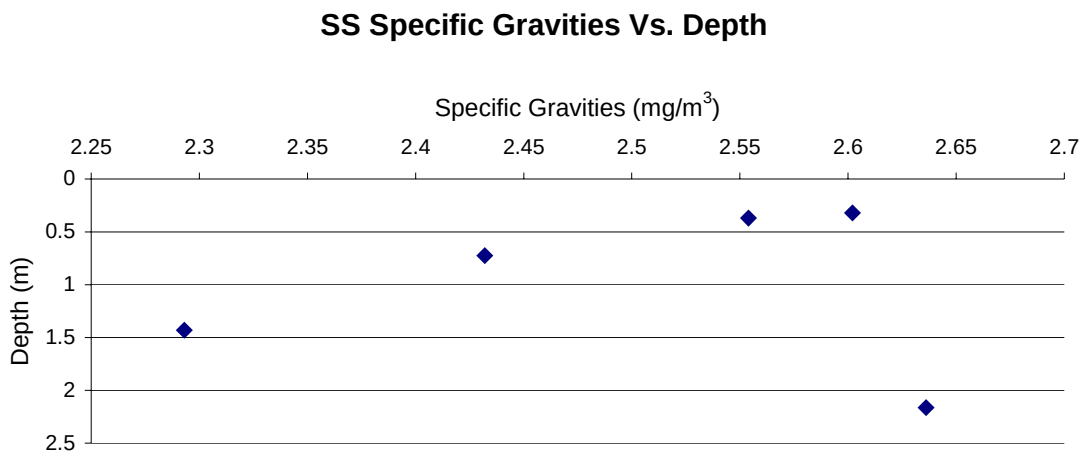

Figure 7.10: Specific Gravities for Sandy Silt.

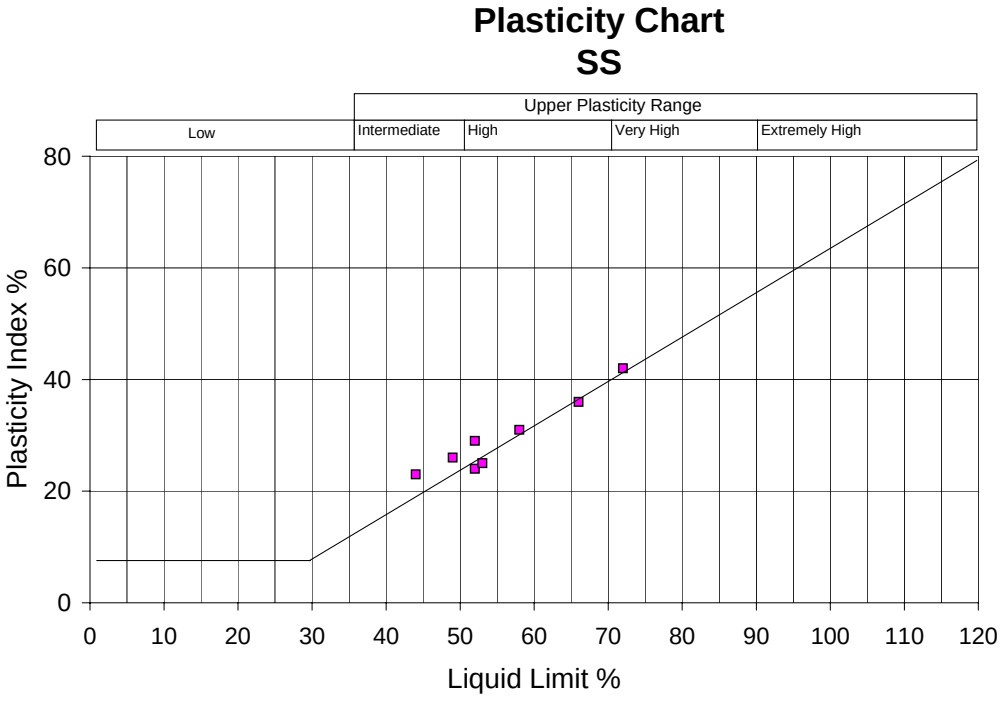

Figure 7.11: Atterberg Limit tests for Sandy Silt.

7.6.3 Silts

Moisture Contents here show a clear trend of decreasing with depth, possibly due to the increasing effective overburden pressure. Samples near the surface plot around 60-70% but values drop to around 35-40% at 2m depth. The specific gravities of this material all plot within a 0.05 wide bracket. Values for specific gravity were between 2.7mg/m^3 and 2.75mg/m^3 with almost no variation with depth. The sample with a value of 2.428mg/m^3 came from site 83/20-Sc001. Two samples were taken from this borehole and both exhibited relatively low specific gravities (2.428mg/m^3 and 2.29mg/m^3).

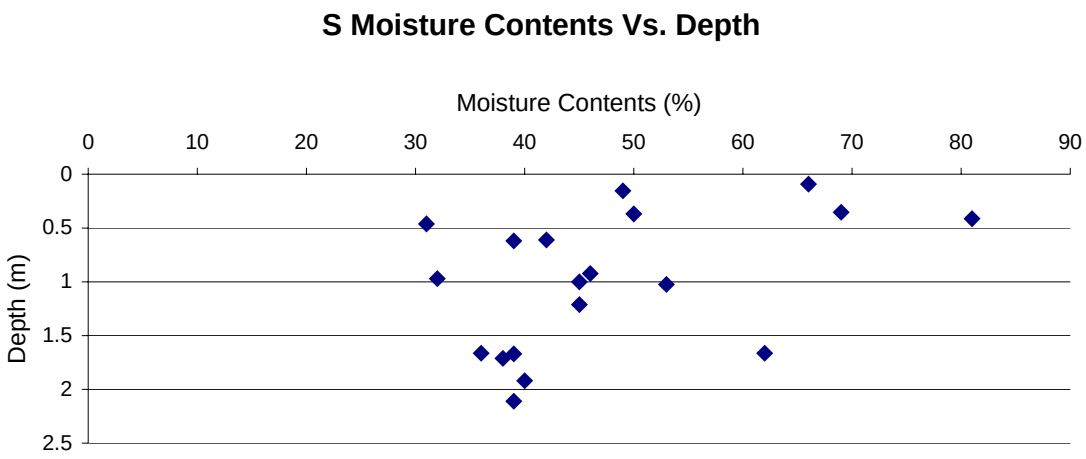

Figure 7.12: Moisture contents for Silts.

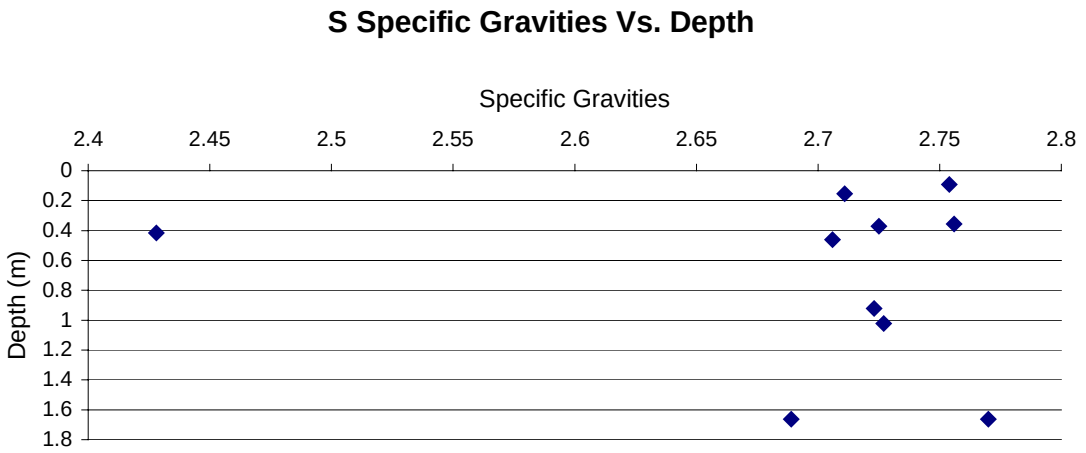

Figure 7.13: Specific Gravities for Silts.

7.6.4 Foraminiferal Sandy Silts

Here we see a strong trend of decreasing values with increasing depth. Values range from 50% down to 20% with depths from 0.2m to 0.6m.

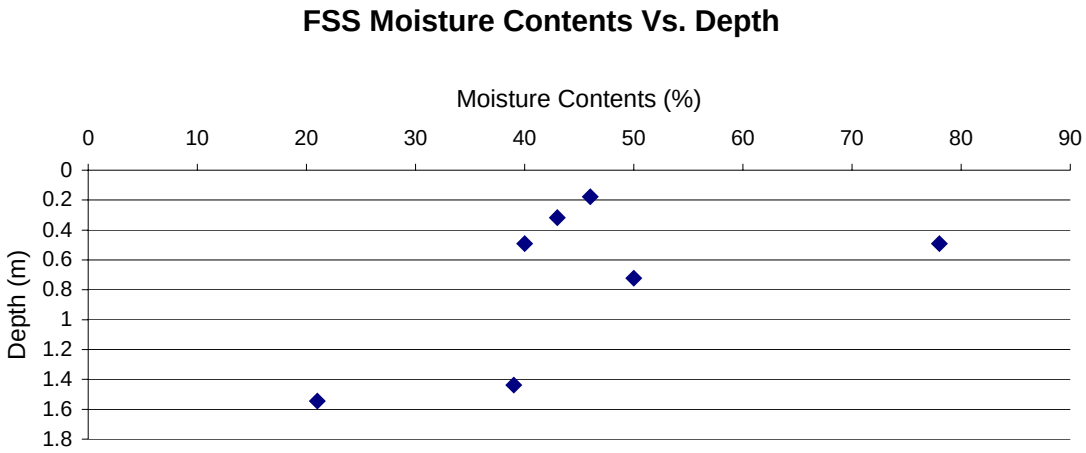

Figure 9.7: Moisture contents for Foraminiferal Sandy Silts.

7.7 Liquidity Indices

Using the principle of the Liquidity index described in Locat (2001) both the values obtained in this study and the values obtained from the preliminary study (Project 98/20) were plotted. However Locat (2001) also proposes that it is possible to predict the undisturbed intact strength, or the rheological properties of clayey material involved in the post-failure stages of mass movement for soft clays.

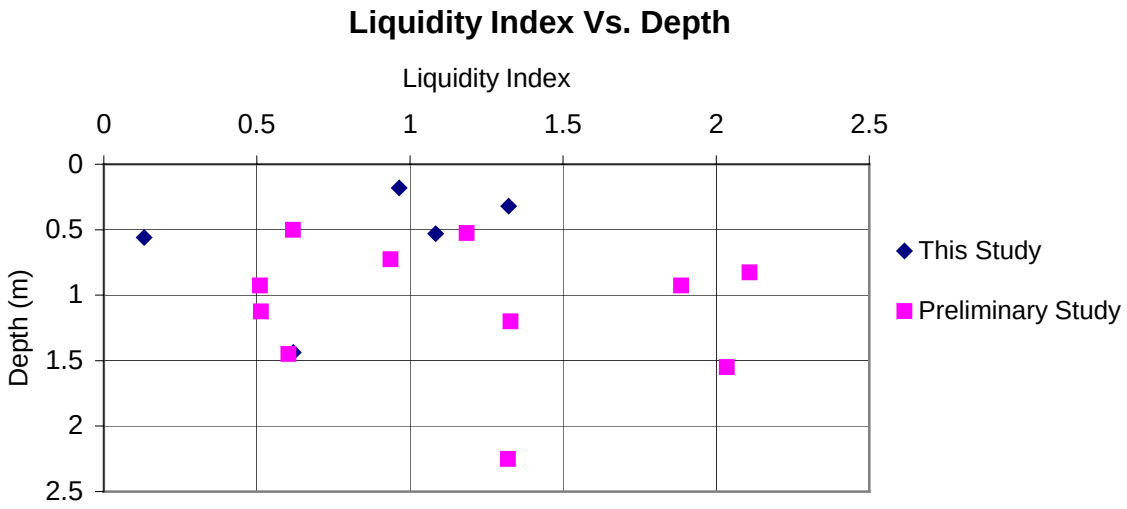

Figure 6.6: Liquidity Indices

The expression used to model the figure below is given as:

$I_L = 3.2543\ \sigma^{-0.396}$

where σ is the calculated remoulded shear strength. The relationship was used to compare in situ values of the liquidity index to those calculated from SEDCON tests (shear strength values from laboratory reconstituted sediments). The materials that Locat (2001) based his analyses on, were described as soft clays. These materials came from a number of sources such as reconstituted sediment from the Eel Margin, in situ values from under Kansai Airport, Japan and field values from Saguenay Fjord, Quèbec.

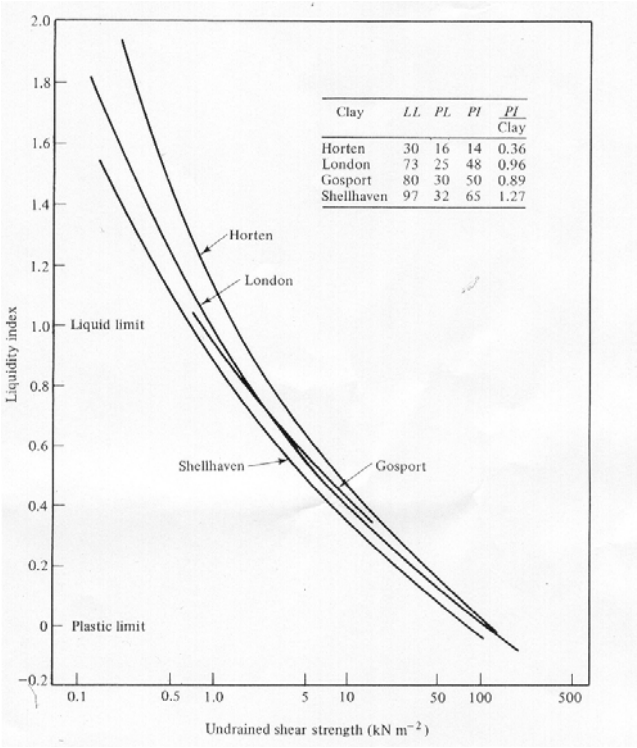

Figure 6.7: Relationship Between shear strength and liquidity index (Atkinson et al, 1978).

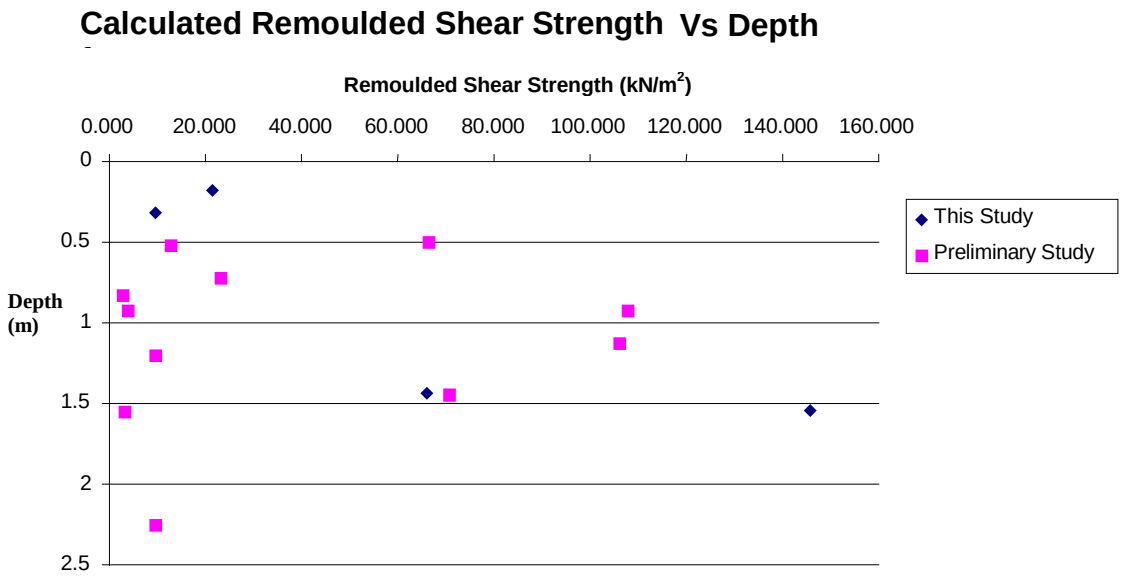

Figure 6.8: Calculated Remoulded Shear Strength from Liquidity Indices

As can be seen from the figures above, these materials have very low remoulded shear strengths and this implies that any of this material is susceptible to shallow slides but less prone to deep-seated catastrophic slides. This is backed up in both figures.

Chapter 8. Stress History

8.1 Introduction

Consolidation is the process through which soil particles are packed more closely over a period of time under the application of continual pressure. It is accompanied by drainage of water from pore spaces between soil particles. The oedometer test used in ~~the~~ this project, is utilized in the determination of the consolidation characteristics of soils of low permeability. It is utilized to examine the stress history of the sample and also to set the value of compressibility of the material. In principle, sequences of 4 to 8 loads are applied to the sample. The sample is then observed for up to 24 hours recording the change in sample height. The degree of consolidation, U, is given as $U=(u_1-u_w)/(u_1-u_0)$ (where u_1 is the initial pore pressure, u_w is the pore pressure at time t and u_0 is the final equilibrium pore pressure). Since this is an average value for the whole sample we can also write $U=\Delta H/\Delta H_f$ where ΔH is the settlement up to time t and ΔH_f is the final overall settlement. Since no actual readings of the pore pressure are made during the test the degree of consolidation is determined using the change in sample height. Therefore, at the beginning of the test t=0, $u=u_1$, $\Delta H=0$ and U=0%. At the end of the test $t=\infty$, $u=u_0$, $\Delta H=\Delta H_f$ and U=100%. However 100% consolidation is never reached and so therefore neither is $t=\infty$, so times for 50% and 90% consolidation are usually obtained. The two main parameters involved are:

1) Compressibility: This is the amount that the soil will compress when loaded and allowed to consolidate. This is expressed in terms of the coefficient of volume compressibility.

2) Time related parameter: This is the rate of compression and therefore the time period over which consolidation will take place.

8.1 Previous Study

Six tests were carried out in the preliminary investigation. The samples tested included two samples of Sandy Silt composition, three samples of Silt composition and one of Carbonate Rich Foraminiferal Silt. By simple comparison with moisture content and previous correlations between moisture content and the compressibility parameter ($C_c/(1+e_0)$ where C_c is the compression index and e_0 is the initial voids ratio) published by others, these samples were found to be less compressible than would have been expected for normally consolidated material when the compressibility parameter was calculated. Normally consolidated materials have never experienced any pressure greater than that due to the overlying material. In this case all samples were observed to be overconsolidated implying that it had experienced more load than should be expected due to the depth of the samples. From this it can be said that the samples were found at a deeper depth at one stage, but this material had been somehow removed, either through erosion or some other process. OCR values for the samples were seen to be typically 3, however samples from site 2 and site 4 were observed to have OCR's of 13 and 8 respectively. Preconsolidation values for these samples generally fell around 40-50kPa. The compression coefficient for the six samples varied between 0.104 and 0.146. However samples from Site 1 and Site 3A were found to be respectively lower (0.042) and higher (0.195) than the rest of the values observed. In order to determine the preconsolidation pressure, an empirical method was employed which was described by Casagrande.

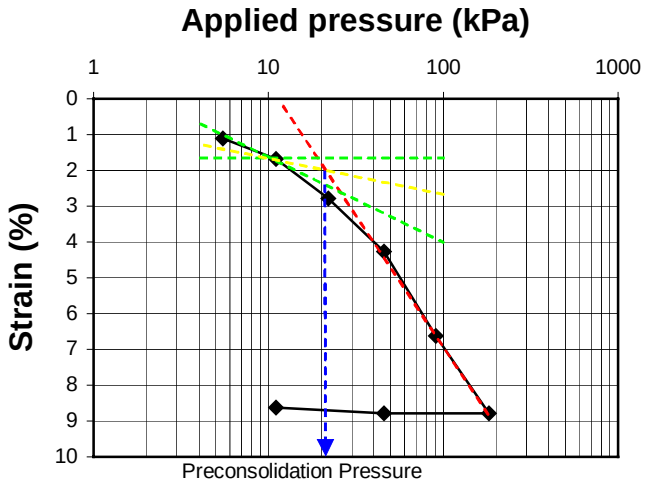

Fig 8.1: Example of Casagrande Method of determining preconsolidation. See below for explanation

In the above example the Casagrande Method for determining the preconsolidation value of a sample is shown. The following constructions are applied. The red dashed line is constructed first. This represents the “virgin stress” line of the material. This is an extension of the latter straight-line part of the graph. The next construction is twofold. First the point of maximum curvature is found on the upper part of the curve, and a tangent is constructed through this point. Next a horizontal line is constructed through the tangent point. The green dashed lines show these. Finally the bisector of the angle formed by the green lines is drawn and the intersection of this line with the red line represents the preconsolidation value of the sample. However this is a subjective analysis and may reflect the influence of sample disturbance and plate embedment.

8.2 New Study

Two samples from a slump body at 83/3-Sc002 (Foraminiferal Sandy Silt) were tested using the conventional maintained load procedure (MSL) with the load being maintained past primary consolidation. Primary consolidation is defined to be "the part of the total compression under load to which the Terzaghi Theory applies. It is the phase during which drainage and pore pressure dissipation occur." Once there was little variation, another increment would be added. Normally samples would be left to consolidate over 24 hours but this is mainly to investigate secondary consolidation, which was of limited use. Secondary consolidation occurs after primary consolidation has virtually finished and is time dependent, and therefore not of use in this case. By simply observing the results of the stress/strain curves and applying the Casagrande approach, preconsolidation values could be determined. The figures for preconsolidation values calculated were 32.25kPa for the first test and 32.3kPa for the second test. Another approach was used which is mentioned in Janbu (1985). OCR values for these materials were recorded to be 2.

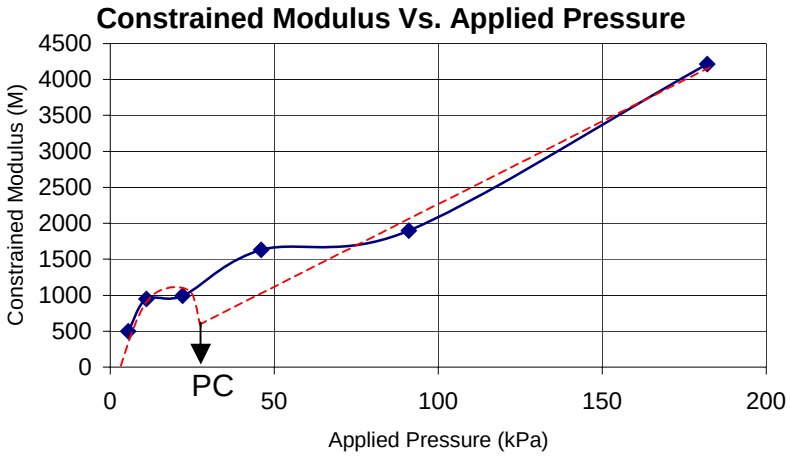

Figure 8.2: Example of Janbu's method of determining preconsolidation pressure. See below for details.

The figure above shows the basic procedure for determining the preconsolidation pressure of a sample using the method described in Janbu (1985). A curve is fitted to the graph of constrained modulus vs. applied pressure, which has an initial parabola representing the structural breakdown of the sample and then a straight line, once again representing the "virgin compression" of the material. The point where the parabola joins the straight "virgin" line is read as the approximate preconsolidation pressure of the material. This approach was used to determine the preconsolidation pressures for the samples tested in the preliminary study (83/20-Sc003, 83/24-Sc003 and 11/20-Sc003). The graphs are plotted below. This gives preconsolidation values of 77kPa, 33kPa and 28.3kPa respectively.

Initial loads are usually given to be $0.25\sigma'_{vo}$, so in this case our first load was 2.5N or 5.5 kPa. The following increments doubled the load each time, finishing at a load of 80N.

Sample disturbance was also quantified by looking at the ratio $\Delta e/e_o$ to the in-situ effective stress. If the value is less than 0.04 the sample is said to be "good to excellent". If the value is 0.04-0.07 the sample is said to be "good to fair". However if the ratio is greater than 0.07 the sample is said to be "poor" and if it is greater than 0.14 it is said to be "very poor". Sample 1 returned a value of 0.18. This implies that the sample disturbance was substantial, giving a sample quality of "very poor". Sample 2 gave a result of 0.12, which describes sample quality as "poor" (Lunne et al, 1997).

Two more samples were also tested but this material was reconstituted, and therefore any stress history within the sample was lost. This was mainly to look at the behaviour of the material to ensure it conformed to the expected behaviour of a silty sand. While the first reconstituted sample (sample 3) showed poor results (due to a leaky oedometer ring

and the drying out of the sample), the second reconstituted sample (sample 4) shows the expected results for a material of this type.

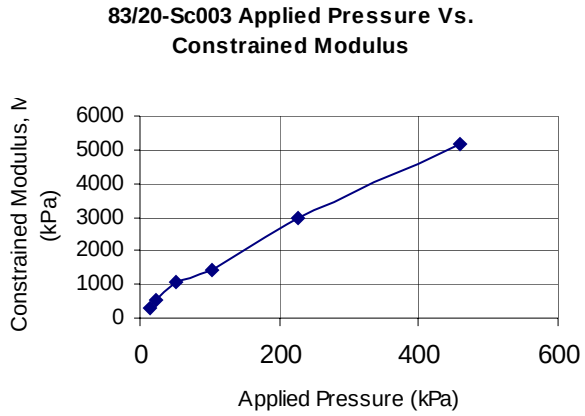

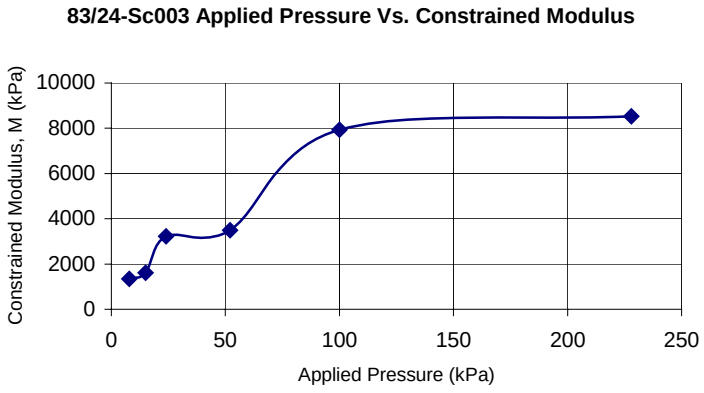

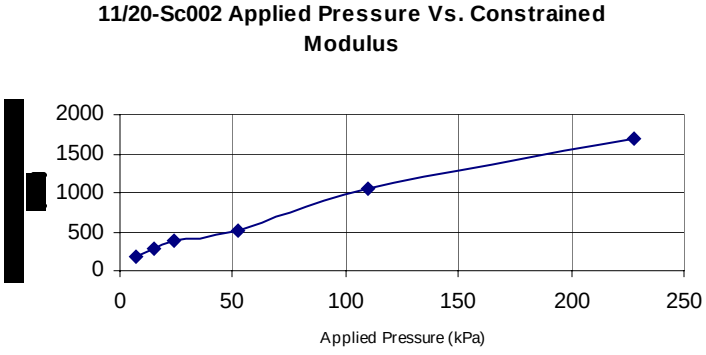

Fig 8.3: Preliminary Study graphs of constrained modulus, M, vs. applied pressure

8.3. Results

83/3-Sc002 Depth: 1.8m Foraminiferal Sandy Silt Sample 1

Increment No.	Load	Compression	H Bar	Sqrt(t_{90})	t_{90}	c_v	M	m_v	k
	KPa	mm	mm	Secs.	(mins)	m^2/year	kPa	m^2/MN	m/s
1	5.5	0.21	18.79	18	5.4	10.60862	498	2.009569	6.6E-09
2	11	0.11	18.68	8.8	1.290667	36.50402	950	1.052632	1.2E-08
3	22	0.21	18.47	16.5	4.5375	14.54724	995	1.004785	4.5E-09
4	46	0.28	18.19	13.5	3.0375	13.10357	1629	0.614035	2.5E-09
5	91	0.45	17.74	13.5	3.0375	26.49875	1900	0.526316	4.3E-09
6	182	0.41	17.33	12.8	2.730667	17.73901	4217	0.237131	1.3E-09

83/3-Sc002(2) Depth:1.8m Foraminiferal Sandy Silt Sample 2

Increment No.	Load	Compression	H Bar	Sqrt(t_{90})	t_{90}	c_v	M	m_v	k
	KPa	mm	mm	Secs.	(mins)	m^2/year	kPa	m^2/MN	m/s
1	5.5	0.11	18.89	15	3.75	151.32549	950	1.052631	4.9E-08
2	11	0.03	18.86	12	2.4	8.55037	1493	0.669856	1.8E-09
3	22	0.09	18.77	10	1.6667	16.73474	1817	0.550239	2.9E-09
4	46	0.12	18.65	8.1	1.0935	9.10166	2497	0.400457	1.1E-09
5	91	0.21	18.44	11.5	2.204166	8.94184	3088	0.323886	9.0E-10
6	182	0.2	18.24	4	0.266666	10.49429	4550	0.219780	7.1E-10

83/3-Sc002(3) Depth 2.8m Reconstituted Sample Sample 3

Increment No.	Load kPa	Compression mm	H Bar mm	Sqrt (t_{90}) secs.	t_{90} mins	c_v M2/year	M kPa	m_v m2/MN	k m/s
1	5.5	0.280	18.173	8.75	1.276	58.132	362.476	2.759	4.97163E-08
2	11.0	0.590	17.583	11.46	2.189	62.329	233.318	4.286	8.28137E-08
3	22.0	0.720	16.863	10.65	1.890	102.836	255.329	3.917	1.24856E-07
4	46.0	1.250	15.613	9.69	1.565	101.567	298.892	3.346	1.05342E-07
5	91.0	1.080	14.533	7.80	1.014	88.610	428.381	2.334	6.41231E-08
6	182.0	0.350	14.183	7.00	0.817	32.161	786.536	1.271	1.26758E-08

83/3-Sc002(4) Depth 2.8m Reconstituted Sample Sample 4

Increment No.	Load kPa	Compression mm	H Bar mm	Sqrt (t_{90}) secs.	t_{90} mins	c_v M2/year	M kPa	m_v m2/MN	k m/s
1	5.5	1.720	17.343	11.25	126.563	114.872	60.958	16.405	5.84E-07
2	11.0	0.480	16.863	9.76	95.258	76.056	95.317	10.491	2.47E-07
3	22.0	1.370	15.493	8.62	74.218	59.176	117.477	8.512	1.56E-07
4	46.0	1.790	13.703	10.50	110.250	66.491	163.603	6.112	1.26E-07
5	91.0	2.775	10.928	6.27	39.313	59.155	213.247	4.689	8.60E-08
6	182.0	3.365	7.563	5.00	25.000	33.339	301.698	3.315	3.43E-08

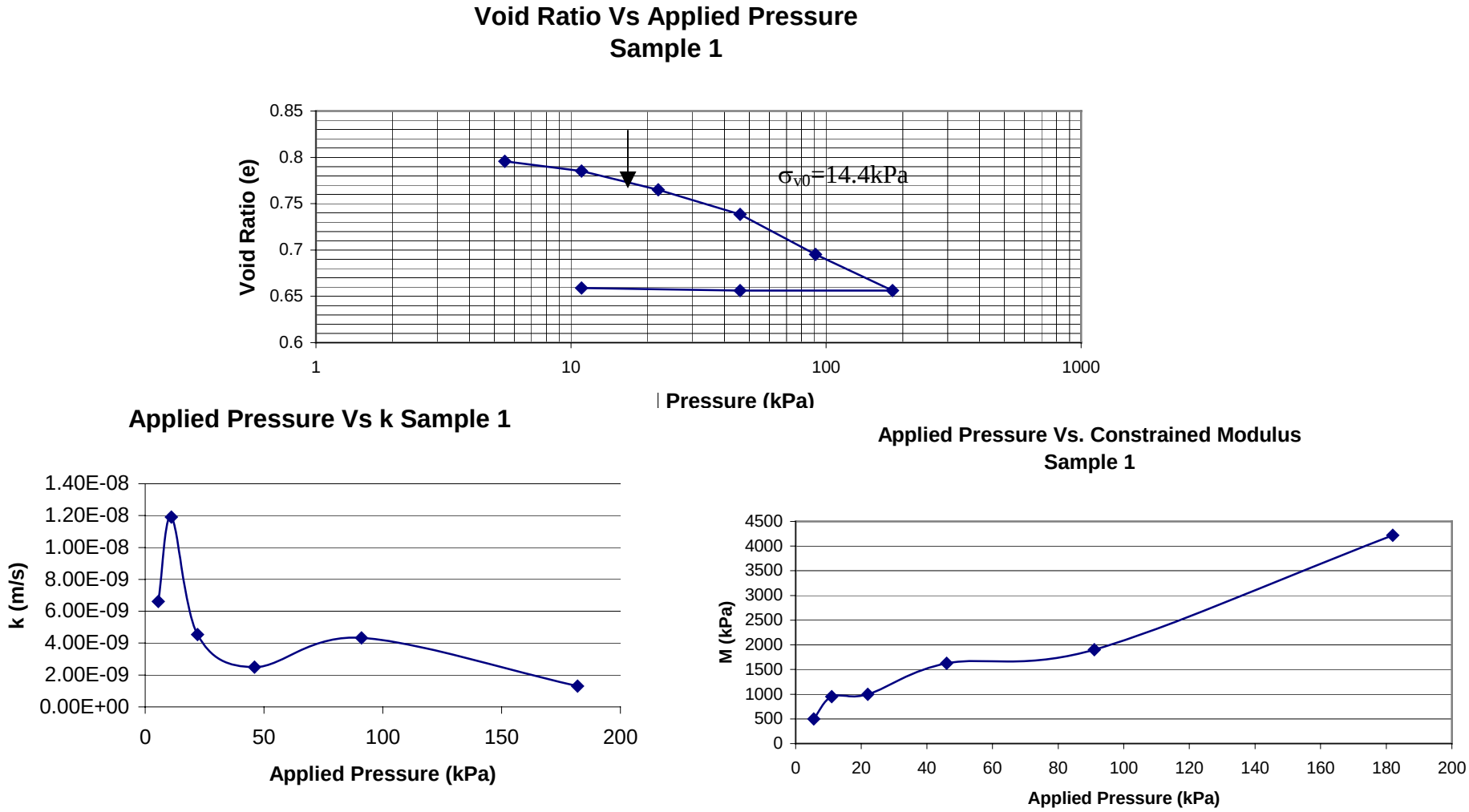

Figure 8.4: Consolidation Test 1 Results.

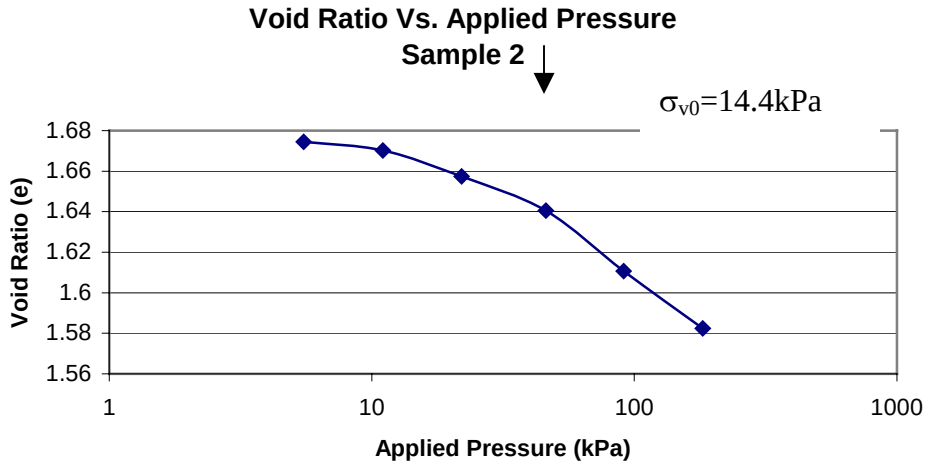

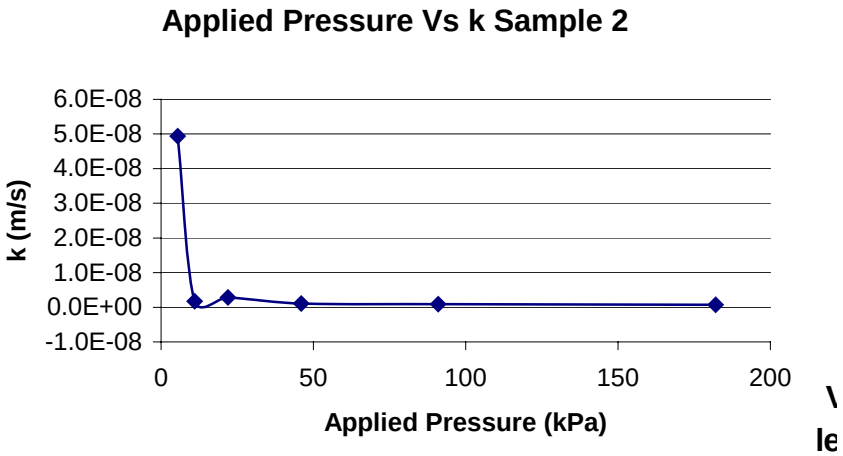

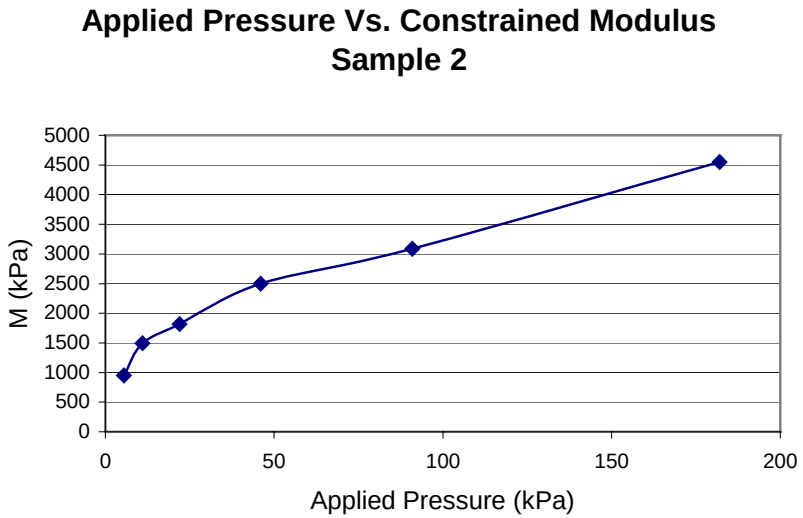

Figure 8.5: Consolidation Test 2 Results.

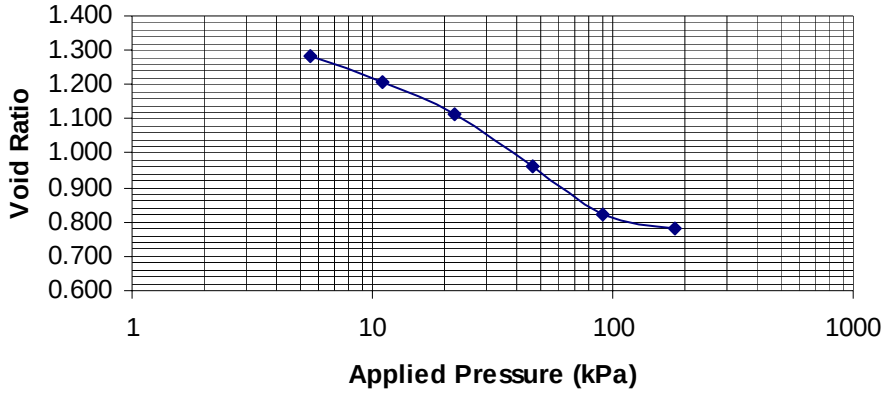

Applied Pressure Vs. Void Ratio
Sample 3

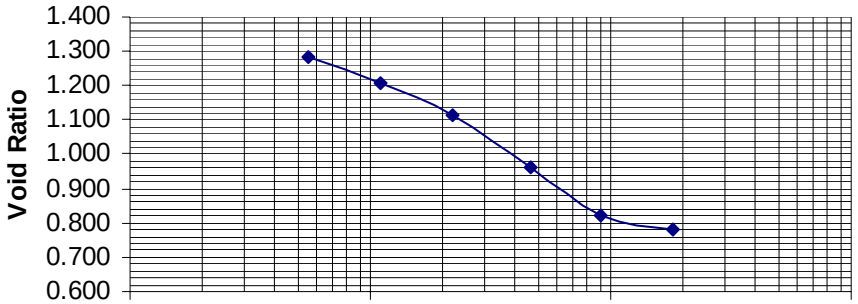

Applied Pressure Vs k
Sample 3

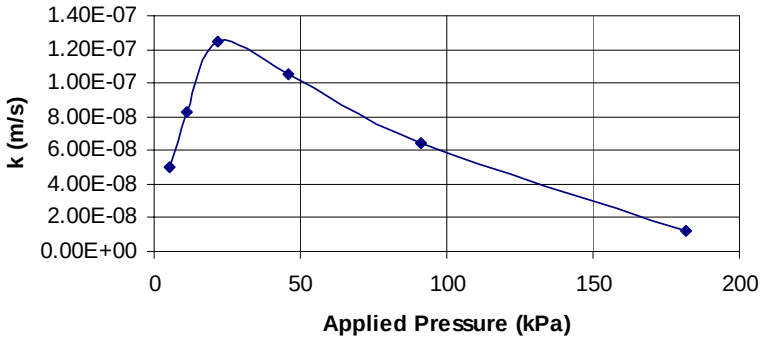

Applied Pres
Samp

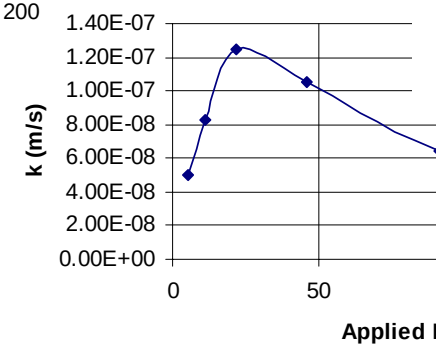

Applied Pressure Vs. M
Sample 3

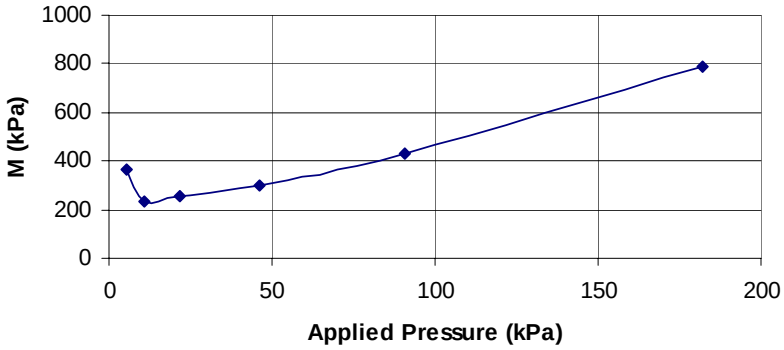

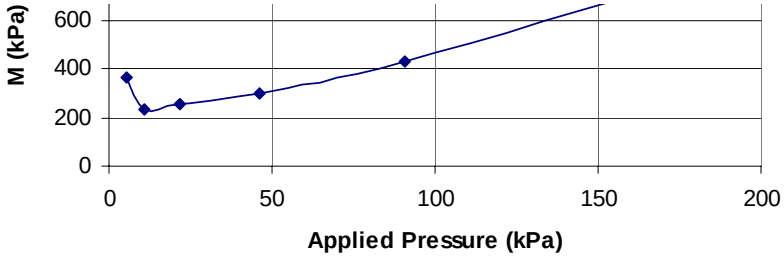

Fig. 8.6: Consolidation Test 3 Results

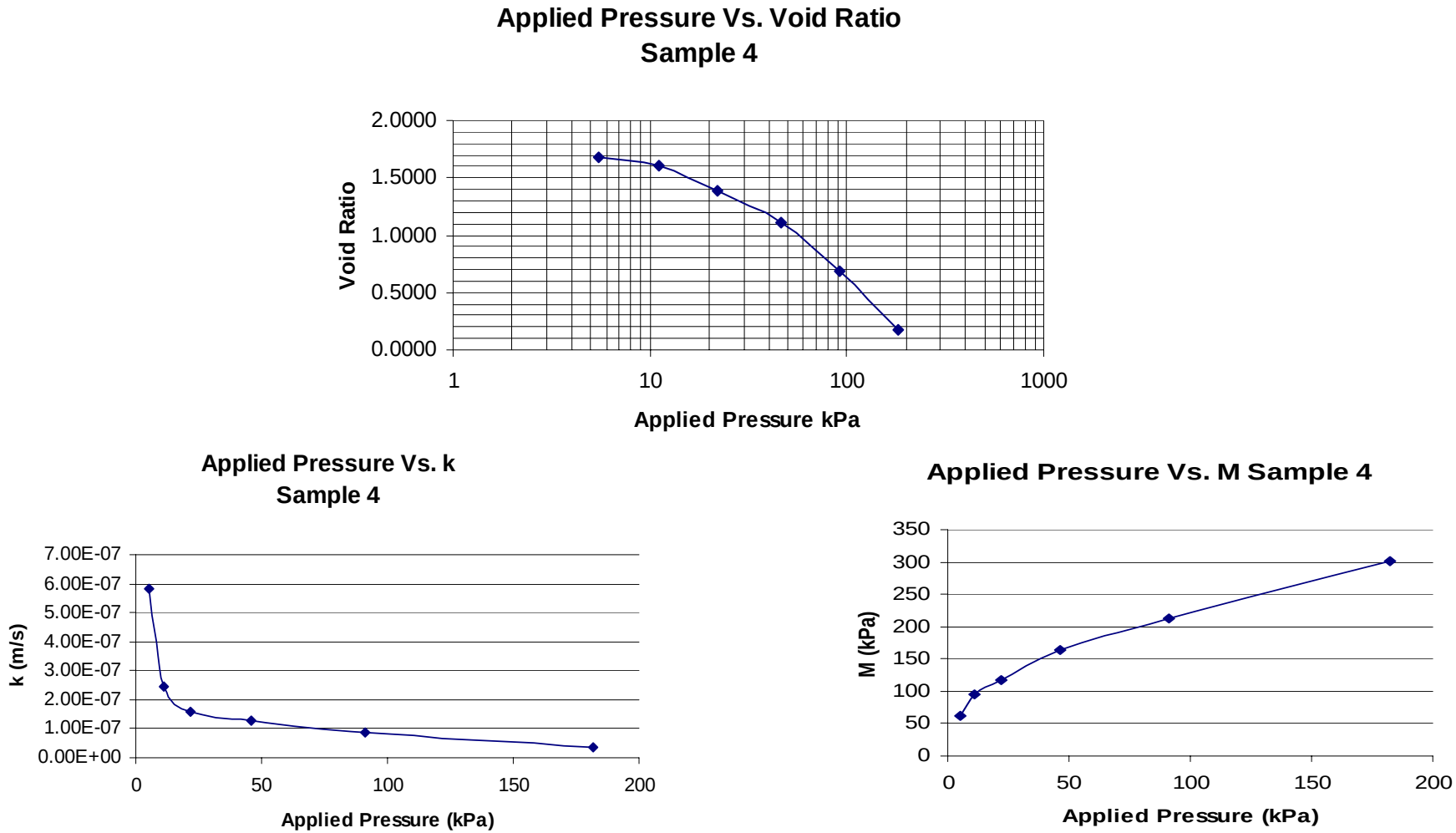

Fig. 8.7: Consolidation Test 4 Results

Chapter 9. Shearbox Test

Shearbox tests were carried out on a sample from 83/3-Sc002 (1.9-2.0m, Foraminiferal Sandy Silt) in order to determine the peak effective stress parameters for the sediment, and also to see how the strength of the sediment varies with density and normal stress. These results will help determine the susceptibility of the material to liquefaction. The method used was as described in BS 1377. The samples used were reconstituted and prepared to a given moisture content (65%), which was recognised as the average value for samples in this area. Three different bulk densities (1.65, 1.785 and 1.85Mg/m^3) were also used and three tests were carried out on these samples with increasing normal stresses (27kPa, 54kPa and 108kPa).

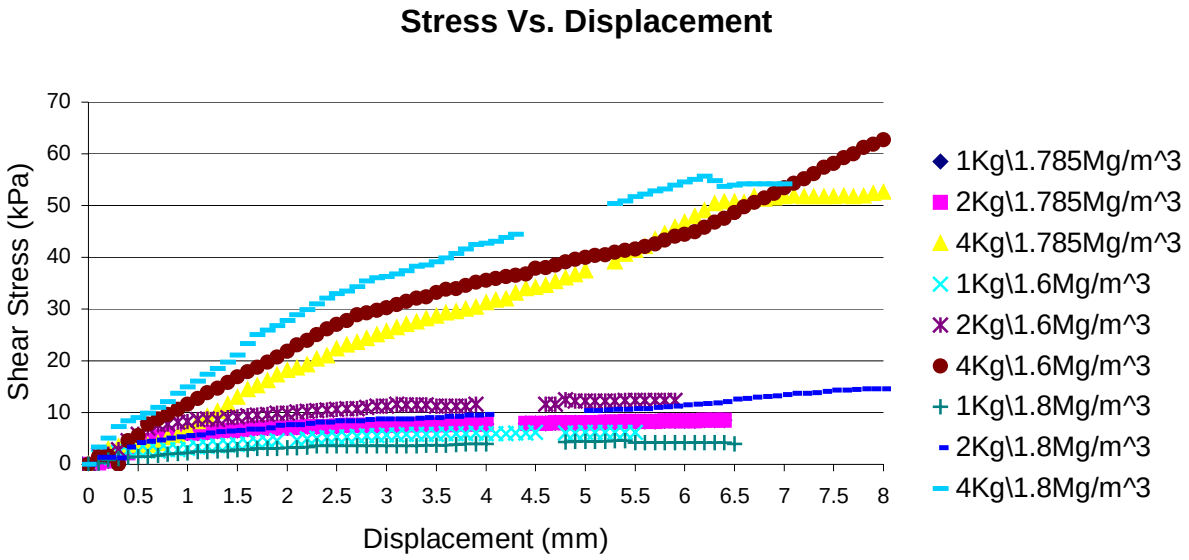

Figure 9.1: Shear Stress vs. Displacement for each test

Figure 9.1 shows shear stress versus the horizontal displacement of the shearbox. The curves here show typical behaviour for a loose granular material with a gradual build up to a peak. These tests show quite clearly that the normal stresses are much more

important than the density of the material. This can be seen in the ~~little~~ small to negligible variation in the curves over various densities at particular normal stresses (Fig. 9.2).

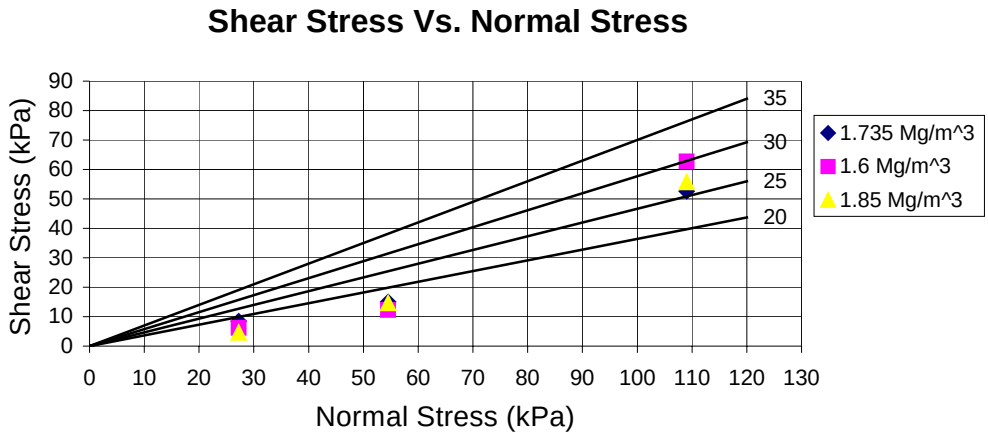

Figure 9.2: Shear Stress vs. Normal Stress for all three tests.

~~Shown above in~~ Figure 9.2 ~~are~~ plots the peak strength values against the normal stresses for the different densities used in the test. The lines labeled from 20 to 35 are ~~simply~~ trend lines representing peak stress conditions of c'=0kN/m^2 and ϕ'=20^o to 35^o. Again the dependence on normal stresses over densities is clear. The results of these tests are c' = 0kN/m^2 and ϕ' = 23.5^o to 26.1^o. These are lower than the values obtained in the preliminary report which reports values ranging from c' = 0kN/m^2 and ϕ' = 32^o to 44^o.

From ~~this~~ these data a number of ~~things~~ conclusions can be ~~said~~drawn. It can be seen that the bulk density of the material has very little effect on the behaviour of the samples. Note the overlap between the different samples with differences only appearing at higher stresses. This means that between these densities (i.e. 1.6 to 1.85 mg/m^3) there is very little difference in behaviour. The strength is very low at low effective stresses and this has serious implications. This means that surface slides are highly probable but more catastrophic deep slides are unlikely.

Chapter 10. Conclusions

Rough tTrends can may be seen observed in the data results of the characterisation tests when presented geographically but these trends are more clearclearer when the data is are presented by lithology type. The main problem with the data is that there are not enough data points to definitely describe trends in these materials. The samples are all shallow (i.e. within the upper 2.5m) and also another factor is that they are geographically quite spread outseparate. The sites are all about 4km^2 in area with up to 5 boreholes present. The Each sites themselves are also over acovers a large area. However, even with this taken into account there are some characteristics which can be ascribed to the various lithologies.

The carbonate carbonate-rich sandy silts can be observed to have moisture contents between 65-73%. Specific gravities for these samples were grouped around 2.5 Mg/m^3. These materials plotted as high plasticity silts on the Atterberg chart. The sandy silts had values of 60-70% moisture content around the surface which dropped to 35% at 2m depth. Values for specific gravity with these samples were 2.6Mg/m^3 at shallow levels and as low as 2.3Mg/m^3 at deeper levels. Again this material plotted as an intermediate to high plasticity silt on the Atterberg chart. The silts had moisture contents between 60-70% at the surface dropping to 35-40% at a depth of 2m. Specific gravities were between 2.7-2.75Mg/m^3. One sample in this suite plotted a very low value of 2.428Mg/m^3, however this borehole exhibited low values for all samples taken from it (83/20-Sc001). The final lithology type was the foraminiferal sandy silt. This was observed to have moisture contents ranging from 20% to 50%, decreasing with depth.

The stress history of these materials seems to imply that they were overconsolidated at some stage in the past and from the tests performed the overconsolidation ratio of the materials was observed to be 2. However from the tests to investigate the stress history of the materials we can also estimate sample quality and the samples tested were found to be of “poor” to “very poor” quality.

The shear strength of some of the samples was also measured. The materials are shown to have low remoulded shear strengths which implies that these materials are susceptible to shallow slides but are less prone to deep-seated slides. Not only was this observed in the shear strength tests but also in the calculations based on the liquidity indices.

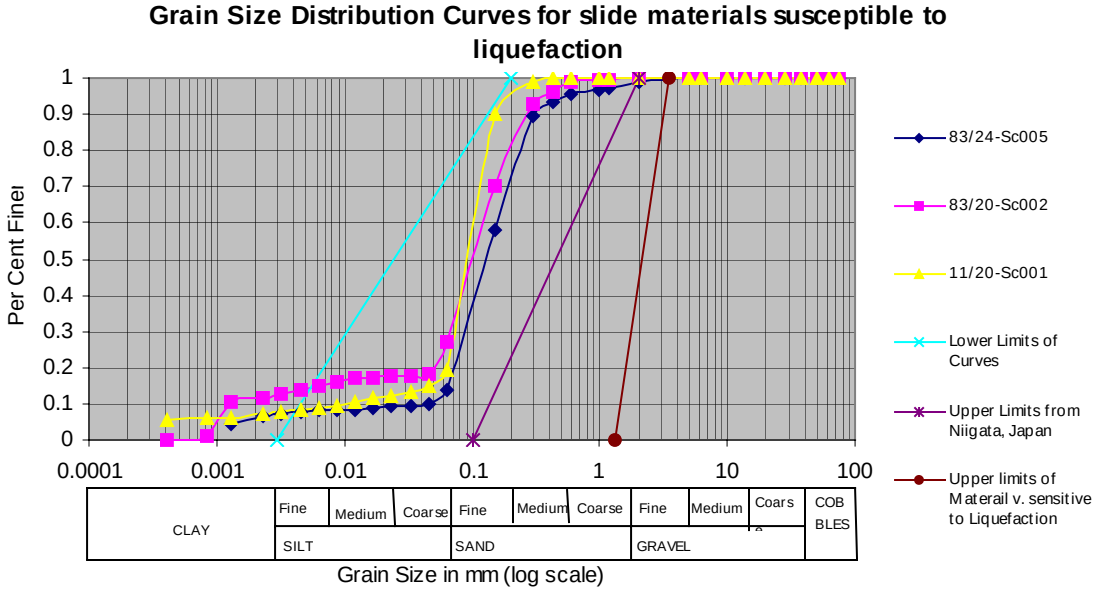

Figure 10.1: Grain size distribution curves for areas with limiting curves for material susceptible for liquefaction. (Bjerrum, 1961; Langer, 1938; Watanaba, 1965; Kishida, 1965).

The material tested during the course of this project could be generally classified as coarse ~~SILT~~ silt fine ~~SAND~~sand. The nature of most of the materials found in this area

implies that they are sensitive to liquefaction (see Figure 10.1). General characteristics show moisture contents ~~in and around~~close to the liquid limits of materials tested and are all either coarse silts or fine sands. Since slopes in this area are generally relatively shallow (0.5-3.5%) compared to ~~what is~~those found on land, the triggers involved are slightly different. Triggers such as earthquakes, rapid sedimentation, liberation of gas hydrates, or diapirism could all be the sources of slides. It appears that at low values of effective stress the angle of internal friction is also low, implying that shallow slides are possible and are more likely to occur than deep-seated failures.

Even though shallow slopes are present, given the nature of the materials, slide propagation would be composed mainly of ~~fluid type~~ movement ,best described by fluid mechanics, due to the potential liquefaction in the sediments. The resulting slides could potentially cover large distances and would move relatively fast, possibly in the form of initially a slump or slide but later on becoming more of a low density flow such as a debris flow or turbidity current.

Once these failures occurred the existing slope would be undermined and further retrogressive propagation could start. As can be seen with the relationship between liquidity index and remoulded shear strength, once disturbed, this material has very low strength and so is susceptible to this retrogressive propagation of the slide. This would lead to more and more material contributing to the slide. Also, due to the nature of the sea bed, the slide would scour the seabed and in turn gain more material and therefore more momentum leading to greater speeds and run-out distances. This would occur because of the lack of binding vegetation on the sea floor, unlike on land where this becomes a factor.

~~1~~Chapter 11. Discussion

One of the most important things in carrying out engineering tests on any type of sample is that the sample itself is undisturbed. This means that the results obtained in the lab best reflect the behaviour of the sediment in its native environment. By its very nature, sampling itself disturbs the sample and so should be taken into account. In this project, it was observed that some of the samples exhibited deformation due to coring. This sample disturbance was quantified in the consolidation test. This manifested itself at various ~~sedimentalogical~~ sedimentological boundaries throughout the cores. Some of these boundaries exhibited "drag" effects along the sleeve of the core. As can be seen in Figure 11.1A, the black band present in the core ~~could be seen~~is curved ~~to be dragged~~ down ~~on~~ to the left-hand side. However this could also be ~~an inherent~~a primary ~~sedimentological~~ sedimentary structure within the sample. Another example of coring effects is the "sleeving" which can occur when some light brown material is smeared out along the walls of the core (see Figure 11.1B). These photos were taken with a digital camera immediately upon splitting of the cores and before sampling (see Appendix ~~4~~4).

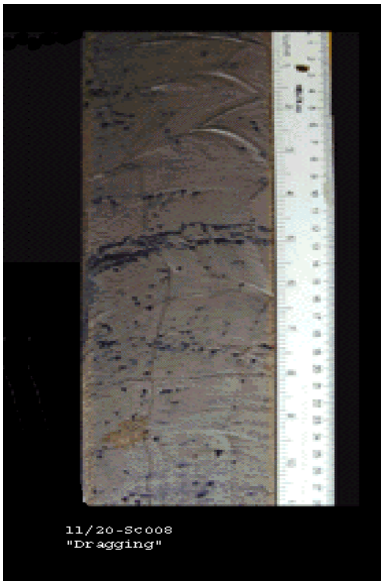

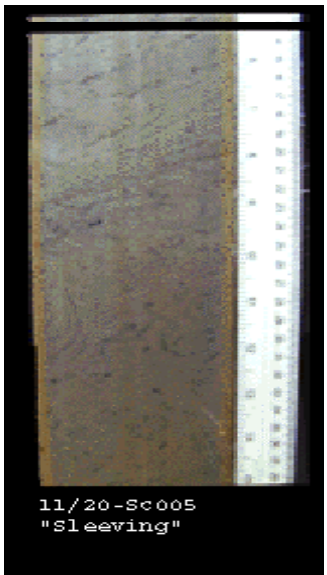

Figure 11.1A: Coring Effects ("Drag") *Figure 11.1B: Coring Effects ("Sleeving")*

A possible solution would be to use a larger diameter corer to minimize the disturbance in the samples or to use a corer with a fixed piston together with an improved cutting head geometry, sharp cutting edge and thin wall, in order to ensure minimum friction both inside and outside the corer. In the paper by Tjelta et al (2002) it is mentioned how all onshore testing was performed on 10cm^2 samples which were trimmed down from 40cm^2 cross sectional area samples.

As mentioned above, one of the most important things to take into account when testing sediments is to ensure they are as undisturbed and unchanged as possible. Therefore samples should be tested as soon as possible after recovery. This gives the truest representation of the natural behaviour of the sediment. Therefore as many standard classification tests as possible should occur on board the survey ship, as well as testing the material in situ. Cone penetration tests, slimline logging and vertical seismic profiling would all be useful, as well as hand vane tests and other on site tests which could be carried out while coring. Unfortunately in this case, the samples were almost two years old before testing began. Ideally, only tests involving remoulded material

should be carried out on shore, with tests requiring “fresh” samples taking place on the ship.

An issue, which should be discussed, is some of the specific gravity readings. Some of these samples exhibited readings lower than that which was expected. This can be put down to variations in sample size. This affects specific gravity readings in the sense that it is harder to ensure there is no air trapped in the sample, the larger the sample. Therefore due to this trapped air, the specific gravity is less than what is expected. This can be seen if the sample size is graphed against the specific gravity. The couple of samples which gave readings of less than 2.2Mg/m^3 all have sample sizes greater than 14g. Ideal sample sizes should be around 10g.

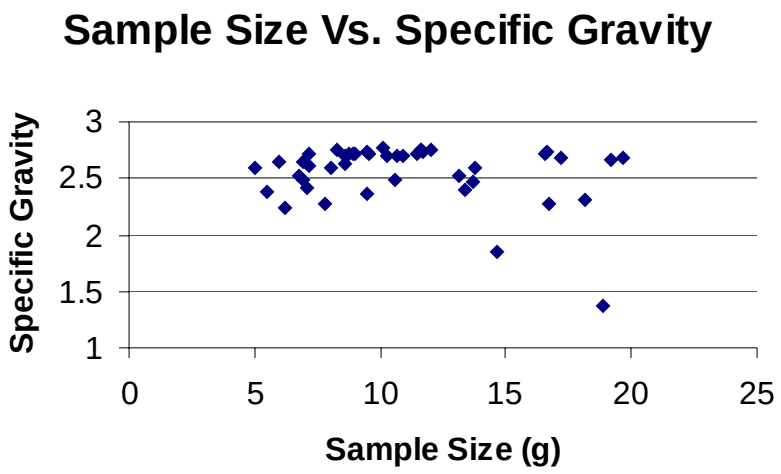

Figure 11.2: Sample size Vs. Specific Gravity

The possibility of dating the sediments and events observed on the TOBI sonar data could also be extremely useful. Not only would it put a timescale on the features observed but also would provide important data such as sedimentation rates in the area. It would help with the interpretation of the area and the potential triggers for the observed slides. A radioisotope method of dating could be suitable in conjunction with or instead

of using planktonic fossils such as forams found in the sediment. This has been carried out as part of the geological investigation of the cores as presented by Lena Øvrebø.

Chapter 12. ~~Bibliography~~References

Andresen, A. and Bjerrum, L. (1968)~~,~~ "Slides in Subaqueous Slopes in Loose Sand and Silt", Marine Geotechnique, Proc. ~~O~~of the Conf. On Marine Geotechnique, 1967, Adrian F. Richards, ed., pp. 221-239

Atkinson, J.H., Bransby, P.L.~~,~~ (1978). The Mechanics of Soils: An Introduction to Critical State Soil Mechanics, Mc Graw-Hill Book Company (UK) Ltd. pp. 339.

Bjerrum, L. (1961). The effective Shear Strength Parameters of Sensitive Clays, NGI Publication 45

Bjerrum, L. (1971).~~,~~ Subaqueous Slope Failures in Norwegian Fjords, NGI publication 88.

Bjerrum, L., Kringstad, S., Kummeneje, O. (1961)., The Shear Strength of a Fine Sand, NGI Publication 45.

Boutwell, G. P. & Schmidt, P. D. (1998)., Pre-instrumented Riverbank Slide, Stability of Natural Slopes in the Coastal Plain, Geotechnical Special Publication 77, ASCE.

Bryn, P., Østomo, S. R., Lien, R., and Berg, K., of Norsk Hydro and Tjelta, T. I., of Statoil, (1998)., Slope Stability in the Deep Water Areas off Mid Norway, OTC paper 8640

BS 1377 Parts 1 and 2 1990, "Methods of test for soils for civil engineering purposes. Classification tests", BSPL, 38 and 68 pages respectively.

Divakarla, P. & Marcari, E. J. (1998)., Stability Analysis of Slopes in Western Puerto Rico, A GIS Approach, Stability of Natural Slopes in the Coastal Plain, Geotechnical Special Publication 77, ASCE.

Edgers, L. and Karlsrud, K. (1985)., Viscous Analysis of Submarine Flows, Behaviour of Offshore Structures, pp. 773-784, Elsevier.

Kishida, H. (1965). Damage of Reinforced Concrete Buildings in Nigata city with Special Reference to Foundation Engineering. Tokyo Building Research institute. 17 + [18] pp. Also published in Soil and Foundation, Vol. 6, No. 1, 1965.

Konert, M., Vandenberghe, J. (1997), Comparison of Laser Grain Size Analysis with Pipette and Sieve Analysis: A Solution for the Underestimated Clay Fraction, Sedimentology 44, 523-535.

Langer, K. (1938), see Terzaghi, K., and Peck, R. B. (1948). Soil Mechanics in Engineering Practice. New York, John Wiley & Sons., pp. 102-105.

Locat, J. (2001), Instabilities along Ocean Margins; A Geomorphological and Geotechnical Perspective, Marine and Petroleum Geology 18 503-512.

Leroueil, S., Vaunat, J., Picarelli, L., Locat, J., Lee, H., and Faure, R. (1996). Geotechnical Characterisation of Slope Movements. In K. Senneset (Ed.) Proceedings of the 7th International Symposium on Landslides, Trondheim, Norway (pp. 53-74).

Lunne, T., Berre, T. & Strandvik, S., (1997). Sample Disturbance Effects in Soft Low Plasticity Norwegian Clay. Proc. Sym. on Recent Developments in Soil and Pavement Mechanics, Rio de Janerio, June 1997, p81-92, published by Balkema.

Martin, R. E. & Seli, J. J., (1998),. Landslide Evaluation in Virginia Coastal Plain, Stability of Natural Slopes in the Coastal Plain, Geotechnical Special Publication 77, ASCE.

Nadim, F. and Kalsnes, B. and Eide, A. (1997). Analysis of Submarine Slope Stability under Seismic Action, NGI Publication 201.

Praeg, D. & Shannon, P.M., (2000). Shallow Seismic Site Surveys from Blocks 83/24,83/20, 75/10, 16/28, 11/20, 78/28: An Interpretation and Seismic Integration with Boreholes. *Technical Report from PIP/RSG, UCD Contribution to RSG Project 98/23.*

Shannon, P.M., O'Reilly, B.M., Readman, P.W., Jacob, A.W.B., & Kenyon, N. (2001). Slope failure features on the margin of the Rockall Trough. In: Shannon, P.M., Haughton, P.D.W. & Corcoran, D.V. (eds) The Petroleum Exploration of Ireland's Offshore Basins. Geological Society, London, Special Publication, 188.

Skaven-Haug, S. (1955). Submarine Slides in Trondheim Harbour. Teknisk Ukeblad, Vol. 102. pp. 133-144. Also published in Norwegian Geotechnical Institute Publication 7

Silva, A., Baxter, C., Bryant W., Bradshaw, A. and LaRosa, P. (2000). The Stress-Strain Behaviour and Stress State of Gulf of Mexico Clays in Relation to Slope Processes, OTC 12091, OTC Conference 2000.

Silva, A. J., Bryant, W. R., Young, A. G., Schultheiss, P., Dunlap, W. A., Sykora G., Bean, D., and Honangen, C. (1999). Long Coring in Deep Water for Seabed Research, Geohazard Studies and Geotechnical Investigations, OTC Paper No. 10923, OTC Conference 1999.

Terzaghi, K. (1950). Shear Characteristics of quicksand and soft clay, Proceedings of the Seventh Texas Conference on Soil Mechanics and Foundation Engineering, Austin [10] pp.

Terzaghi, K. (1956). Varieties of Submarine Slope Failures. Proceedings of the Eighth Texas Conference on Soil Mechanics and Foundation Engineering. 41pp. Reprint, Harvard Soil Mechanics Series No. 52. Also published as Norwegian Geotechnical Institute Publication 25

Terzaghi, K. and Peck, R. B. (1948). Soil Mechanics in Engineering Practice. New York, John Wiley & Sons. 566 pp.

Tjelta, T.I., Strout, J., Solheim, A., Mokkelbost, K.H., Berg, K., Bryn, P. (2002), Geological and Geotechnical Investigations of in the Storegga Slide Area, International Conference Offshore Site Investigation and Geotechnics, Sustainability through Diversity, 26-28 November 2002.

Watanabe, T. (1965). Niigata earthquake: feature on the damage and related problems, University of Tokyo, Collected papers of the faculty of engineering, Department of Civil Engineering, vol. 3, Report 6501.

Øvrebø, L. K., ~~Haughton, P., Shannon, P.,~~ Geological Analysis of Gravity Cores from The Rockall Trough, PhD. Thesis U.C.D., ~~to be published~~in preparation.

Appendix 1: Raw Data: Moisture Contents

Site 1
Borehole No 83/24-Sc001
Box No. 1

Date	Site			
11/12/00	1			
BS1377: Part 2: 1990				
Sample No.	1E	1E	2E	2E
Container No.	104	6	15	2103
Mass of wet soil & container (m_2)	38.89	36.04	40.35	37.52
Mass of dry soil & container (m_3)	29	24.3	29.55	25.74
Mass of container (m_1)	13.93	9.13	14.2	8.77
Mass of moisture (m_2-m_3)	9.89	11.74	10.8	11.78
Mass of dry soil (m_3-m_1)	15.07	15.17	15.35	16.97
Moisture Content (w=((m2-m3)/(m3-m1))*100)	65.62707366	77.38958471	70.35830619	69.41661756
Depth of Sample (m)	0.11-0.265	0.11-0.265	0.38-0.5	0.38-0.5
Average Moisture Content	71.50832918		69.88746187	

Borehole No. 83/24-Sc002
Box No. 1

Date	Site

02/11/00	1					
BS1377: Part 2: 1990						
Sample No.	1E	1E	2E	2E	3E	3E
Container No.	131	2	17	18	31	34
Mass of wet soil & container (m_2)	38.05	34.63	44.67	37.27	35.96	38.39
Mass of dry soil & container (m_3)	28.05	25.88	32.7	27.6	26.85	28.53
Mass of container (m_1)	14.1	14.1	14.07	14.08	14.01	14.01
Mass of moisture (m_2-m_3)	10	8.75	11.97	9.67	9.11	9.86
Mass of dry soil (m_3-m_1)	13.95	11.78	18.63	13.52	12.84	14.52
Moisture Content (w=((m2-m3)/(m3-m1))*100)	72	74	64	72	71	68
Depth of Sample	0.14-0.22	0.14-0.22	0.27-0.37	0.27-0.37	0.475-0.585	0.475-0.585
Average Moisture Content	73		68		69	

Borehole No. 83/24-Sc003
Box No. 2

Date	Site	Borehole No.
29/01/01	1	83/24/Sc003
BS1377: 1990: Part 2		Box1
Sample No.	1	2
Container No.	I	B1A
Mass of wet soil & container (m_2)	27.47	36.4
Mass of dry soil & container (m_3)	20	24.99
Mass of container (m_1)	9.1	8.58
Mass of moisture (m_2-m_3)	7.47	11.41
Mass of dry soil (m_3-m_1)	10.9	16.41
Moisture Content (w=((m2-m3)/(m3-m1))*100)	68.532	69.53077
Depth of Sample	59.5-85cm	
Average Moisture Content	69.031	

Borehole No. 83/24-Sc005
Box No. 1

Date	Site	Borehole No.
05/12/00	1	83/24-Sc005

BS1377: Part 2: 1990: 4.3/4.4				
Sample No.	5E	5E	4E	4E
Container No.	15	2	21	131
Mass of wet soil & container (m_2)	37.91	39.65	41.25	39.65
Mass of dry soil & container (m_3)	25.84	29.23	29.89	25.31
Mass of container (m_1)	8.73	14.06	14.26	14.09
Mass of moisture (m_2-m_3)	12.07	10.42	11.36	14.34
Mass of dry soil (m_3-m_1)	17.11	15.17	15.63	11.22
Moisture Content (w=((m2-m3)/(m3-m1))*100)	70.5435	68.6882004	72.6807	127.807
Depth of Sample	0.33-0.41		0.145-0.165	
Average Moisture Content	69.6159		100.244	

Borehole No. 83/24-Sc005
Box No. 3

Tested to BS1377: 1990: Part 2

Date	Site	Borehole No.
01/12/00	1	83/24-sc005(3)

Sample No.	1E	1E	2E	2E	3E	3E
Container No.	15	18	11	21	2	9
Mass of wet soil & container (m_2), g	28.73	34.56	40.12	46.5	24.7	29.16
Mass of dry soil & container (m_3), g	20.7	26.59	29.19	32.9	20.51	23.17
Mass of container (m_1), g	8.71	14.08	14.14	14.26	14.07	14
Mass of moisture (m_2-m_3, g	8.03	7.97	10.93	13.6	4.19	5.99
Mass of dry soil (m_3-m_1), g	11.99	12.51	15.05	18.64	6.44	9.17
Moisture Content (w=((m_2-m_3)/(m_3-m_1))*100), %	66.9725	63.709	72.6246	72.9614	65.0621	65.3217
Depth of Sample						
Average Moisture Content (w%)	65.3408		72.793		65.1919	

Site 1A
Borehole No. 83/20-Sc001
Box No. 1

Date	Site	Borehole No.
29/01/01	1A	83/20/Sc001
BS 1377: 1990: Part 2		Box 1 of 2
Sample No.		
Container No.	1	7
Mass of wet soil & container (m_2)	21.63	33.13
Mass of dry soil & container (m_3)	15.79	22.32
Mass of container (m_1)	8.75	8.77
Mass of moisture (m_2-m_3)	5.84	10.81
Mass of dry soil (m_3-m_1)	7.04	13.55
Moisture Content (w=((m2-m3)/(m3-m1))*100)	82.95455	79.77859779
Depth of Sample	25-72cm	
Average Moisture Content	81.36657	

Box No. 2
Moisture Contents

Date	Site	Borehole No.
29.01.01	1A	83/20/Sc001
BS 1377: 1990: Part 2		Box 2 of 2
Sample No.		
Container No.	3	2
Mass of wet soil & container (m_2)	37.34	39.76
Mass of dry soil & container (m_3)	27.75	30.12
Mass of container (m_1)	8.57	8.91
Mass of moisture (m_2-m_3)	9.59	9.64
Mass of dry soil (m_3-m_1)	19.18	21.21
Moisture Content (w=((m2-m3)/(m3-m1))*100)	50	45.45025931
Depth of Sample		
Average Moisture Content	47.72513	

Borehole No. 83/20-Sc002
Box No. 1

Date	Site	Borehole No.

13/03/01	1A	83/20-Sc002
BS 1377: 1990: Part 2		Box 1 of 2
Sample No.		
Container No.	B1A	7
Mass of wet soil & container (m_2)	29.69	24.46
Mass of dry soil & container (m_3)	24.1	21.19
Mass of container (m_1)	8.57	8.77
Mass of moisture (m_2-m_3)	5.59	3.27
Mass of dry soil (m_3-m_1)	15.53	12.42
Moisture Content (w=((m2-m3)/(m3-m1))*100)	35.9948	26.328502
Depth of Sample		
Average Moisture Content	31.1617	

Box No. 2

Date	Site	Borehole No.
13/03/01	1A	83/20-Sc002
BS 1377: 1990: Part 2		Box 2 of 2
Sample No.	2	
Container No.	3	I
Mass of wet soil & container (m_2)	36.68	31.64
Mass of dry soil & container (m_3)	31.66	27.9
Mass of container (m_1)	8.56	9.11
Mass of moisture (m_2-m_3)	5.02	3.74
Mass of dry soil (m_3-m_1)	23.1	18.79
Moisture Content (w=((m2-m3)/(m3-m1))*100)	21.7316	19.90420436
Depth of Sample	1.41-1.68	
Average Moisture Content	20.8179	

Borehole No. 83/20-Sc005

Box No. 2

Date	Site	Borehole

		No.
13/03/01	1A	83/20-Sc005

BS 1377: 1990: Part 2

Sample No.	1	
Container No.	N1	2
Mass of wet soil & container (m_2)	45.73	43.38
Mass of dry soil & container (m_3)	36.38	35.26
Mass of container (m_1)	8.72	8.9
Mass of moisture (m_2-m_3)	9.35	8.12
Mass of dry soil (m_3-m_1)	27.66	26.36
Moisture Content (w=((m2-m3)/(m3-m1))*100)	33.80333	30.80424886
Depth of Sample (m)	0.83-1.11	
Average Moisture Content	32.30379	

Site 2
Borehole No. 16/28-Sc001
Box No. 2

Date	Site	Borehole No.		
30/05/01	2	16/28-Sc001		
BS 1377: 1990: Part 2				
Sample No.	1E	1E	2E	2E
Container No.	14	2	18	23
Mass of wet soil & container (m_2)	25.31	27.04	28.58	26.38
Mass of dry soil & container (m_3)	20.39	21.4	22.17	20.94
Mass of container (m_1)	14.1	14.06	14.08	14.06
Mass of moisture (m_2-m_3)	4.92	5.64	6.41	5.44
Mass of dry soil (m_3-m_1)	6.29	7.34	8.09	6.88
Moisture Content (w=((m2-m3)/(m3-m1))*100)	78.21939587	76.83923706	79.23362176	79.06976744
Depth of Sample	0.45-0.53		0.615-0.72	
Average Moisture Content	77.52931646		79.1516946	

Borehole No. 16/28-Sc002
Box No. 1

Date	Site	Borehole No.
30/05/01	2	16/28-Sc002
BS 1377: 1990: Part 2		
Sample No.	16/28-Sc001 (2) 1E	16/28-Sc001 (2) 1E
Container No.	131	9
Mass of wet soil & container (m_2)	33.35	29.6
Mass of dry soil & container (m_3)	27.25	24.35
Mass of container (m_1)	14.12	14
Mass of moisture (m_2-m_3)	6.1	5.25
Mass of dry soil (m_3-m_1)	13.13	10.35
Moisture Content (w=((m2-m3)/(m3-m1))*100)	46.458492	50.72463768
Depth of Sample	0.055-0.18	
Average Moisture Content	48.59156484	

Site 3
Borehole No. 11/20-Sc006
Box No. 2

Date	Site	Borehole No.		
19/04/01	3A	11/20-Sc006(2)		
BS 1377: 1990: Part 2				
Sample No.	2/3 1E	2/3 1E	2/3 2E	2/3 2E
Container No.	9	131	23	18
Mass of wet soil & container (m_2)	27.73	30.01	29.51	35.42
Mass of dry soil & container (m_3)	23.11	24.8	24.72	28.77
Mass of container (m_1)	14	14.13	14.05	14.07
Mass of moisture (m_2-m_3)	4.62	5.21	4.79	6.65
Mass of dry soil (m_3-m_1)	9.11	10.67	10.67	14.7
Moisture Content (w=((m2-m3)/(m3-m1))*100)	50.71350165	48.8284911	44.89222	45.23809524
Depth of Sample	0.58-0.865		1.07-1.35	
Average Moisture Content	49.77099637		45.06516	

Box No. 3

Date	Site	Borehole No.
19/04/01	3A	11/20-Sc006(3)
BS 1377: 1990: Part 2		
Sample No.	3/3 1E	3/3 1E
Container No.	14	2
Mass of wet soil & container (m_2)	33.05	43.04
Mass of dry soil & container (m_3)	27.77	34.92
Mass of container (m_1)	14.11	14.06
Mass of moisture (m_2-m_3)	5.28	8.12
Mass of dry soil (m_3-m_1)	13.66	20.86
Moisture Content (w=((m2-m3)/(m3-m1))*100)	38.653	38.9261745
Depth of Sample	1.99-1.23	
Average Moisture Content	38.78959	

Borehole No. 11/20-Sc007
Box No. 1

Date	Site	Borehole No.
27/04/01	3A	11/20-Sc007
BS 1377: 1990: Part 2		
Sample No.	1E(1)	1E(1)
Container No.	131	2
Mass of wet soil & container (m_2)	30.51	29.21
Mass of dry soil & container (m_3)	25.8	24.98
Mass of container (m_1)	14.12	14.09
Mass of moisture (m_2-m_3)	4.71	4.23
Mass of dry soil (m_3-m_1)	11.68	10.89
Moisture Content (w=((m2-m3)/(m3-m1))*100)	40.32534247	38.84297521
Depth of Sample	0.39-0.59	
Average Moisture Content	39.58415884	

Borehole No. 11/20-Sc008
Box No. 1

Date	Site	Borehole No.
25/04/01	3	11/20-Sc008
BS 1377: 1990: Part 2		
Sample No.	1E(1)	1E(1)
Container No.	7	13
Mass of wet soil & container (m_2)	22	25.14
Mass of dry soil & container (m_3)	17.87	19.97
Mass of container (m_1)	8.77	8.75
Mass of moisture (m_2-m_3)	4.13	5.17
Mass of dry soil (m_3-m_1)	9.1	11.22
Moisture Content (w=((m2-m3)/(m3-m1))*100)	45.38461538	46.07843137
Depth of Sample	0.115-0.24	
Average Moisture Content	45.73152338	

Box No. 2

Date	Site	Borehole No.
25/04/01	3	11/20-Sc008
BS 1377: 1990: Part 2		
Sample No.	2E(2)	2E(2)
Container No.	2	107
Mass of wet soil & container (m_2)	31.47	33.5
Mass of dry soil & container (m_3)	24.22	25.98
Mass of container (m_1)	8.68	8.93
Mass of moisture (m_2-m_3)	7.25	7.52
Mass of dry soil (m_3-m_1)	15.54	17.05
Moisture Content (w=((m2-m3)/(m3-m1))*100)	46.65379665	44.10557185
Depth of Sample		
Average Moisture Content	45.37968425	

Borehole No. 11/20-Sc010
Box No. 3

Date	Site	Borehole No.		
15/05/01	3	11/20-Sc010		
BS 1377: 1990: Part 2				
Sample No.	1E	1E	2E	2E
Container No.	14	2	9	131
Mass of wet soil & container (m_2)	23.94	42.41	31.02	29.54
Mass of dry soil & container (m_3)	21.11	34.22	26.18	25.21
Mass of container (m_1)	14.11	14.07	14	14.12
Mass of moisture (m_2-m_3)	2.83	8.19	4.84	4.33
Mass of dry soil (m_3-m_1)	7	20.15	12.18	11.09
Moisture Content (w=((m2-m3)/(m3-m1))*100)	40.42857143	40.64516129	39.73727422	39.04418
Depth of Sample	1.86-2.76m		1.62-1.72m	
Average Moisture Content	40.53686636		39.39072908	

Site 3A
Borehole No. 11/20-Sc001
Box No. 1

Date	Site	Borehole No.		
31/05/01	3A	11/20-Sc001		
BS 1377: 1990: Part 2				
Sample No.	1E	1E	2E	2E
Container No.	17	18	3	15
Mass of wet soil & container (m_2)	37.15	43.22	47.05	33.07
Mass of dry soil & container (m_3)	30.28	34.4	36.6	27.2
Mass of container (m_1)	14.07	14.07	13.92	14.2
Mass of moisture (m_2-m_3)	6.87	8.82	10.45	5.87
Mass of dry soil (m_3-m_1)	16.21	20.33	22.68	13
Moisture Content (w=((m2-m3)/(m3-m1))*100)	42.38125	43.38416134	46.07584	45.15385
Depth of Sample	0.07-0.565		0.855-0.99	
Average Moisture Content	42.8827		45.61484	

Box No. 2

Date	Site	Borehole No.
31/05/01	3A	11/20-Sc001
BS 1377: 1990: Part 2		
Sample No.	1E	1E
Container No.	4	5
Mass of wet soil & container (m_2)	30.53	36.53
Mass of dry soil & container (m_3)	24.8	29.3
Mass of container (m_1)	8.74	9.04
Mass of moisture (m_2-m_3)	5.73	7.23
Mass of dry soil (m_3-m_1)	16.06	20.26
Moisture Content (w=((m2-m3)/(m3-m1))*100)	35.6787	35.68608095
Depth of Sample	1.61-1.715	
Average Moisture Content	35.68239	

Borehole No. 11/20-Sc002

Box No. 1

Date	Site	Borehole No.		
16/03/01	3A	11/20-Sc002(1)		
BS 1377: 1990: Part 2				
Sample No.	1E(1)	1E(1)	2E(1)	2E(1)
Container No.	131	23	104	21
Mass of wet soil & container (m_2)	35.6	32.21	31.22	32.37
Mass of dry soil & container (m_3)	27.3	24.81	24.1	24.98
Mass of container (m_1)	14.13	14.07	13.92	14.25
Mass of moisture (m_2-m_3)	8.3	7.4	7.12	7.39
Mass of dry soil (m_3-m_1)	13.17	10.74	10.18	10.73
Moisture Content (w=((m2-m3)/(m3-m1))*100)	63.02202	68.90130354	69.94106	68.87232
Depth of Sample	0.0-0.185		0.27-0.44	
Average Moisture Content	65.96166		69.40669	

Box No. 3

Date	Site	Borehole No.
16/03/01	3A	11/20-Sc002(3)
BS 1377: 1990: Part 2		
Sample No.	1E(3)	1E(3)
Container No.	18	17
Mass of wet soil & container (m_2)	32.37	27.85
Mass of dry soil & container (m_3)	25.43	22.58
Mass of container (m_1)	14.08	14.07
Mass of moisture (m_2-m_3)	6.94	5.27
Mass of dry soil (m_3-m_1)	11.35	8.51
Moisture Content (w=((m2-m3)/(m3-m1))*100)	61.14537	61.92714454
Depth of Sample	1.77-2.18	
Average Moisture Content	61.53626	

Borehole No. 11/20-Sc003

Box No. 1

Date	Site	Borehole No.		
23/03/01	3A	11/20-Sc003(1)		
BS 1377: 1990: Part 2				
Sample No.	1E	1E	2E	2E
Container No.	104	21	23	18
Mass of wet soil & container (m_2)	27.65	26.87	26.36	26.64
Mass of dry soil & container (m_3)	23.07	22.76	22.17	22.57
Mass of container (m_1)	13.92	14.26	14.07	14.08
Mass of moisture (m_2-m_3)	4.58	4.11	4.19	4.07
Mass of dry soil (m_3-m_1)	9.15	8.5	8.1	8.49
Moisture Content (w=((m2-m3)/(m3-m1))*100)	50.05464	48.35294118	51.7284	47.93875
Depth of Sample	0.105-0.205		0.32-0.42	
Average Moisture Content	49.20379		49.83357	

Box No. 2

Date	Site	Borehole No.
23/03/01	3A	11/20-Sc003(2)
BS 1377: 1990: Part 2		
Sample No.	3E(2)	3E(2)
Container No.	17	131
Mass of wet soil & container (m_2)	33.73	26.54
Mass of dry soil & container (m_3)	26.86	22.24
Mass of container (m_1)	14.07	14.03
Mass of moisture (m_2-m_3)	6.87	4.3
Mass of dry soil (m_3-m_1)	12.79	8.21
Moisture Content (w=((m2-m3)/(m3-m1))*100)	53.71384	52.37515225
Depth of Sample	0.73-1.315	
Average Moisture Content	53.0445	

Borehole No. 11/20-Sc004

Box No. 2

Date	Site	Borehole No.
11/04/01	3A	11/20-Sc004(2&3)
BS 1377: 1990: Part 2		
Sample No.	11/20-Sc004(2)	11/20-Sc004(2)
Container No.	17	18
Mass of wet soil & container (m_2)	35.46	33.33
Mass of dry soil & container (m_3)	29.28	27.52
Mass of container (m_1)	14.08	14.08
Mass of moisture (m_2-m_3)	6.18	5.81
Mass of dry soil (m_3-m_1)	15.2	13.44
Moisture Content (w=((m2-m3)/(m3-m1))*100)	40.65789474	43.22916667
Depth of Sample	0.38-0.84	
Average Moisture Content	41.9435307	

Box No. 3

Date	Site	Borehole No.
11/04/01	3A	11/20-Sc004(3)
BS 1377: 1990: Part 2		
Sample No.	11/20-Sc004(3)	11/20-Sc004(3)
Container No.	23	131
Mass of wet soil & container (m_2)	39.17	33.01
Mass of dry soil & container (m_3)	32.33	27.84
Mass of container (m_1)	14.06	14.14
Mass of moisture (m_2-m_3)	6.84	5.17
Mass of dry soil (m_3-m_1)	18.27	13.7
Moisture Content (w=((m2-m3)/(m3-m1))*100)	37.43842365	37.73722628
Depth of Sample	1.595-1.83	
Average Moisture Content	37.58782496	

Appendix 1.2: ***Raw Data: Specific Gravity of fine-grained soils***
Site 1
Borehole No. 83/24-Sc002
Box No. 1

DATE 13/03/2001
Borehole Number 83/24-Sc002 Box 1
Test Method BS1377: 1990: Part 2

Test Number	1	2	3	4	5	6
Specimen Reference	1E(A)	1E(B)	2E(A)	2E(B)	3E(A)	3E(B)
Pyknometer Number	775	3422	3440	838	769	3398
Mass of bottle, soil and water, m_3 g	80.535	85.244	85.377	82.552	91.283	87.066
Mass of bottle and soil, m_2 g	33.31	37.127	38.172	35.628	44.582	41.735
Mass of bottle full of water, m_4 g	77.331	81.547	80.43	78.109	84.066	80.374
Mass of bottle, m_1 g	27.79	31.175	30.13	28.42	33.156	31.089
Mass of soil, m_2-m_1 g	5.52	5.9518	8.0423	7.2083	11.426	10.646
Mass of water in full bottle, m_4-m_1 g	49.541	50.372	50.3	49.689	50.91	49.285
Mass of water used, m_3-m_2 g	47.225	48.118	47.205	46.924	46.701	45.331
Volume of soil particles, (m_4-m_1)-(m_3-m_2) mL	2.316	2.2548	3.0953	2.7654	4.2092	3.954
Particle Density, r_s=(m2-m1)r_L/((m4-m1)-(m3-m1)) Mg/m^3	2.3834	2.6396	2.5982	2.6066	2.7146	2.6924
Average Value, r_s Mg/m^3	2.5115		2.6024		2.7035	

Borehole No. 83/24-Sc003
Box No. 2

DATE 13/03/01
Borehole No. 83/24-Sc003 Box 2
Test Method BS 1377: 1990: Part 2

Test Number		1	2
Specimen Reference		83/24/Sc003(1)	83/24/Sc003(1)
Pyknometer Number		775	769
Mass of bottle, soil and water, m_3	g	85.5692	91.9424
Mass of bottle and soil, m_2	g	41.4161	46.4455
Mass of bottle full of water, m_4	g	77.4264	84.1675
Mass of bottle, m_1	g	27.726	33.1021
Mass of soil, m_2-m_1	g	13.6901	13.3434
Mass of water in full bottle, m_4-m_1	g	49.7004	51.0654
Mass of water used, m_3-m_2	g	44.1531	45.4969
Volume of soil particles, (m_4-m_1)-(m_3-m_2)	mL	5.5473	5.5685
Particle Density, r_s=(m2-m1)r_L/((m4-m1)-(m3-m1))	Mg/m^3	2.467885278	2.396228787
Average Value, r_s	Mg/m^3	2.432057032	

Borehole No. 83/24-Sc005
Box No. 1

DATE 13/03/01
Test Method Small Pyknometers
Method of Preparation BS 1377: 1990: Part 2

Test Number		1	2	3	4
Specimen Reference		4E	4E	5E	5E
Pyknometer Number		3398	775	769	3422
Mass of bottle, soil and water, m_3	g	83.8774	81.9535	92.6463	89.5686
Mass of bottle and soil, m_2	g	37.2598	35.6151	46.9254	44.271
Mass of bottle full of water, m_4	g	80.4634	77.5762	84.1908	81.653
Mass of bottle, m_1	g	31.0878	27.7941	33.1414	31.1493
Mass of soil, m_2-m_1	g	6.172	7.821	13.784	13.1217
Mass of water in full bottle, m_4-m_1	g	49.3756	49.7821	51.0494	50.5037
Mass of water used, m_3-m_2	g	46.6176	46.3384	45.7209	45.2976
Volume of soil particles, (m_4-m_1)-(m_3-m_2)	mL	2.758	3.4437	5.3285	5.2061
Particle Density, r_s=(m2-m1)r_L/((m4-m1)-(m3-m1))	Mg/m^3	2.237854	2.2711	2.58684	2.52045
Average Value, r_s	Mg/m^3	2.254479		2.55365	

Borehole No. 83/24-Sc005
Box No. 3

DATE	06/12/2000
Borehole Number	83/24-Sc005(III)
Test Method	Small Pyknometers
Method of Preparation	BS 1377: 1990: Part 2

Specimen Reference	1E(A)	1E(B)	2E(A)	2E(B)	3E(A)	3E(B)
Pyknometer Number	3398	3422	775	838	3440	769
Mass of bottle, soil and water, m_3, g	84.6037	84.73	81.632	82.354	85.716	88.537
Mass of bottle and soil, m_2, g	38.2143	36.173	34.585	35.344	38.634	40.067
Mass of bottle full of water, m_4, g	80.4428	81.639	77.536	78.202	80.419	84.246
Mass of bottle, m_1, g	31.1138	31.146	27.797	28.407	30.066	33.177
Mass of soil, m_2-m_1, g	7.1005	5.0274	6.7882	6.9372	8.5678	6.8896
Mass of water in full bottle, m_4-m_1, g	49.329	50.493	49.739	49.795	50.353	51.069
Mass of water used, m_3-m_2, g	46.3894	48.557	47.047	47.01	47.082	48.47
Volume of soil particles, (m_4-m_1)-(m_3-m_2), mL	2.9396	1.9357	2.6922	2.7851	3.2706	2.5983
Particle Density, r_s=(m2-m1)r_L/((m4-m1)-(m3-m1)), Mg/m^3	2.41546	2.5972	2.5214	2.4908	2.6196	2.6516
Average Value, r_s, Mg/m^3	2.50633		2.5061		2.6356	

Site 1A
Borehole No. 83/20-Sc001
Box No. 1

DATE 21/03/01
Test Method Small Pyknometers
Method of Preparation BS 1377: 1990: Part 2

Test Number		3	4
Specimen Reference		83/20/Sc001(1)	83/20/Sc001(1)
Pyknometer Number		838	3398
Mass of bottle, soil and water, m_3	g	84.4935	85.9125
Mass of bottle and soil, m_2	g	38.9468	40.5586
Mass of bottle full of water, m_4	g	78.1557	80.4268
Mass of bottle, m_1	g	28.3596	31.052
Mass of soil, m_2-m_1	g	10.5872	9.5066
Mass of water in full bottle, m_4-m_1	g	49.7961	49.3748
Mass of water used, m_3-m_2	g	45.5467	45.3539
Volume of soil particles, (m_4-m_1)-(m_3-m_2)	mL	4.2494	4.0209
Particle Density, r_s=(m2-m1)r_L/((m4-m1)-(m3-m1))	Mg/m^3	2.491457618	2.364296551
Average Value, r_s	Mg/m^3	2.427877084	

DATE 21/03/01
Test Method Small Pyknometers
Method of Preparation BS 1377: 1990: Part 2

Test Number		5	6
Specimen Reference		83/20/Sc001(2)	83/20/Sc001(2)
Pyknometer Number		3422	3440
Mass of bottle, soil and water, m_3	g	91.867	89.8025
Mass of bottle and soil, m_2	g	49.2456	46.7696
Mass of bottle full of water, m_4	g	81.5917	80.4163
Mass of bottle, m_1	g	31.1147	30.0397
Mass of soil, m_2-m_1	g	18.1309	16.7299
Mass of water in full bottle, m_4-m_1	g	50.477	50.3766
Mass of water used, m_3-m_2	g	42.6214	43.0329
Volume of soil particles, (m_4-m_1)-(m_3-m_2)	mL	7.8556	7.3437
Particle Density, r_s=(m2-m1)r_L/((m4-m1)-(m3-m1))	Mg/m^3	2.308022303	2.278129553
Average Value, r_s	Mg/m^3	2.293075928	

Borehole No. 83/20-Sc002
Box No. 1

DATE 11/04/01
Test Method BS 1377: 1990: Part 2
Method of Preparation Small Pyknometers

Test Number	1	2
Specimen Reference	83/20-Sc002(1)	83/20-Sc002(1)
Pyknometer Number	838	3398
Mass of bottle, soil and water, m_3, g	84.2185	85.8377
Mass of bottle and soil, m_2, g	37.9669	39.6853
Mass of bottle full of water, m_4, g	78.182	80.4254
Mass of bottle, m_1, g	28.3995	31.0921
Mass of soil, m_2-m_1, g	9.5674	8.5932
Mass of water in full bottle, m_4-m_1, g	49.7825	49.3333
Mass of water used, m_3-m_2, g	46.2516	46.1524
Volume of soil particles, (m_4-m_1)-(m_3-m_2), mL	3.5309	3.1809
Particle Density, r_s=(m2-m1)r_L/((m4-m1)-(m3-m1)) Mg/m^3	2.709620777	2.701499576
Average Value, r_s Mg/m^3	2.705560176	

Box No. 2
DATE 11/04/01
Test Method Small Pyknometer
Method of Preparation BS 1377: 1990: Part 2

Test Number	3	4
Specimen Reference	83/20-Sc002(2)	83/20-Sc002(2)
Pyknometer Number	769	3440
Mass of bottle, soil and water, m_3 g	91.1049	86.8773
Mass of bottle and soil, m_2 g	44.0443	40.374
Mass of bottle full of water, m_4 g	84.2442	80.4008
Mass of bottle, m_1 g	33.15	30.077
Mass of soil, m_2-m_1 g	10.8943	10.297
Mass of water in full bottle, m_4-m_1 g	51.0942	50.3238
Mass of water used, m_3-m_2 g	47.0606	46.5033
Volume of soil particles, (m_4-m_1)-(m_3-m_2) mL	4.0336	3.8205
Particle Density, r_s=(m2-m1)r_L/((m4-m1)-(m3-m1)) Mg/m^3	2.700887545	2.695196964
Average Value, r_s Mg/m^3	2.698042254	

Site 3A
Borehole No. 11/20-Sc001
Box No. 1
Date 31/05/01
Test Method BS 1377: 1990: Part 2
Method of Preparation Small Pyknometers

Test Number	1	2	3	4
Specimen Reference	1E(1)		2E(1)	
Pyknometer Number	3440	838	3422	769
Mass of bottle, soil and water, $m_{3,g}$	91.1531	90.1599	92.1443	94.6383
Mass of bottle and soil, $m_{2,}$ g	47.2918	47.5996	47.7834	49.7248
Mass of bottle full of water, $m_{4,}$ g	80.3738	78.1565	81.5971	84.18323
Mass of bottle, $m_{1,}$ g	30.069	28.4008	31.1422	33.1751
Mass of soil, m_2-$m_{1,}$ g	17.2228	19.1988	16.6412	16.5497
Mass of water in full bottle, m_4-$m_{1,}$ g	50.3048	49.7557	50.4549	51.00813
Mass of water used, m_3-$m_{2,}$ g	43.8613	42.5603	44.3609	44.9135
Volume of soil particles, $(m_4-m_1)-(m_3-m_2)$, mL	6.4435	7.1954	6.094	6.094625
Particle Density, $r_s=(m2-m1)r_L/((m4-m1)-(m3-m1))$, Mg/m^3	2.672895166	2.668205	2.730752	2.715458
Average Value, $r_{s,}$ Mg/m^3	2.670549926		2.723105	

Box No. 2
Date 31/05/01
Test Method BS 1377: 1990: Part 2
Method of Preparation Small Pyknometers

Test Number	1	2
Specimen Reference	1E(2)	
Pyknometer Number	775	3398
Mass of bottle, soil and water, $m_{3,}$ g	89.4093	92.7463
Mass of bottle and soil, $m_{2,}$ g	46.6987	50.7602
Mass of bottle full of water, $m_{4,}$ g	84.2178	80.3951
Mass of bottle, $m_{1,}$ g	27.8088	31.0985
Mass of soil, m_2-$m_{1,}$ g	18.8899	19.6617
Mass of water in full bottle, m_4-$m_{1,}$ g	56.409	49.2966
Mass of water used, m_3-$m_{2,}$ g	42.7106	41.9861
Volume of soil particles, $(m_4-m_1)-(m_3-m_2)$,mL	13.6984	7.3105
Particle Density, $r_s=(m2-m1)r_L/((m4-m1)-(m3-m1))$,$Mg/m^3$	1.3789859	2.689515
Average Value, $r_{s,}$ Mg/m^3	2.0342505	

Borehole No. 11/20-Sc002
Box No. 1

Date 31/05/01

Test Method BS 1377: 1990: Part 2

Method of Preparation Small Pyknometers

Test Number	1	2	3	4
Specimen Reference	1E(1)		2E(1)	
Pyknometer Number	769	3440	3422	775
Mass of bottle, soil and water, m_3, g	91.6234	88.0431	89.0205	82.7777
Mass of bottle and soil, m_2, g	44.7344	42.1094	42.7964	36.0433
Mass of bottle full of water, m_4, g	84.2305	80.3873	81.6086	77.5091
Mass of bottle, m_1, g	33.1389	30.0767	31.1551	27.7796
Mass of soil, m_2-m_1, g	11.5955	12.0327	11.6413	8.2637
Mass of water in full bottle, m_4-m_1, g	51.0916	50.3106	50.4535	49.7295
Mass of water used, m_3-m_2, g	46.889	45.9337	46.2241	46.7344
Volume of soil particles, (m_4-m_1)-(m_3-m_2),mL	4.2026	4.3769	4.2294	2.9951
Particle Density, r_s=(m2-m1)r_L/((m4-m1)-(m3-m1)),Mg/m^3	2.75913	2.74914	2.75247	2.75907
Average Value, r_s,Mg/m^3	2.75413		2.75577	

Box No. 3

Date 31/05/01

Test Method BS 1377: 1990: Part 2

Method of Preparation Small Pyknometers

Test Number	5	6
Specimen Reference	1E(3)	
Pyknometer Number	838	3398
Mass of bottle, soil and water, m_3, g	84.9352	86.8903
Mass of bottle and soil, m_2, g	39.0723	41.2135
Mass of bottle full of water, m_4, g	78.1691	80.4087
Mass of bottle, m_1, g	24.416	31.07
Mass of soil, m_2-m_1, g	14.6563	10.1435
Mass of water in full bottle, m_4-m_1, g	53.7531	49.3387
Mass of water used, m_3-m_2, g	45.8629	45.6768
Volume of soil particles, (m_4-m_1)-(m_3-m_2),mL	7.8902	3.6619
Particle Density, r_s=(m2-m1)r_L/((m4-m1)-(m3-m1)),Mg/m^3	1.857532	2.77001
Average Value, r_s,Mg/m^3	2.313771	

Borehole No. 11/20-Sc003
Box No. 1

Date 31/05/01
Test Method BS 1377: 1990: Part 2
Method of Preparation Small Pyknometers

Test Number	1	2	3	4
Specimen Reference	1E		2E	
Pyknometer Number	838	769	775	3398
Mass of bottle, soil and water, m3, g	83.6925	89.854	83.5452	84.9267
Mass of bottle and soil, m2, g	37.1503	42.0404	37.2671	38.2131
Mass of bottle full of water, m4, g	78.1705	84.2339	77.5205	80.4152
Mass of bottle, m1, g	28.4039	33.1326	27.7714	31.0703
Mass of soil, m2-m1, g	8.7464	8.9078	9.4957	7.1428
Mass of water in full bottle, m4-m1, g	49.7666	51.1013	49.7491	49.3449
Mass of water used, m3-m2, g	46.5422	47.8136	46.2781	46.7136
Volume of soil particles, (m4-m1)-(m3-m2),mL	3.2244	3.2877	3.471	2.6313
Particle Density, rs=(m2-m1)rL/((m4-m1)-(m3-m1)),Mg/m3	2.71257	2.70943	2.73572	2.71455
Average Value, rs,Mg/m3	2.711		2.72514	

Box No. 2

Date 31/05/01
Test Method BS 1377: 1990: Part 2
Method of Preparation Small Pyknometers

Test Number	5	6
Specimen Reference	3E	
Pyknometer Number	3440	3422
Mass of bottle, soil and water, m3, g	86.0829	89.0774
Mass of bottle and soil, m2, g	39.0541	42.9117
Mass of bottle full of water, m4, g	80.4029	81.6277
Mass of bottle, m1, g	30.0655	31.1731
Mass of soil, m2-m1, g	8.9886	11.7386
Mass of water in full bottle, m4-m1, g	50.3374	50.4546
Mass of water used, m3-m2, g	47.0288	46.1657
Volume of soil particles, (m4-m1)-(m3-m2),mL	3.3086	4.2889
Particle Density, rs=(m2-m1)rL/((m4-m1)-(m3-m1)),Mg/m3	2.71674	2.73697
Average Value, rs,Mg/m3	2.72686	

Appendix 1.3: Raw Data: Plasticity Indices

Borehole Number 83/24-Sc002 Box 1
Liquid Limit (Cone Penetrometer) and Plastic Limit
Test to BS1377: Part 2: 1990: 4.3/4.4

Date	06/11/00		Sample	1E			
Test No.	1	2	3	4	5	6	7
Type of Test	LL	LL	LL	LL	PL	PL	PL
Initial Reading (mm)	0	0	0	0			
Final Reading (mm)	16.8	19.8	22.35	23.85			
Core Penetration (mm)	16.8	19.8	22.35	23.85			
Container No.	11	9	15	23	103	104	14
Mass of wet soil + container (g)	28.58	25.6	25.51	27.27	30.69	33.11	29.14
Mass of dry soil + container (g)	22.46	20.64	20.67	21.72	25.24	27.08	24.57
Mass of container (g)	14.14	14	14.2	14.07	14.06	13.96	14.1
Mass of Moisture (g)	6.12	4.96	4.84	5.55	5.45	6.03	4.57
Mass of dry soil (g)	8.32	6.64	6.47	7.65	11.18	13.12	10.47
Moisture Content (w%)	74	75	75		49	46	44

Liquid Limit 74.45
Plastic Limit 46
Plasticity Index 28

Date	06/11/00		Sample	2E			
Test No.	1	2	3	4	5	6	7
Type of Test	LL	LL	LL	LL	PL	PL	PL
Initial Reading (mm)	0	0	0	0			
Final Reading (mm)	15	17.9	20.25	24.1			
Core Penetration (mm)	15	17.9	20.25	24.1			
Container No.	17	34	18	31	2	131	12
Mass of wet soil + container (g)	21.88	30.93	28.81	30.59	22.63	27.23	22.07
Mass of dry soil + container (g)	19.12	24.79	23.46	24.45	20.83	24.37	20.36
Mass of container (g)	14.07	13.94	14.08	14	14.09	14.12	14
Mass of Moisture (g)	2.76	6.14	5.35	6.14	1.8	2.86	1.71
Mass of dry soil (g)	5.05	10.85	9.38	10.45	6.74	10.25	6.36
Moisture Content (w%)	55	57	57	59	27	28	27

Liquid Limit 58
Plastic Limit 27
Plasticity Index 30

Date	06/11/00		Sample	3E			
Test No.	1	2	3	4	5	6	7
Type of Test	LL	LL	LL	LL	PL	PL	PL
Initial Reading (mm)	0	0	0	0			
Final Reading (mm)	17	19.5	21.1	24			
Core Penetration (mm)	17	19.5	21.1	24			
Container No.	12	131	2	31	18	34	17
Mass of wet soil + container (g)	25.13	25.65	27.51	25.72	29.49	28.19	25.87
Mass of dry soil + container (g)	20.75	21.05	22.14	21.06	26.08	24.94	23.06
Mass of container (g)	14.01	14.13	14.08	14.01	14.09	13.95	14.08
Mass of Moisture (g)	4.38	4.6	5.37	4.66	3.41	3.25	2.81
Mass of dry soil (g)	6.74	6.92	8.06	7.05	11.99	10.99	8.98
Moisture Content (w%)	64.99	66.47	66.63	66.10	28.44	29.57	31.29

Liquid Limit 66
Plastic Limit 30
Plasticity Index 36

Date	27/11/00		Sample	4E			
Test No.	1	2	3	4	5	6	7
Type of Test	LL	LL	LL	LL	PL	PL	PL
Initial Reading (mm)	0	0	0	0			
Final Reading (mm)	13.5	17.4	21.25	22.9			
Core Penetration (mm)	13.5	17.4	21.25	22.9			
Container No.	9	104	103	21	11	18	2
Mass of wet soil + container (g)	29.04	26.91	27.55	38.81	20.84	22.7	21.53
Mass of dry soil + container (g)	24.13	22.53	22.86	30.18	19.58	21.08	20.16
Mass of container (g)	14	13.92	14.06	14.25	14.15	14.08	14.07
Mass of Moisture (g)	4.91	4.38	4.69	8.63	1.26	1.62	1.37
Mass of dry soil (g)	10.13	8.61	8.80	15.93	5.43	7	6.09
Moisture Content (w%)	48	51	53	54	23	23	22

Liquid Limit 52
Plastic Limit 23
Plasticity Index 29

Box No.3
Liquid Limit (Cone Penetrometer) and Plastic Limit

Test to BS1377: Part 2: 1990: 4.3/4.4

Date	27/11/00		Sample	4E			
Test No.	1	2	3	4	5	6	7
Type of Test	LL	LL	LL	LL	PL	PL	PL
Initial Reading (mm)	0	0	0	0			
Final Reading (mm)	13.5	17.4	21.25	22.9			
Core Penetration (mm)	13.5	17.4	21.25	22.9			
Container No.	9	104	103	21	11	18	2
Mass of wet soil + container (g)	29.04	26.91	27.55	38.81	20.84	22.7	21.53
Mass of dry soil + container (g)	24.13	22.53	22.86	30.18	19.58	21.08	20.16
Mass of container (g)	14	13.92	14.06	14.25	14.15	14.08	14.07
Mass of Moisture (g)	4.91	4.38	4.69	8.63	1.26	1.62	1.37
Mass of dry soil (g)	10.13	8.61	8.80	15.93	5.43	7	6.09
Moisture Content (w%)	48	51	53	54	23	23	22

Liquid Limit	52
Plastic Limit	23
Plasticity Index	29

Site 1A
Borehole No. 83/20-Sc001
Box No. 1

Liquid Limit (Cone Penetrometer) and Plastic Limit
Test to BS1377: Part 2: 1990: 4.3/4.4

DATE 02/04/01

Test No.	1	2	3	4	5	6	7
Type of Test	LL	LL	LL	LL	PL	PL	PL
Initial Reading (mm)	0	0	0	0			
Final Reading (mm)	19.6	23.2	26.5	26.9			
Core Penetration (mm)	19.6	23.2	26.5	26.9			
Container No.	14	2	17	131	104	9	21
Mass of wet soil + container (g)	23.18	23.64	23.74	25.1	17.33	17.89	17.59
Mass of dry soil + container (g)	19.22	19.45	19.45	20.27	16.57	17.04	16.88
Mass of container (g)	14.14	14.09	14.1	14.11	13.94	14.01	14.27
Mass of Moisture (g)	3.96	4.19	4.29	4.83	0.76	0.85	0.71
Mass of dry soil (g)	5.08	5.36	5.35	6.16	2.63	3.03	2.61
Moisture Content (w%)	77.953	78.172	80.187	78.409	29	28	27

Liquid Limit	52
Plastic Limit	28.05107
Plasticity Index	23.94893

Liquid Limit (Cone Penetrometer) and Plastic Limit
Test to BS1377: Part 2: 1990: 4.3/4.4

DATE 02/04/01

Test No.	1	2	3	4	5	6	7
Type of Test	LL	LL	LL	LL	PL	PL	PL
Initial Reading (mm)	0	0	0	0			
Final Reading (mm)	19.6	23.2	26.5	26.9			
Core Penetration (mm)	19.6	23.2	26.5	26.9			
Container No.	14	2	17	131	104	9	21
Mass of wet soil + container (g)	23.18	23.64	23.74	25.1	17.33	17.89	17.59
Mass of dry soil + container (g)	19.22	19.45	19.45	20.27	16.57	17.04	16.88
Mass of container (g)	14.14	14.09	14.1	14.11	13.94	14.01	14.27
Mass of Moisture (g)	3.96	4.19	4.29	4.83	0.76	0.85	0.71
Mass of dry soil (g)	5.08	5.36	5.35	6.16	2.63	3.03	2.61
Moisture Content (w%)	77.953	78.172	80.187	78.409	29	28	27

Liquid Limit	52
	28.05107
Plastic Limit	
	23.94893
Plasticity Index	3

Box No. 2
Liquid Limit (Cone Penetrometer) and Plastic Limit
Test to BS1377: Part 2: 1990: 4.3/4.4
DATE 02/04/01

Type of Test	LL	LL	LL	LL	PL	PL	PL
Initial Reading (mm)	0	0	0	0			
Final Reading (mm)	16.4	19.2	20.5	21.8			
Core Penetration (mm)	16.4	19.2	20.5	21.8			
Container No.	9	131	14	2			
Mass of wet soil + container (g)	23.7	28.67	31.45	27.99			
Mass of dry soil + container (g)	20.65	24.1	25.99	23.53			
Mass of container (g)	14	14.13	14.11	14.07			
Mass of Moisture (g)	3.05	4.57	5.46	4.46			
Mass of dry soil (g)	6.65	9.97	11.88	9.46			
Moisture Content (w%)	45.865	45.838	45.960	47.146			

Liquid Limit 46
Too
Plastic Limit Sandy
Plasticity Index

Borehole No. 83/20-Sc004
Box No. 2
Plasticity Index
Liquid Limit (Cone Penetrometer) and Plastic Limit
Test to BS1377: Part 2: 1990: 4.3/4.4
Date 11/04/01

Test No.	1	2	3	4	5	6	7
Type of Test	LL	LL	LL	LL	PL	PL	PL
Initial Reading (mm)	0	0	0	0			
Final Reading (mm)	16.5	19.3	20	21.5			
Core Penetration (mm)	16.5	19.3	20	21.5			
Container No.	131	14	2	9	23	18	17
Mass of wet soil + container (g)	31.45	29.19	30.525	31.72	21.4	21.08	21.86
Mass of dry soil + container (g)	25.84	24.28	25.10	25.83	20.04	19.78	20.41
Mass of container (g)	14.14	14.1	14.06	14	14.06	14.075	14.08
Mass of Moisture (g)	5.61	4.91	5.43	5.89	1.36	1.3	1.45
Mass of dry soil (g)	11.7	10.18	11.04	11.83	5.98	5.705	6.33
Moisture Content (w%)	47.949	48.232	49.139	49.789	22.742	22.787	22.907

Liquid Limit	49
Plastic Limit	23
Plasticity Index	26

Sample Photos

Site 1

83/24-Sc001 Box 1

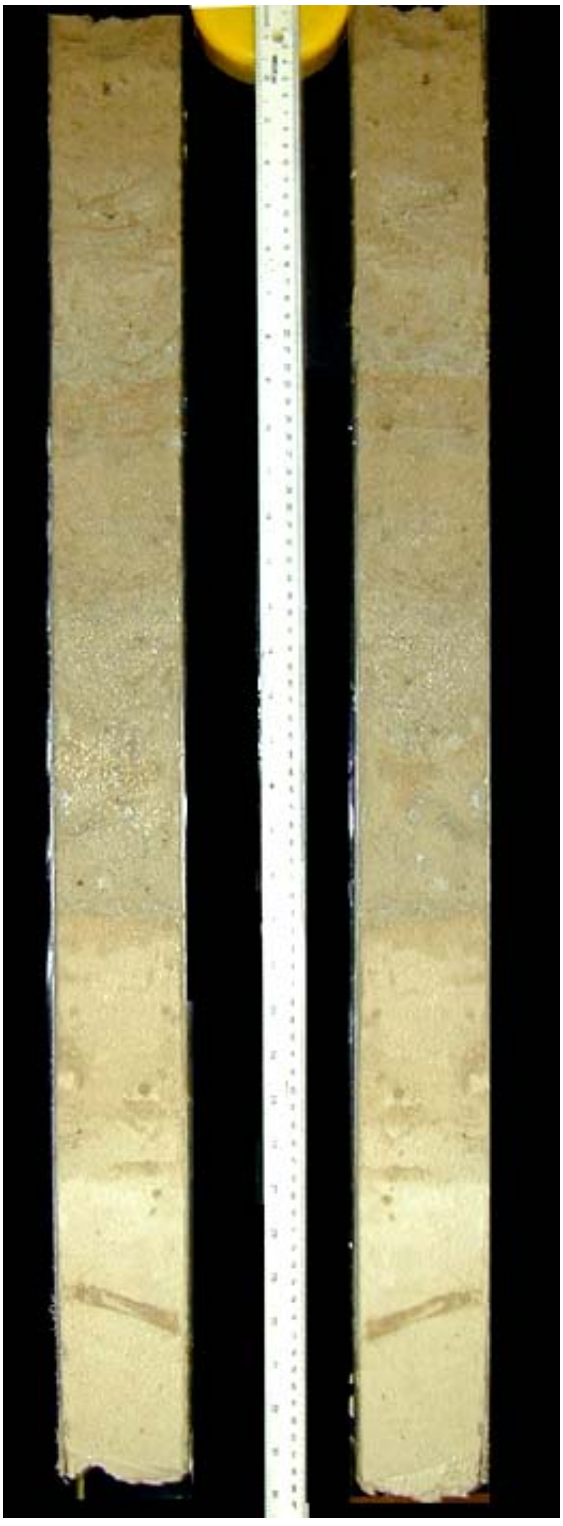

83/24-Sc001 Box 2

83/24-Sc002 Box 1

83/24-Sc003 Box 1

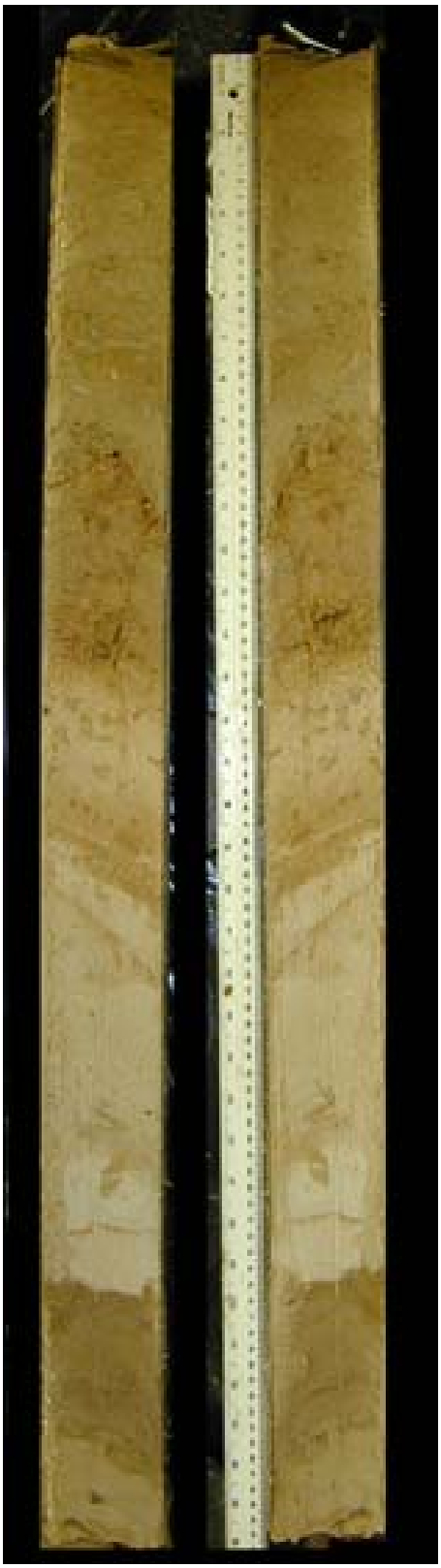

83/24-Sc004 Box 1

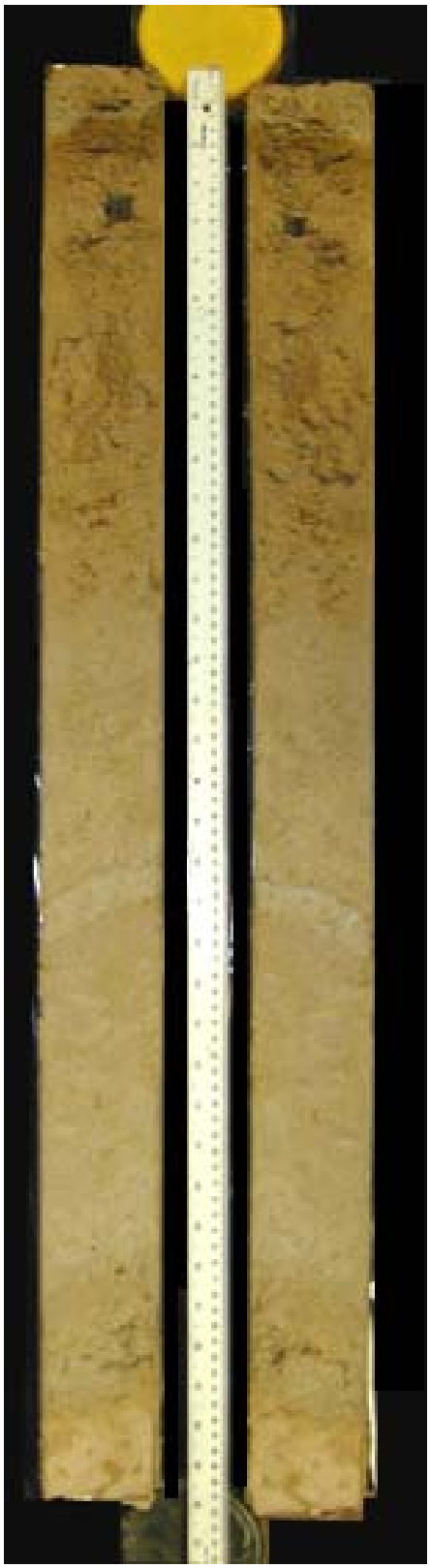

83/24-Sc004 Box 2

83/24-Sc005 Box 1

83/24-Sc005 Box 2

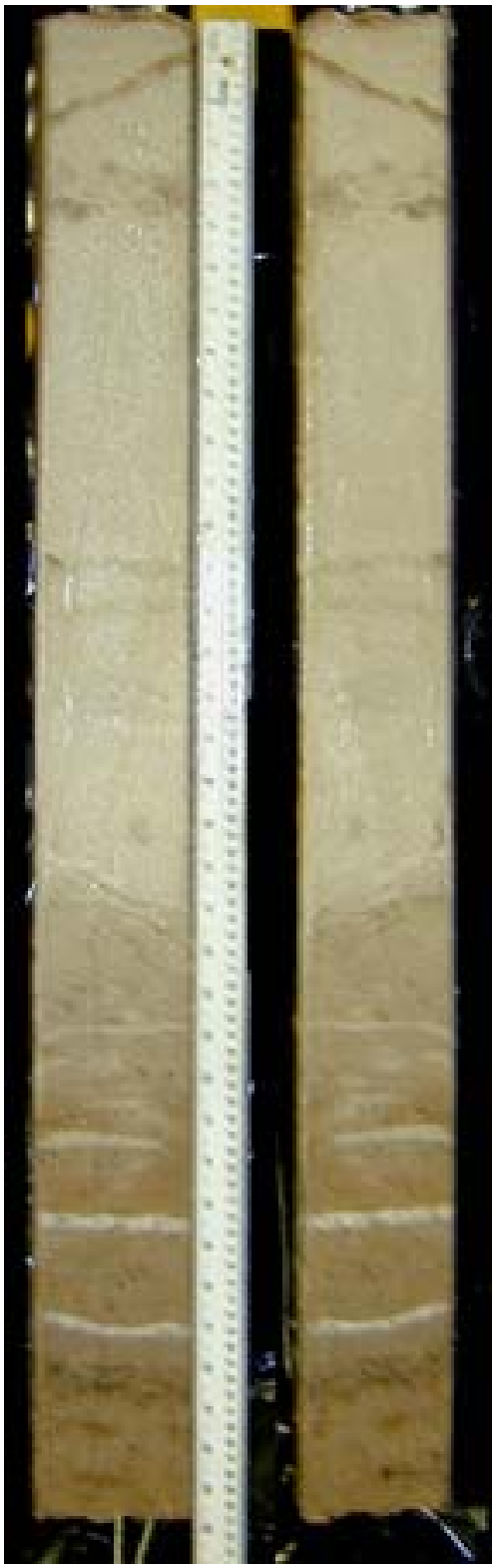

83/24-Sc005 Box 3

Site 1A

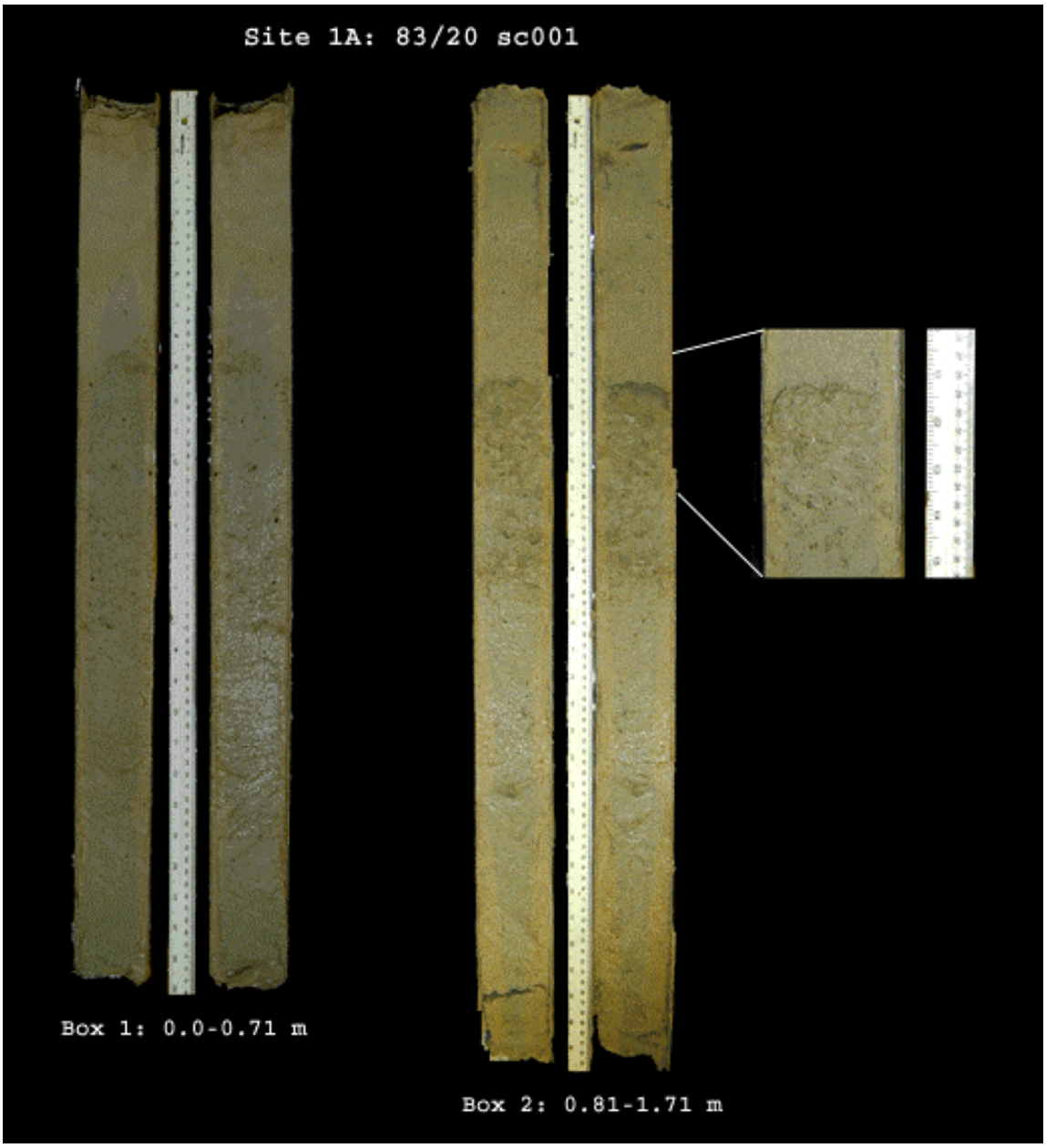


Site 1A: 83/20 sc002
Box 1: 0.0-0.71 m
Box 2: 0.81-1.71 m

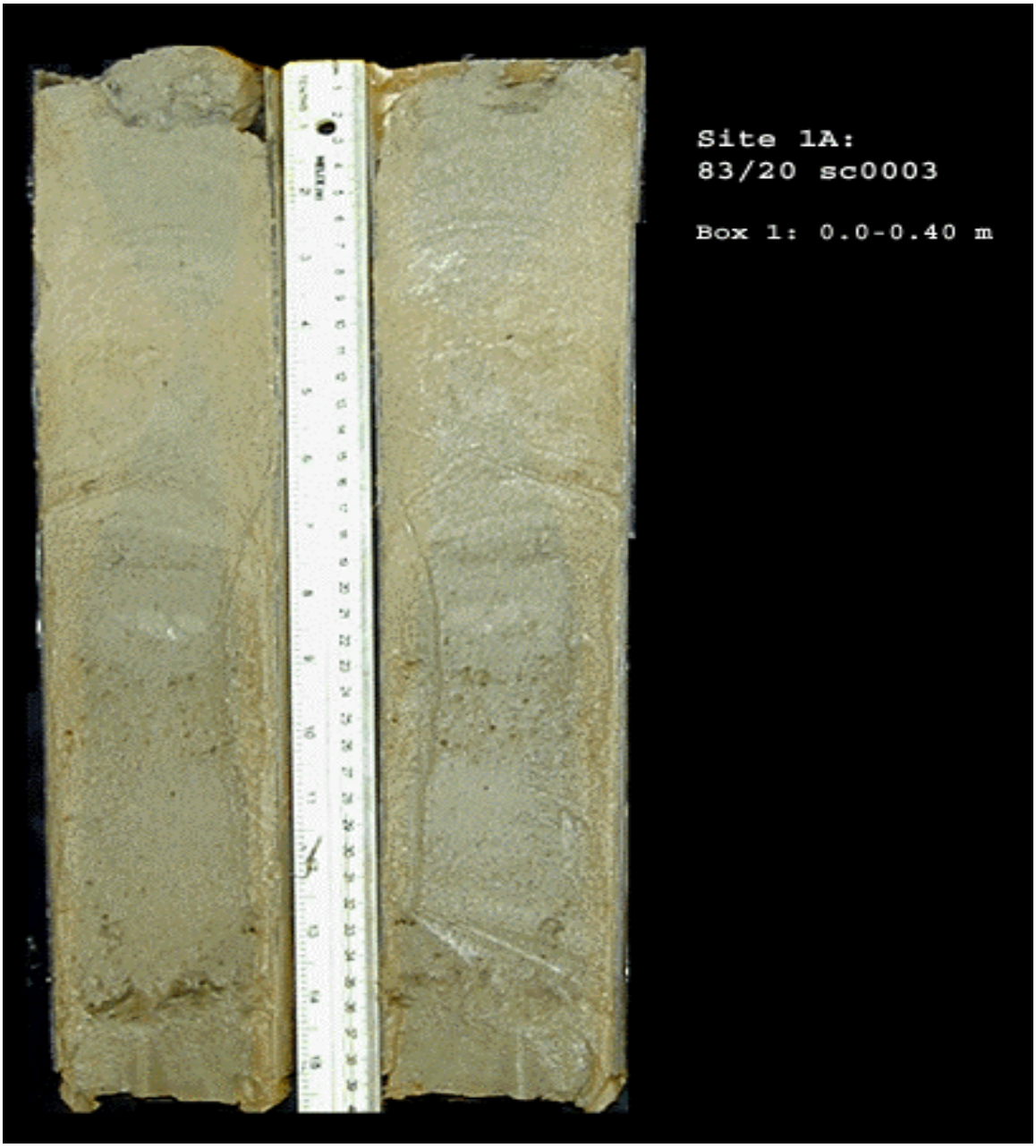
Site 1A:
83/20 sc0003
Box 1: 0.0-0.40 m

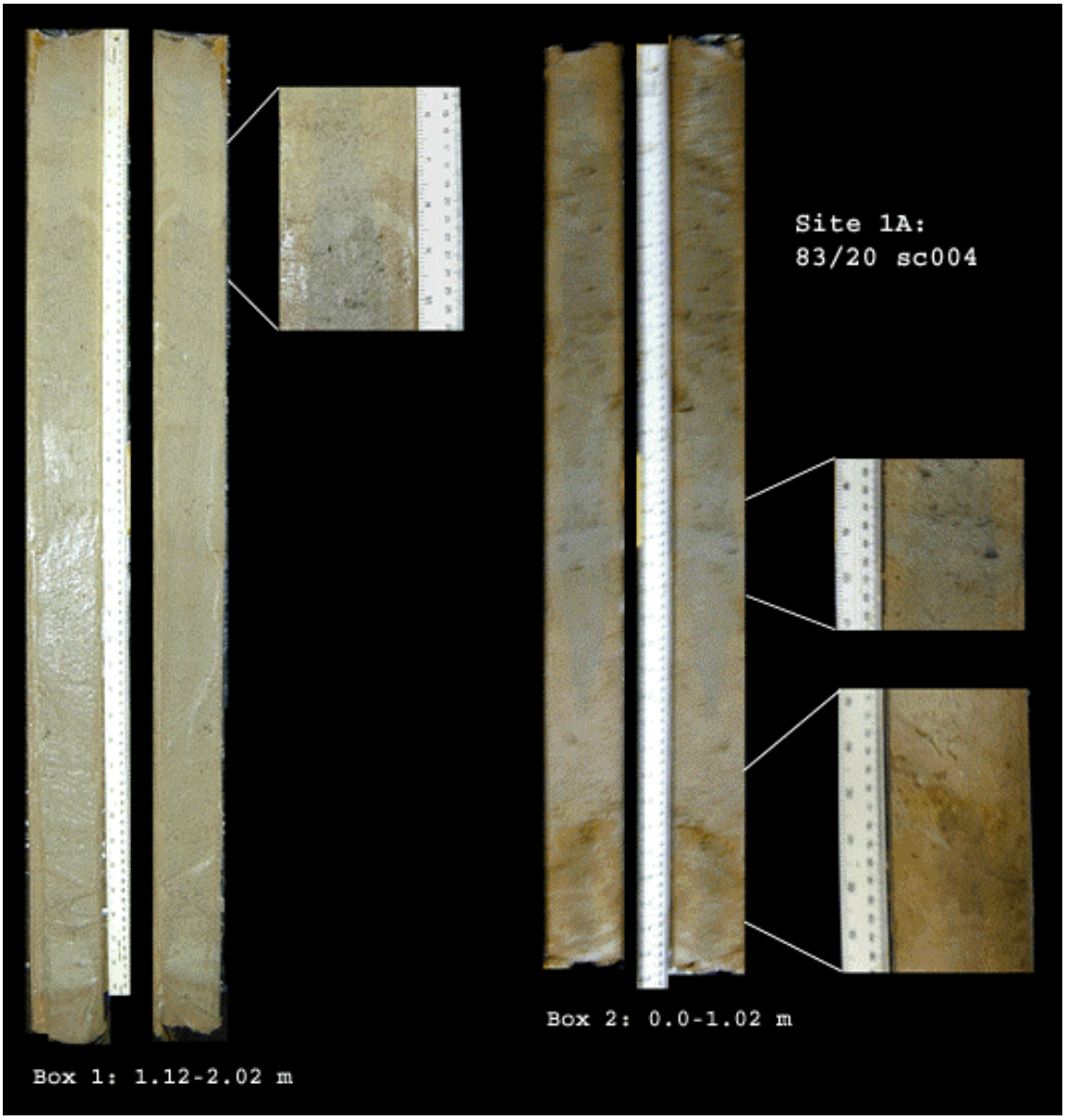
Site 1A:
83/20 sc004
Box 1: 1.12-2.02 m
Box 2: 0.0-1.02 m

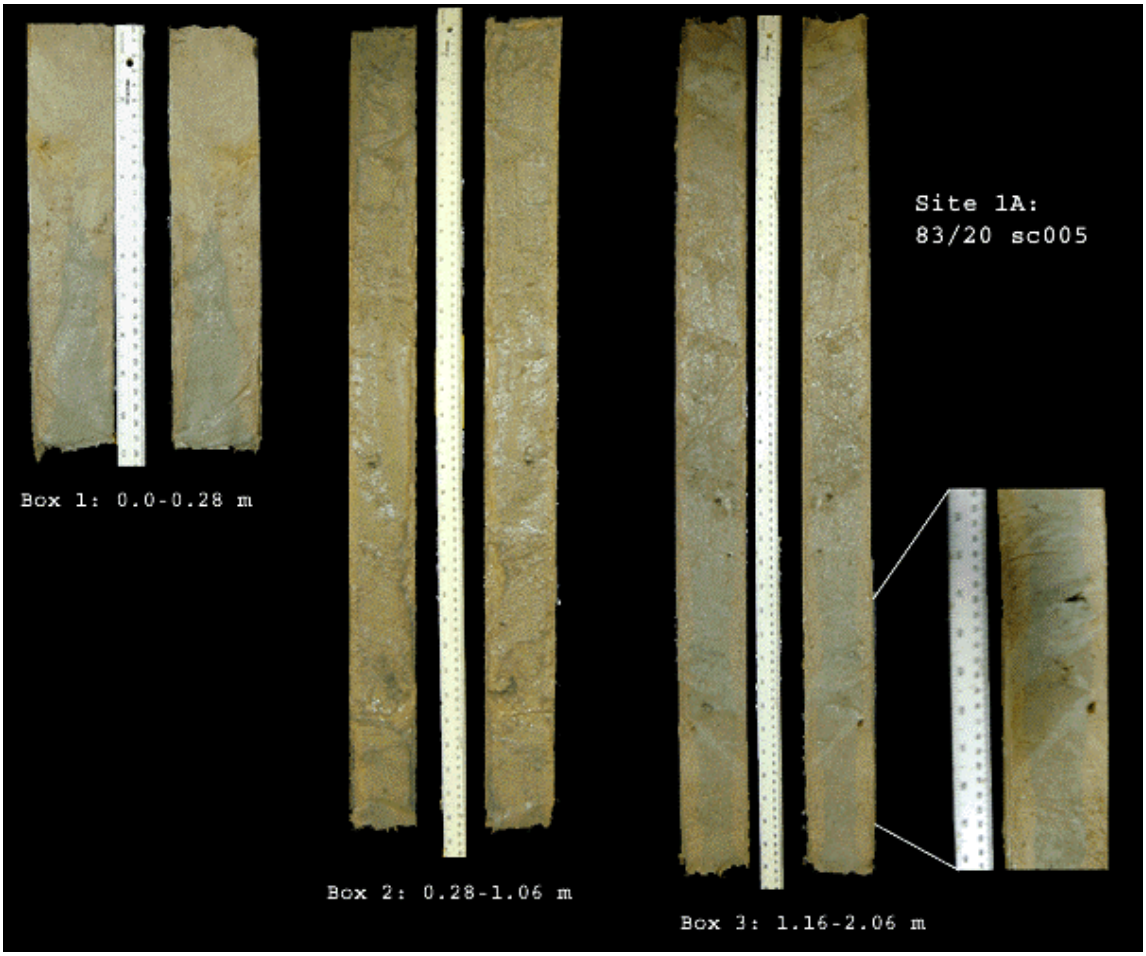
Site 1A:
83/20 sc005
Box 1: 0.0-0.28 m
Box 2: 0.28-1.06 m
Box 3: 1.16-2.06 m

Site 2

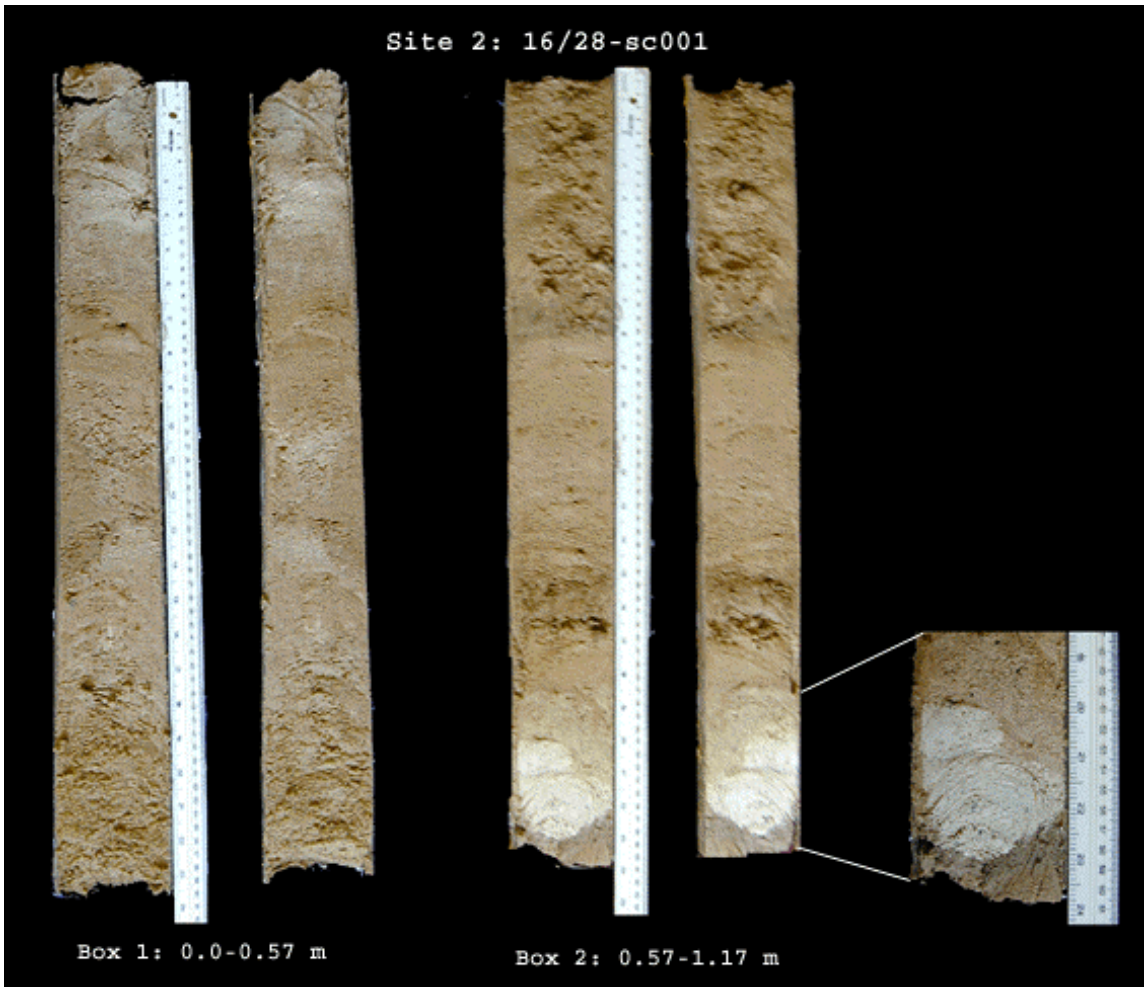

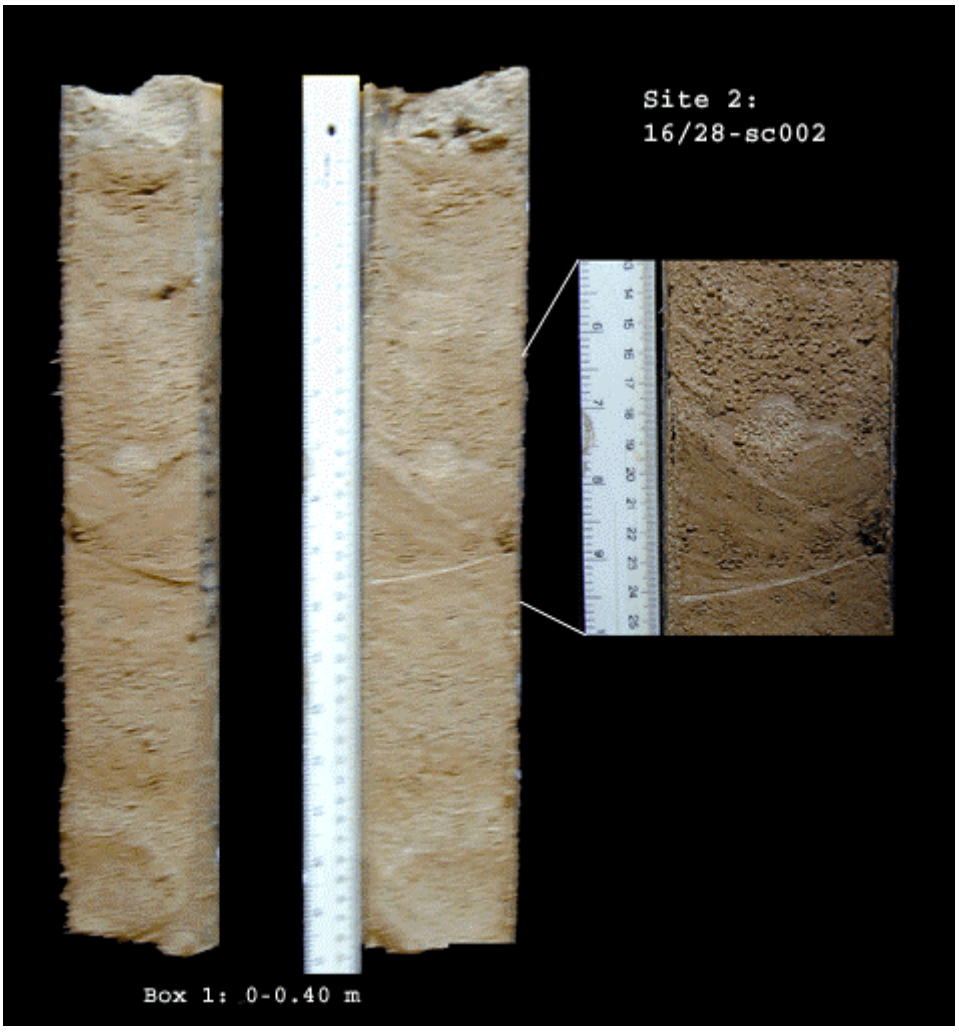
Site 2:
16/28-sc002
Box 1: 0-0.40 m

Site 3

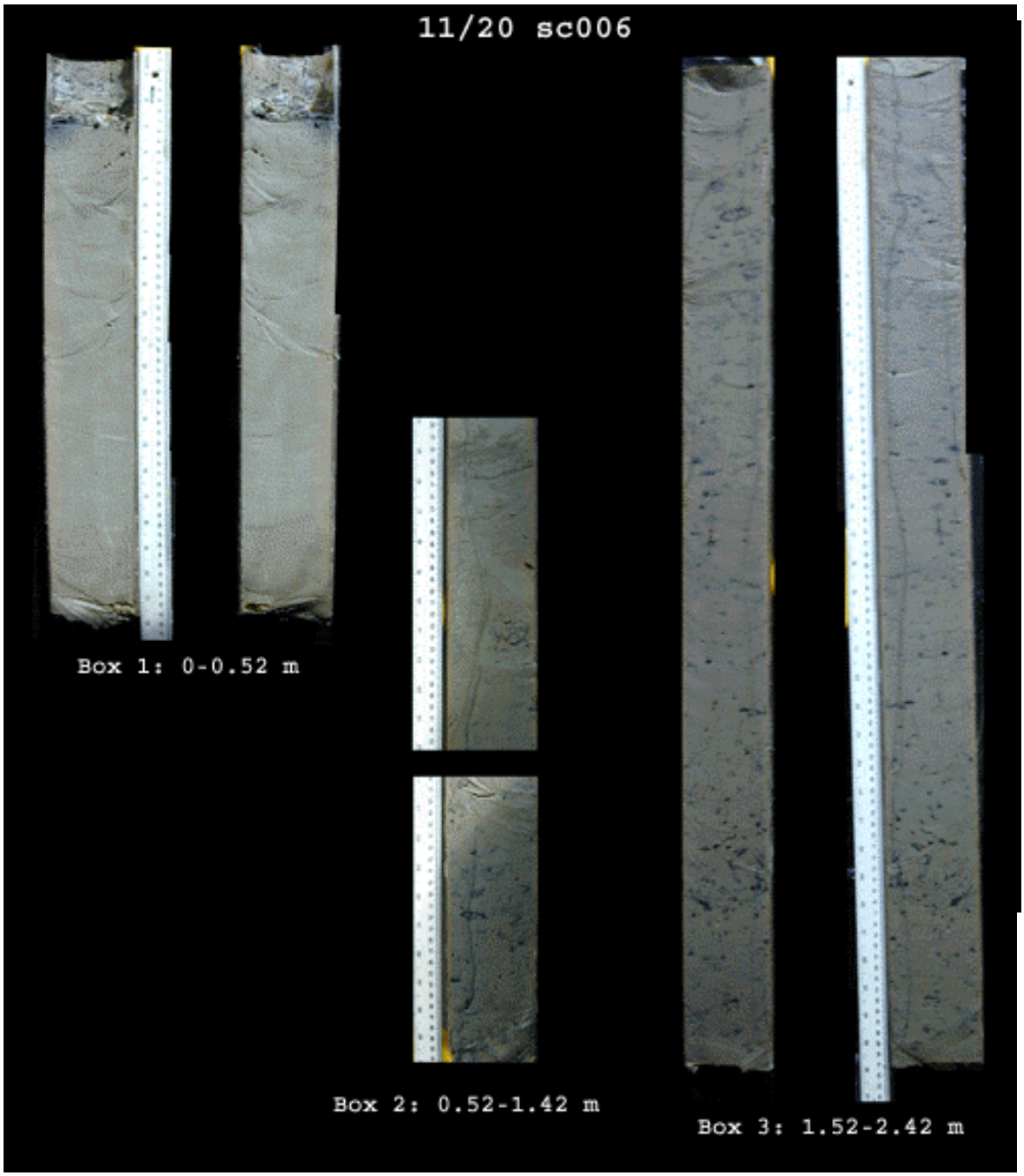

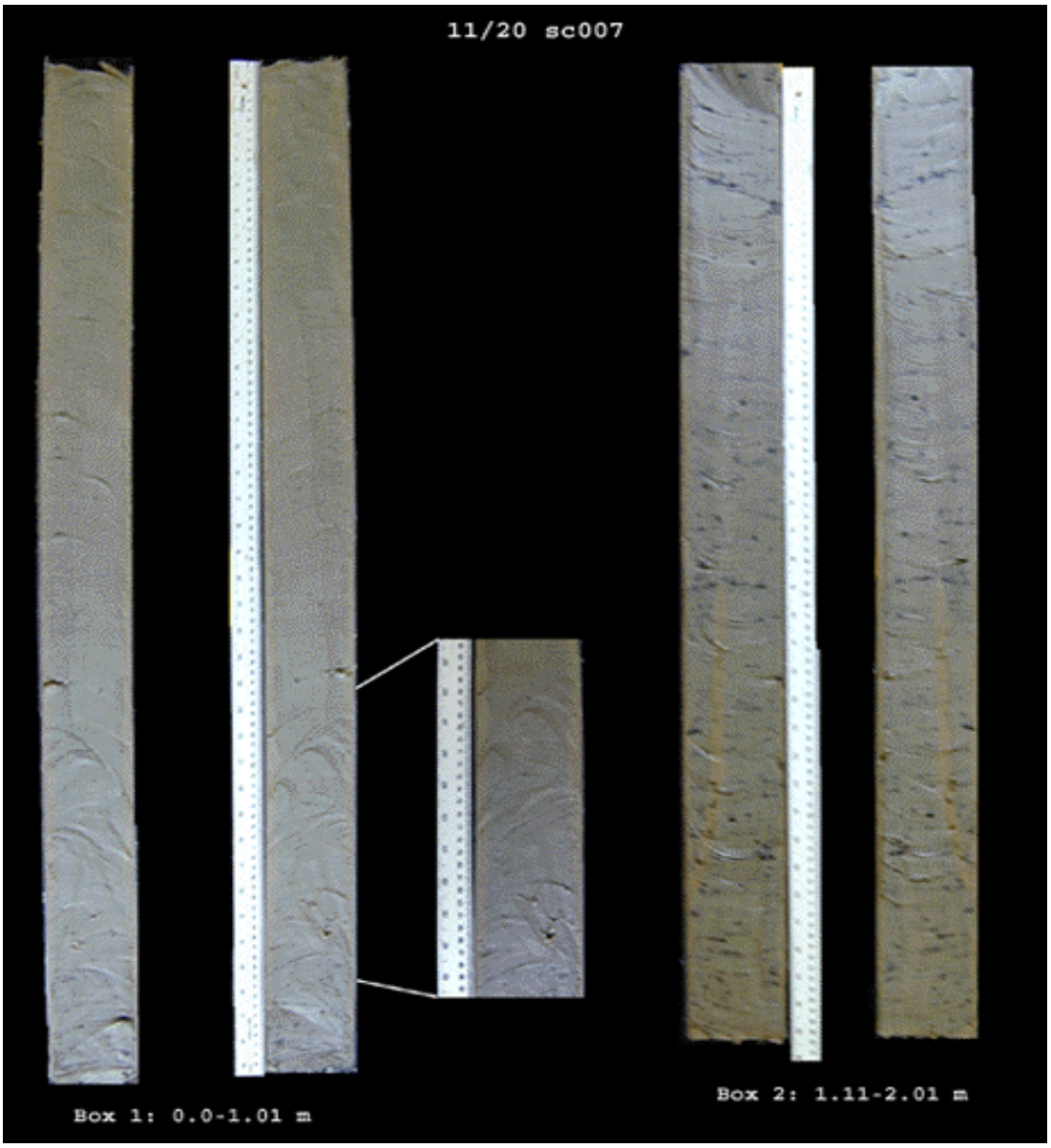
11/20 sc007
Box 1: 0.0-1.01 m
Box 2: 1.11-2.01 m

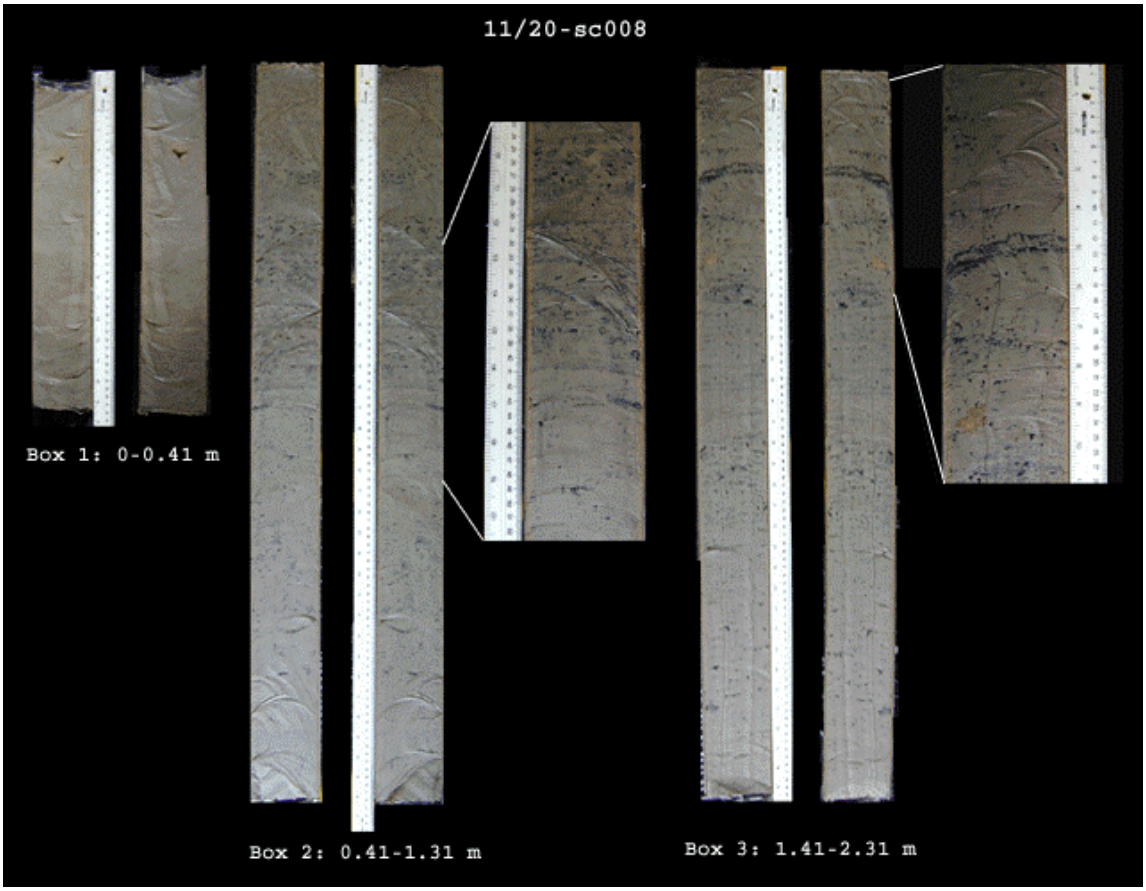
11/20-sc008
Box 1: 0-0.41 m
Box 2: 0.41-1.31 m
Box 3: 1.41-2.31 m

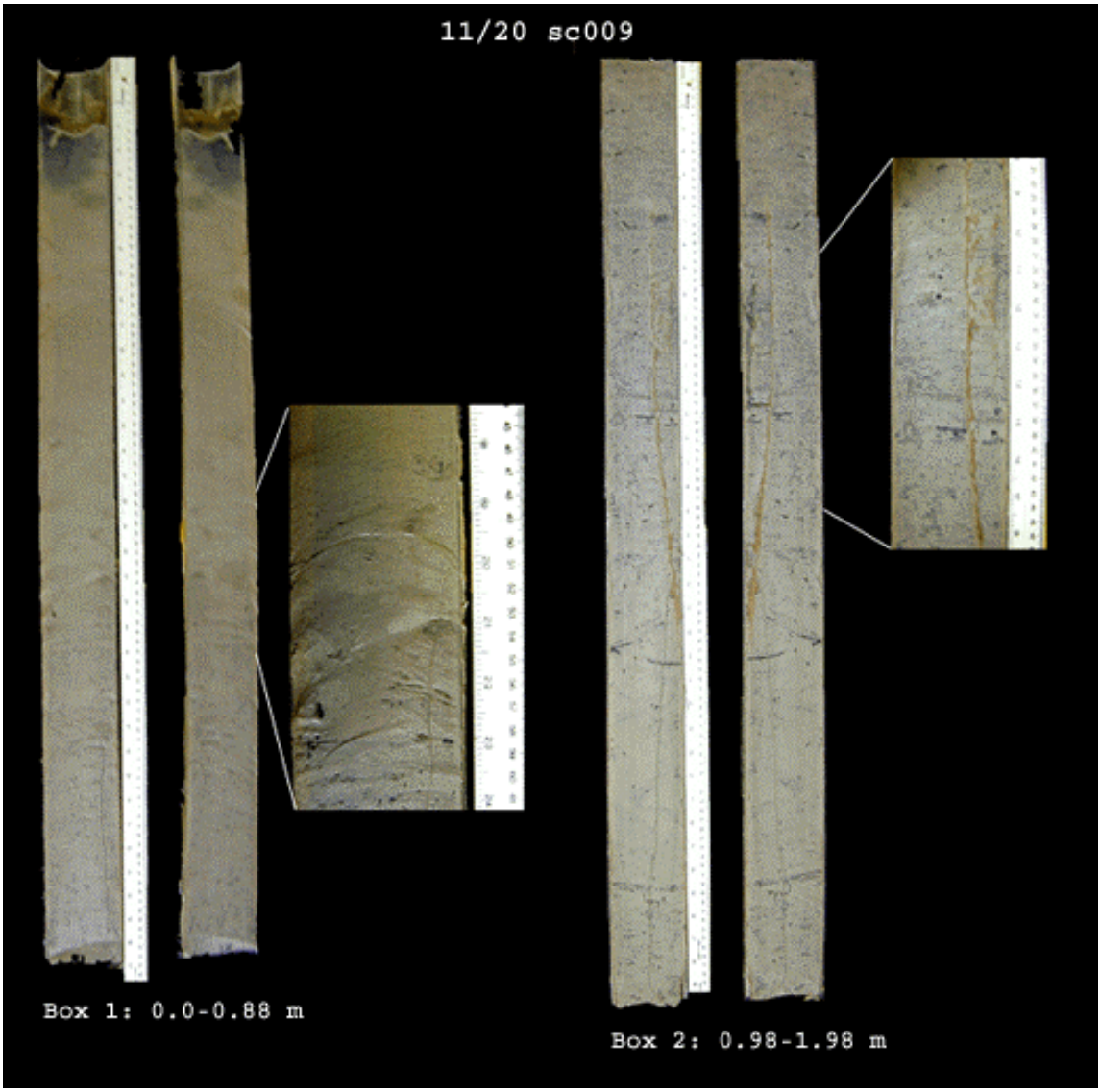
11/20 sc009
Box 1: 0.0-0.88 m
Box 2: 0.98-1.98 m


11/20 sc001
Box 1: 0.0-0.92 m
Box 2: 1.02-1.92 m

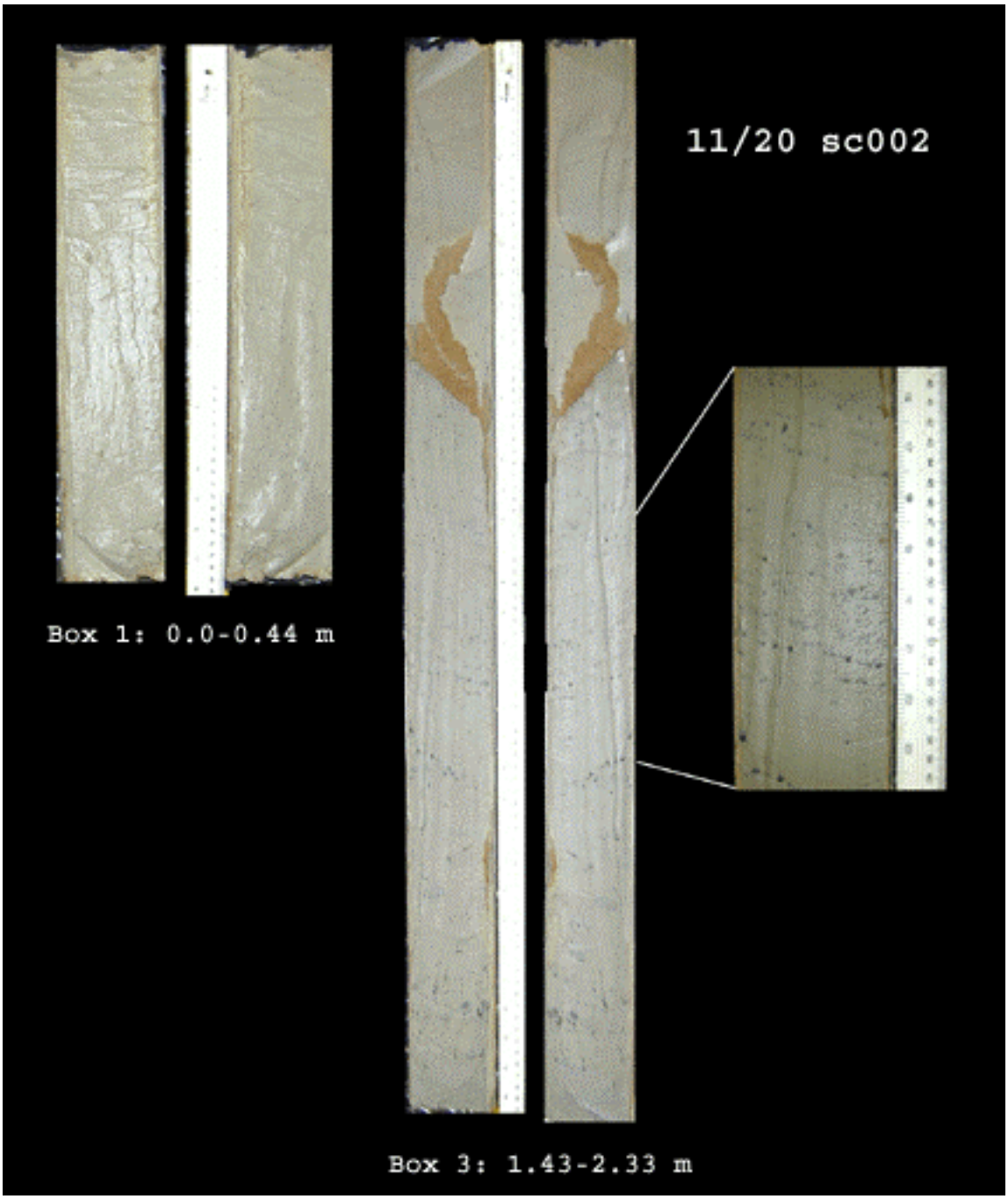
11/20 sc002
Box 1: 0.0-0.44 m
Box 3: 1.43-2.33 m

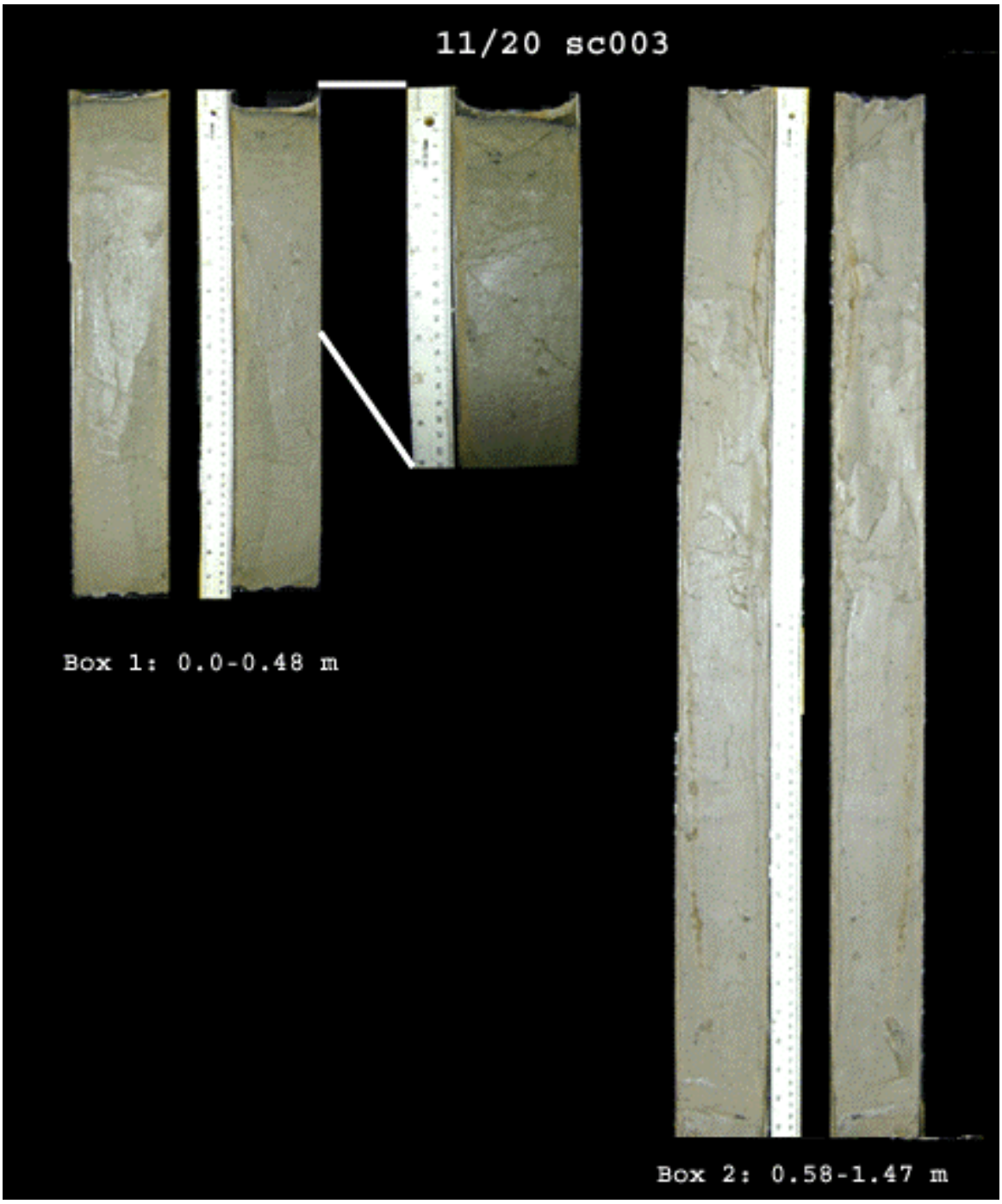
11/20 sc003
Box 1: 0.0-0.48 m
Box 2: 0.58-1.47 m

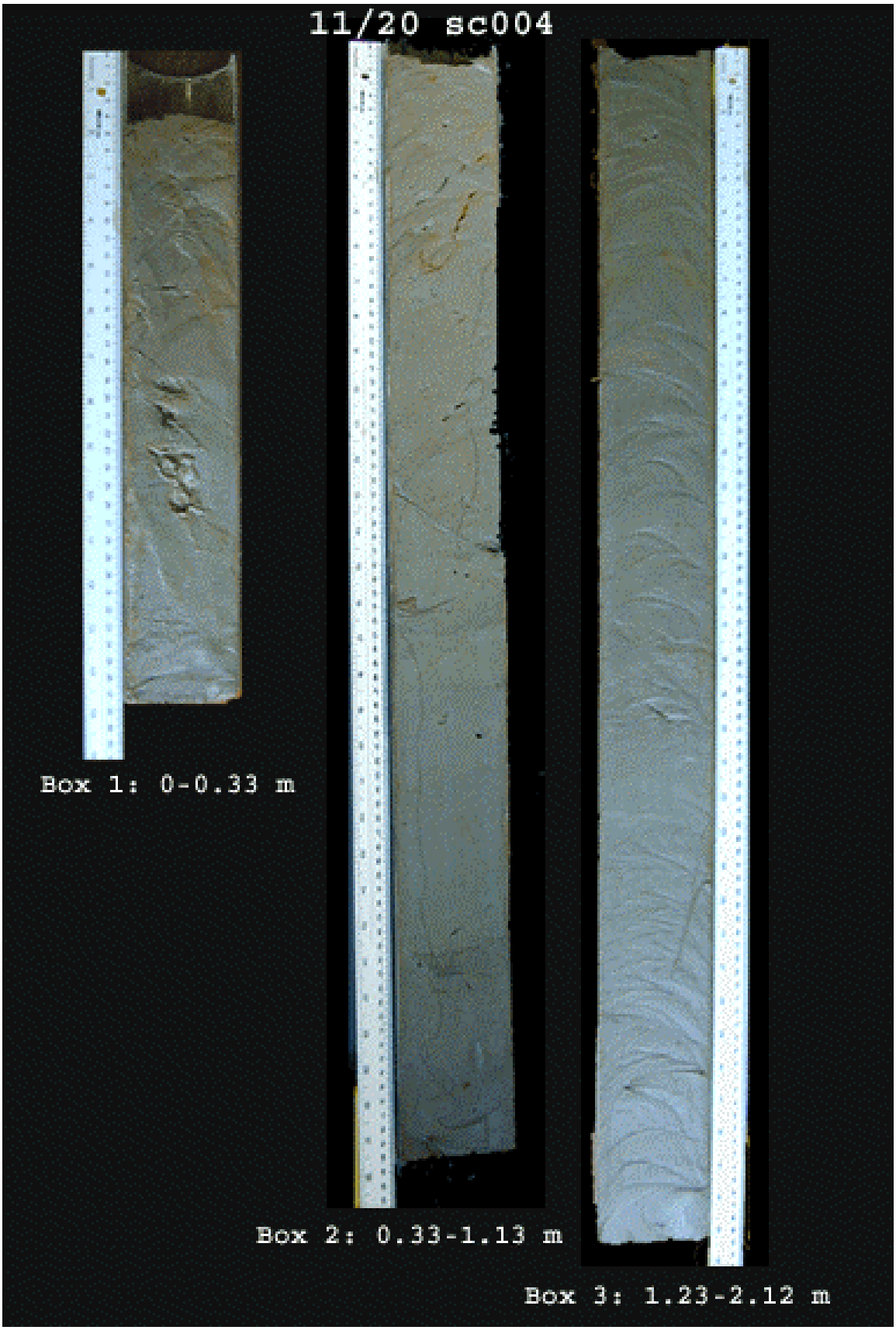
11/20 sc004
Box 1: 0-0.33 m
Box 2: 0.33-1.13 m
Box 3: 1.23-2.12 m

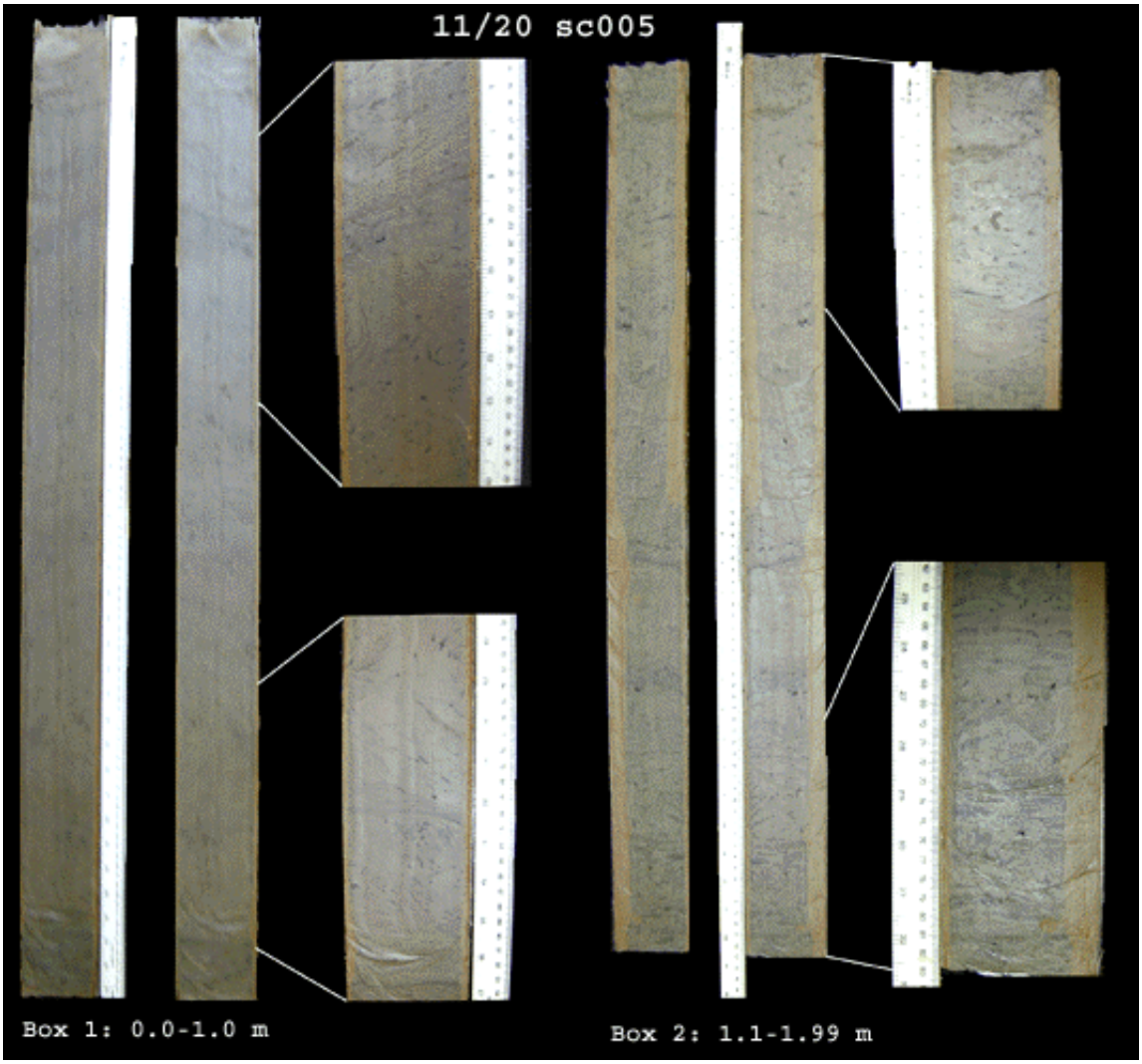
11/20 sc005
Box 1: 0.0-1.0 m
Box 2: 1.1-1.99 m

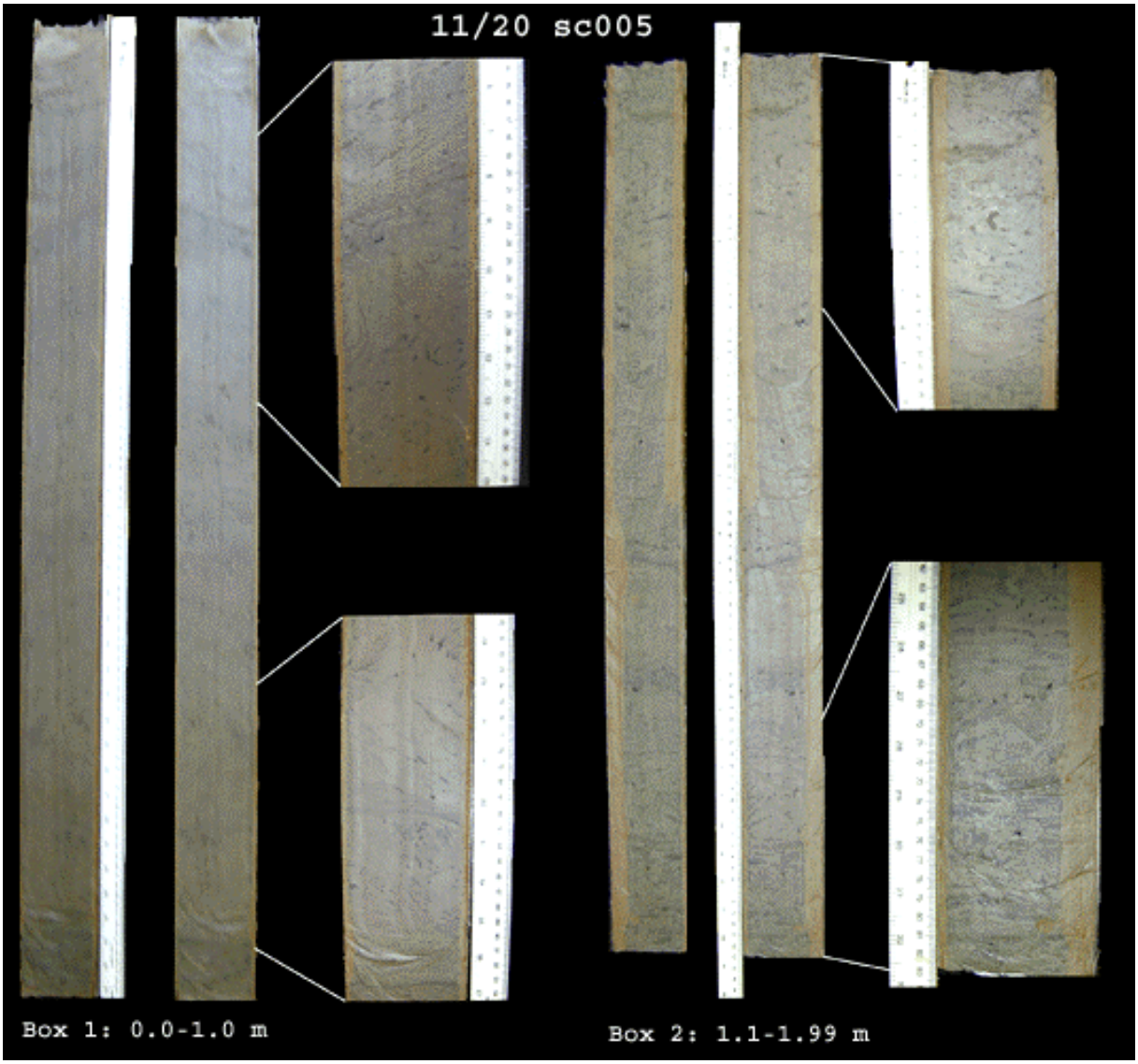
11/20 sc005
Box 1: 0.0-1.0 m
Box 2: 1.1-1.99 m